ADDIS ABABA UNIVERSITY

ADDIS ABABA INSTITUTE OF TECHNOLOGY

SCHOOL OF CIVIL AND ENVIRONMENTAL ENGINEERING

Early Age Thermal Behavior of Bagasse Ash Concrete Under Different Ambient Temperatures

By Amanuel Bersisa

July, 2019

Addis Ababa

A Thesis in Structural Engineering

A Thesis

Submitted in Partial Fulfillment of the Requirements for the Degree of Master of Science

The undersigned have examined the thesis entitled "Early Age Thermal Behavior of Bagasse Ash Concrete Under Different Ambient Temperatures" presented by **Amanuel Bersisa**, a candidate for the degree of **Master of Science** and hereby certify that it is worthy of acceptance.

Dr. - Ing. Adil Zekeria		
Advisor	Signature	Date
Dr. Esayas G/Youhannes		
Internal Examiner	Signature	Date
Dr. - Ing. Girma Zerayouhannes		
External Examiner	Signature	Date
Dr. - Ing. Henok Fikre		
Chair Person	Signature	Date

UNDERTAKING

I confirm that research work titled "Early Age Thermal Behavior of Bagasse Ash Concrete under Different Ambient Temperatures" is my own work. The work has not been presented elsewhere for assessment. Where material has been used from other sources, it has been properly acknowledged / referred.

Amanuel Bersisa

ABSTRACT

Bagasse ash can be optimized as a partial cement replacing material in a concrete mixture. Other than guaranteeing mechanical properties, this pozzolana could be used as a thermal retarder for mass concrete placement, despite the fact that its property was not examined under various ambient temperatures. This research aims at studying the early age thermal and mechanical properties of bagasse ash concrete under different ambient temperatures. A semi-adiabatic temperature rise data of four different concrete mixtures (containing pure Portland cement, 6.5%, 13% and 20% dosage of bagasse ash by volume) are determined. Insulated concrete specimens of size 30*30*40cm^3 were cast and the internal heat of hydration was measured at three different locations for every 30 minutes of interval. For simulating different ambient temperatures, a chamber has been constructed in the AAiT material laboratory. The temperature chamber is capable of simulating average ambient temperatures of 25.15^0, 35.54^0 and 43.77^0 C.

As the experimental outcomes indicate, there is reduction in early age compressive, splitting tensile, and flexural strength of concrete containing different dosages of bagasse ash. On the other hand, enhancement of strength is observed in bagasse ash concrete specimens at late age testing (with exception of 20% replacement level). The laboratory testing program revealed that, the presence of bagasse ash in the concrete mixture shifts temperature rise-time curve, reduces the total heat of hydration and decreases the thermal gradient in the specimens. Moreover, the total heat of hydration of all mixtures was significantly influenced as the ambient temperature increased, but mixtures containing bagasse ash show slower heat liberation rate relative to the control group.

Heat of hydration and thermal cracking risk were also simulated using Hacon-3 finite element software. The FES results show a good agreement with the real measurement in temperature gauges. The presence of bagasse ash in concrete up to 13% decreases the cracking risk. However, incorporating bagasse ash at a higher dosage could retard the strength development and consequently escalates the risk of cracking. This investigation proves, the main driving force that controls early age cracking risk depends on both strength development and heat liberation of concrete.

Key words: Bagasse ash, Semi-adiabatic temperature rise, Temperature chamber, Heat of hydration, Ambient temperature, Thermal gradient, Thermal cracking risk.

ACKNOWLEDGMENTS

I would first like to take this opportunity to thank God for being my strength and guide in writing this thesis. I express my deepest gratitude to my thesis advisor Dr. - Ing. Adil Zekeria for devoting much time to consult, guide and read my work over and over again. Your assistance on both research as well as on my career have been indispensable.

Beside my advisor, the door to Dr. Esayas G.Youhannes office was always open whenever I had a question about my research work; hence, I am very thankful for his unconditional cooperation. I would also like to thank AAiT material laboratory staffs and experts from different field of study for partaking in this research.

Ethiopian road authority is playing a vital role in producing educated manpower by sponsoring educational programs. Therefore, I would like to thank ERA for sponsoring my MSc. program collaborating with AAiT. Finally, yet importantly, I would like to thank my mother: Seblewongle Dejenie for supporting me spiritually throughout my life.

TABLE OF CONTENTS

LIST OF TABLES

LIST OF FIGURES

ABBREVIATIONS, SIGNS, AND SYMBOLS

A.S.L.	Above Sea Level
AAiT	Addis Ababa Institute of Technology
ACI	American Concrete Institute
ASTM	American Standard Testing Material
ASCE	American Society of Civil Engineering
C–S–H	Calcium Silicate Hydrate
C_2S	Di-Calcium-silicate
C_3S	Tri-Calcium-Silicate
C_4AF	Tetra-Calcium-Alumino-Ferrite
C_3A	Tri-Calcium Aluminate
EMA	Ethiopian Mapping Authority
FES	Finite Element Software
FEM	Finite Element Method
GGBFS	Ground Granulated Blast Furnace Slug
GOE	Government of Ethiopia
LOI	Loss of Ignition
MPa	Mega Pascal
NMA	National Meteorological Agency
NRMCA	National Ready Mix Concrete Association
PC	Portland Cement
SCM	Supplementary Cementitious Materials
SCB	Sugarcane Bagasse
SCBA	Sugarcane Bagasse Ash
USDA	United States Department of Agriculture
XRD	X-Ray Diffraction

CHAPTER 1 INTRODUCTION

1.1 MOTIVATION

With amplified environmental awareness, the recycling of industrial byproducts has become an attractive alternative for disposal. Besides disposal management, several reports show that utilization of waste material like plastics, coal bottom ash, bagasse ash, coal fly ash, cement kiln dust, etc. in concrete enhances its texture, strength and durability. Bagasse is among the industrial by-product found abundantly in Ethiopia. Off course, there is some traditional way of using bagasse ash as a fertilizer for the production of crops, but it can be utilized for other purposes as well. According to studies, bagasse ash can partially replace cement due to its pozzolana behavior. Using this type of advantage is quite crucial in order to minimize environmental pollution resulted from the emission of CO_2 when producing cement. Besides the abundance of bagasse ash disposed of existing sugar factories, other factories of different production capacity are under construction along with the various irrigation projects. By 2020 the bagasse ash production (estimated amount of 1.9Million ton) from the local factories will reach into a figure around 16.01% of the over-all cement need of the time. (Geremewu, 2017)

Application of pozzolana material in concrete hinge on the hydration of cement and possibly modifies the reaction momentum. As hydration is an exothermic reaction, it will possess heat on concrete sections. If the volume concrete section is large, hydration heat accumulated at the interior of the structure is not easy to be lost so that, the temperature inside the concrete rise. The temperature difference between the inner and surface concrete will produce a thermal gradient. At early age, thermal dilution will impose compressive stress on the concrete section, which result formation of surface cracks. Through time the concrete surface cools and tries to shrink; therefore, the specimen will be under tension. When the tensile strength of the concrete is not enough to resist the tensile stress, through crack will be produced. (Neville, 2011; Bobko et al., 2015)

Figure 1.1 Early Age Thermal Cracking on a Massive Foundation (https://www.concretebridgeviews.com)

Factors such as ambient temperature affect the rate of hydration and heat evolution of both pozzolana and cementitious materials. Therefore, studies should have to be carried out on different environmental conditions before one can use pozzolana and cement in real life construction works.

According to NMA (2007), the temperature which covers a wide range of land in Ethiopia, varies from 20^0 to 45^0 Celsius. Though wide coverage of temperature and humidity range of Ethiopia, papers done on bagasse ash concrete are conducted on specific target temperature, which makes the applicability of the studies not comprehensive.

1.2 RESEARCH NEED

Scientists have been documenting climate-related shifts due to the emanation of CO_2 and disposal of a waste products. Production of cement is the third-largest source of anthropogenic emission of carbon dioxide, in which it covers up to 5% of the total amount (Raja, 2014; Mikulclc et al., 2013). Besides the increment of carbon dioxide due to cement production, the demand and cost of this construction material is inflating (Joshua et al., 2018). Counting the odds constructions are not altered for a while, as it is crucial for human development. Through all this, the utilization of supplementary cementitious materials

from the by-product of industries come in to picture. The use of SCMs conserves energy and has environmental benefits due to reduction in carbon dioxide emission since the manufacturing of cement declines. Furthermore, recycling of SCMs help to regulate an abundance of industrial by-products (Abdulkadir et al., 2014; Awad et al., 2017)

Among SCMs, Bagasse ash is the earlier one. Researches have been giving a clue for utilizing bagasse ash as partial replacement for cement to a certain optimum level. As per previous studies, Cement can be replaced by 10% to 15% of bagasse ash with an insured good mechanical property of concrete. Although there is a good beginning, the early age thermal properties, shrinkage, long-term and early age mechanical properties of concrete containing this pozzolana are not fully addressed.

Gremew (2017) had tried to investigate the application of bagasse ash for rigid pavement. The research result was overwhelming and gives a clue that bagasse ash can be used as a thermal retarder. As a part of consecutive research, further study should be carried out to investigate the early age thermal property of bagasse ash concrete under different ambient temperature.

1.3 OBJECTIVES AND SCOPE OF RESEARCH

The general objective of this study is investigating the early age thermal behavior of bagasse ash concrete under different ambient temperatures. Furthermore, the influence of Bagasse ash on the development of early age mechanical properties (compressive and tensile strength) of concrete is also a part of this study.

The main scope is defined as follows: -

- To review the existing knowledge of Cement hydration, pozzolana reaction, thermal cracking and utilization of bagasse ash in concrete.
- Performing comprehensive experimental programs to investigate the influence bagasse ash on strength development of young concrete.
- Undertaking experimental investigations to study the effect of ambient temperatures on the heat evolution of concrete containing bagasse ash and validating the outcomes using finite element software.

1.4 SCIENTIFIC APPROACH

The first crucial step was a critical state-of-art report. Information's and previous studies are structured in a compressive way in order to find gaps and supportive feedbacks. Preceding step was designing of experimental programs and preparation of experimental setups. Experiment programs are classified into two major part. The first part includes chemical and physical characterization of construction materials. The second part incorporates early age thermal and mechanical properties investigation.

For major experimental program, 40*30*30 cm^3 concrete samples were used to measure early age heat evolution using thermocouples. The specimens were insulated using Styrofoam in five directions. The upper part was left uninsulated for examining the effect of ambient temperature on the response concrete specimens. For simulating different ambient temperatures, Chamber has been constructed at AAiT material laboratory.

1.5 ORGANIZATION OF THESIS

CHAPTER 1 of this paper states the motivation for the study. The research needs, research goals and the corresponding scientific approach is emphasized in this chapter.

CHAPTER 2 of this report provides thorough discussion about cement hydration, heat evolution, influence factor on the heat of hydration, abundance, and application of bagasse ash on concrete, etc.

CHAPTER 3 documents physical and chemical characterization of construction materials. The adopted research methods and test setups to achieve the research goals are also a part of this section.

CHAPTER 4 present major experimental program results. The mechanical properties and heat evolution of different concrete mixture were discussed based on scientific explanation.

CHAPTER 5 deals with finite element modeling for prediction of early age thermal crack risk. The modeling issues, input parameters and analyses results are well documented.

CHAPTER 6 offers conclusions and recommendations for future works.

CHAPTER 2 LITERATURE REVIEW

2.1 CEMENT HYDRATION AND HEAT EVOLUTION

When water and cement are mixed, the constituent compounds undergo a chemical reaction termed hydration, which results in new compounds called hydration product. Among the cement constitutes both C_3S and C_2S react with water to produce an amorphous calcium silicate hydrate known as C–S–H gel, which is the main glue that binds the sand and coarse aggregate particles together in concrete. (Kim, 2010, Perumal et al., 2016; Neville, 2011)

Cement hydration is an exothermic reaction, which produces a high amount of heat. The amount of heat generated in the concrete depends on different factors including cement type, chemical composition, casting temperature and ambient temperature. (Lagundžija and Thiam, 2017; Meadows, 2007)

2.1.1 Hydration of Ordinary Portland Cement

Ordinary Portland cement is composed largely of four types of minerals: alite (C3S), belite (C_2S), aluminate (C_3A), and alumino-ferrite (C_4AF). When the various compounds are present all together in cement, their rates of hydration will be affected by compound interactions.

Tri-calcium-silicate (C_3S) or alite is responsible for the major engineering properties of concrete. The Portland cement clinker may contain about 40–60% C_3S (Neville, 2011). The hydration reaction of C_3S is exothermic and can be expressed by stoichiometric Equation 2.1 (Kim, 2010).

$$2C_3S + 11H \rightarrow C_3S_2H_8(C\text{-}S\text{-}H) + 3CH \text{ (Calcium Hydroxide)} \quad \text{.....(2.1)}$$

$$2C_2S + 9H \rightarrow C_3S_2H_8(C\text{-}S\text{-}H) + CH \text{ (Calcium Hydroxide)} \quad \text{.....(2.2)}$$

Di-calcium-silicate (C_2S) or belite is another important component of cement clinker. The PC clinker may contain about 12–30% C_2S (Neville, 2011). Like C_3S, the hydration reaction of C_2S is also exothermic, which can be expressed by the stoichiometric equation as shown in Equation 2.2. The principal hydration product alite and belite is calcium silicate hydrate (C-S-H) and calcium hydroxide.

The PC clinker may contain 3–14% tri-calcium-aluminate (C_3A) or aluminate. Even if the amount of tri-calcium aluminate (C_3A) occurred in cement is small, the relationship of this

constitute with other compounds should have to be a point of interest. The reaction of this compound at pure state is very volatile and will result a flash set. Since C_3A reacts with water immediately, in order to avoid flash setting, gypsum is added (Neville, 2011). The hydration products of C_3A are commonly formed of ettringite in the first stage (Equation 2.3) and mono-sulfo-aluminate later as shown on Equation 2.4 (Kim, 2010). Tri-calcium aluminate (C_3A) contributes little to the strength of cement paste.

$$2C_3A + 3CSH_2 + 26H \rightarrow C_6AS_3H_{32}\,(ettringite) \quad \text{.....(2.3)}$$

$$C_3A + C_6AS_3H_{32} + 4H \rightarrow 3C_4ASH_{12}\,(mono\text{-}sulfo\text{-}alu\min ate) \quad \text{.....(2.4)}$$

Researches show that, the hydration of C_3A is retarded by the presence of $Ca(OH)_2$, which is liberated from the hydration of C_3S. The phenomenon occurs because $Ca(OH)_2$ will form a proactive layer on the surface of un-hydrated grains of C_3A. The main purpose of C_3A addition on the cement is in facilitating the burning process of cement clinkers by using it as a heat flux. (Neville, 2011)

Tetra-calcium-alumino-ferrite (C_4AF) or ferrite is a ternary phase (three component system) occurring in cement clinker, resulting from the solid solution of calcium aluminate and calcium ferrite (C_2A-C_2F). The PC clinker may contain around 7%–16% C_4AF. The hydration of tetra-calcium alumino-ferrite (C_4AF) is slower and involve less heat. Two possible hydrates can form depending on the availability of gypsum (Equations 2.5 & 2.6). (Kim, 2010)

$$C_4AF + 3CSH_2 + 21H \rightarrow C_6(A,F)S_3H_{32} + (F,A)H_3 \quad \text{..... ....(2.5)}$$

$$C_4AF + C_6(A,F)S_3H_{32} + 7H \rightarrow 3C_4(A,F)SH_{12} + (F,A)H_3 \quad \text{.....(2.6)}$$

The amount of gypsum added in concrete should have to be at the optimum level. Further increment in gypsum content will leads expansion of concrete and consequent disruption on the setting of cement paste. (Portland cement Association, 1997; Lagundžija and Thiam, 2017)

2.1.2 Hydration of Cement with Supplementary Admixtures

In addition to the former hydration process, the presence of admixture causes different types of chemical reaction. Especially the addition of pozzolana material in cement have a great interaction with calcium hydroxide $Ca(OH)_2$. Calcium hydroxide is formed as tri and di-calcium silicates react with water. The presence of calcium hydroxide as by-product enables secondary hydration by adding pozzolana to the system.

$$SiO_2 \ / \ Al2O_3 + Ca \ (OH)_2 \rightarrow C\text{-}S\text{-}H \ldots \ldots \quad (2.7)$$

As shown in Equation 2.7, additional C-S-H gel can be formed by adding reactive admixture on the formal cement hydration. (Siddique et al., 2011; Kim, 2010; Perumal et al., 2016)

2.1.3 Factors That Influence Cement Hydration and Heat Evolution

The rate and amount of heat liberated during hydration greatly depends on cement type, chemical composition, physical properties of cement, water/cement ratio, the presence of supplementary cementitious material, and curing conditions.

2.1.3.1 Chemical Composition of Cement

The hydration heat of each cement compound is different. The total heat of hydration that compounds possess after complete hydration according to Bogue (1929) is summarized in Table 2.1.

Table 2.1 Heat Evolution of Compounds (Bogue, 1929)

Compound	Heat Evolution after Complete Hydration(J/g) Bogue(1947)	Rate of Reaction with Water
C_3S	500	"Medium"
C_2S	260	"Slow"
C_3A	866	"Fast"
C_4AF	420	"Medium"

Order of hydration rate during the first few days is approximately $C_3A > C_3S > C_4AF > C_2S$. (Bogue, 1929; Kim, 2010)

2.1.3.2 Type of Cement

The amount of heat generated by each class of cement varies according to the proportion of its respective compounds, as each has different heat of hydration. Figure 2.1 shows the heat generation rates for different types of cement under adiabatic conditions.

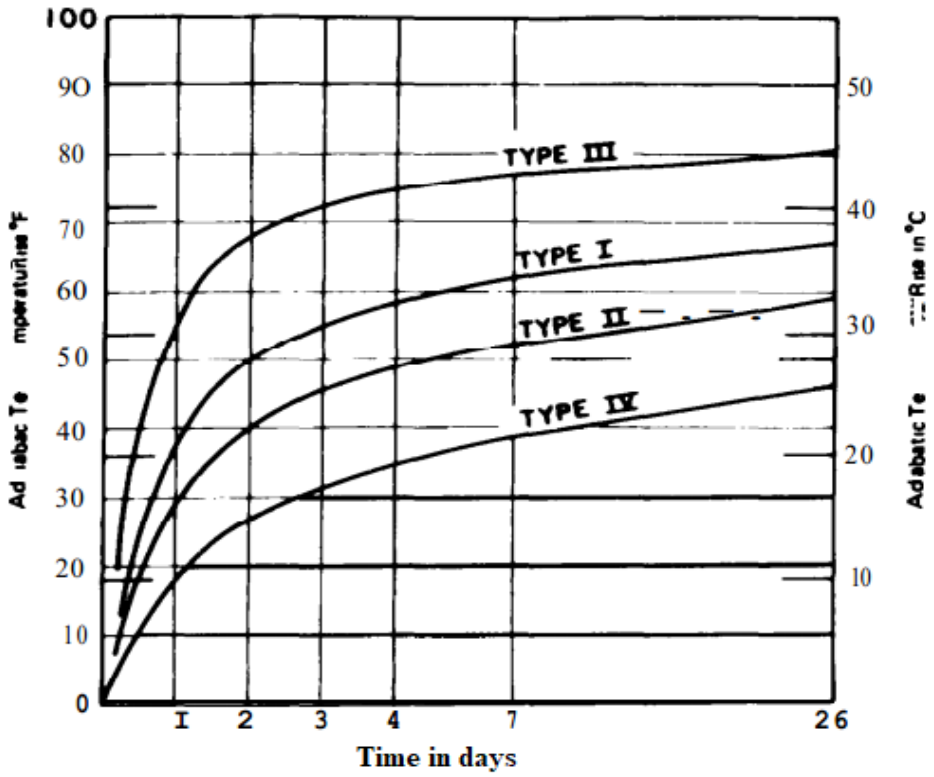

Figure 2.1 Temperature Rise for Mass Concrete Under Adiabatic Condition of Different Cement Type, (Containing 223kg/m^3 of Cement) (ACI 207, 1995).

2.1.3.3 Fineness

Fineness represents the material available for making contact with water so that it hydrates. Higher fineness provides a greater surface area to be wetted, which results in acceleration of the reaction between cement and water. This increases the rate of heat liberation at early ages, but may not influence the total amount of heat developed over several weeks (Portland cement Association, 1997). Wang, (2014) had studied the effect of Blaine fineness in the heat generation of cement hydration. The research shows that heat generation from hydration of coarser cement during early age was lower because of slower cement hydration.

2.1.3.4 Water/Cement Ratio

According to Kim (2010) for full hydration, the range of water to cement ratio should be 0.4-0.42. Since the hydration is the major source of heat, it will upsurge for an increase in water to cement ratio (Portland cement Association, 1997). According to Wang et al. (2014), the heat of hydration at early age is higher for lower water to cement ratio.

2.1.3.5 Casting and Ambient Temperature

The environmental temperature is also important in determining the heat of hydration. Cement hydration at higher environmental temperature is accelerated at early ages but decelerated later on (Kim, 2010). Since seasonal change becomes significant, it should be considered on mass concrete structures, which is constructed for a long period of time.

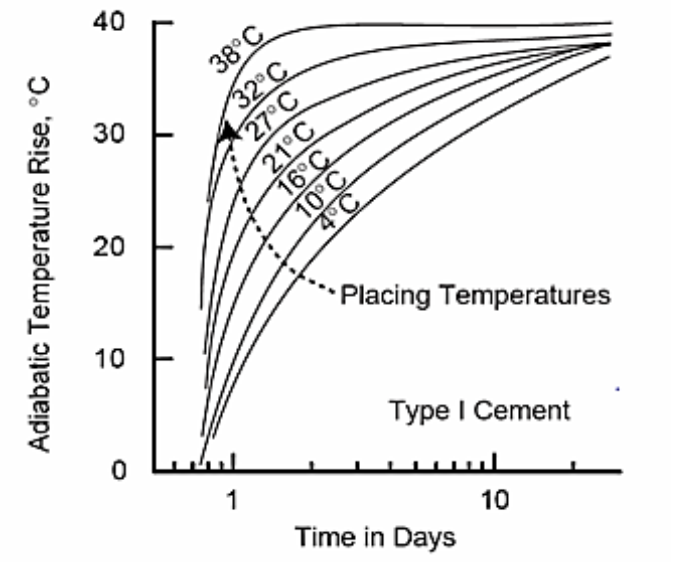

Figure 2.2 The Effect of Placing Temperature on Adiabatic Temperature Rise (ACI 207, 1995)

2.1.3.6 Supplemental Cementitious Materials (SCMs)

SCMs has been widely used as partial replacements for Portland cement. The proper use of pozzolana has advantages in reduction of a heat of hydration. The pozzolana reaction generates less heat than ordinary Portland cement because the reaction is similar to a C_2S reaction. Various studies have shown that partial replacement of cement by Fly ash, GGBF Slag and Bagasse ash will significantly decrease hydration heat. (Geremew, 2017; Meadows, 2007; Parham and Chini, 2005)

2.2 MASS CONCRETE AND THERMAL CRACKING

2.2.1 Definition of Mass-Concrete

According to ACI 207, Mass concrete is defined as "any volume of concrete with dimensions large enough to require that measures be taken to cope with generation of heat from hydration of the cement and attendant volume change, to minimize cracking". The

other precaution for mass concrete should be taken even for a thinner section, if higher heat generating concrete mixing, higher cementitious materials content or faster hydrating mixtures is used. (NRMCA, 2009)

According to Ulm and Coussy (2001), the definition of Mass-concrete is given by hydration-heat diffusion length: the gauge length that relates thermal diffusivity and characteristics hydration time which varies with the degree of hydration and temperature. Structural concrete is then defined as Mass-concrete when the maximum distance of any point in the concrete to its nearest free surface is greater than the hydration heat diffusion length.

2.2.2 Thermal Cracking

Cracking in concrete structures are two types. Crack induced due to an external load, that are included in the conventional structural design calculation, and material type resulted by temperature differential or restrained condition. Early age concrete cracking is caused by restrained volume changes (i.e. autogenous shrinkage and thermal dilation) in hardening concrete structures and it is serious threat to aesthetics, tightness, and durability. (Klemczak & Knoppik-Wróbel, 2011)

During the hydration of cement, heat is generated. In thin concrete sections, the generated heat dissipates to the atmosphere relatively quickly in a way the temperature of concrete is not greatly influenced. On contrast, the temperature in thicker sections will not be lost easily, rather it will accumulate on the interior part while the temperature at the outer edges remains relatively low. The uneven temperature distribution throughout the concrete element is known a thermal gradient. It results in non-uniform volume change across the element's cross-section, thereby inducing stresses to cause thermal cracks. (Lagundžija et al., 2017; Bobko et al., 2013; ACI 207, 1995)

2.2.3 Mitigation Strategies of Thermal Cracking

2.2.3.1 Thermal Reducing Binders

Low-heat generating concrete mixtures are always a wise choice for mass concrete to minimize potential thermal problems. Low-heat binders such as class F fly ash or slag as cement replacements, and the minimum amount of total cementitious materials can greatly

reduce the temperature evolution when there is a thermal cracking risk. (Thomas, 1994. Belie et al, 2018)

2.2.3.2 Pre Cooling of Concrete

The concrete temperature at the time of placement has a great impact on the maximum heat on concrete. Methods to precool concrete include shading and sprinkling of aggregate piles, use of chilled mix water, and replacement of mix water by ice. Efforts to cool aggregates have the most pronounced effects on the concrete heat evolution because they represent 70 to 85% of the weight of concrete. (ACI 207, 1995; Lagundžija & Thiam, 2017)

2.2.3.3 Post Cooling of Concrete

Post-cooling is most effectively achieved by using embedded cooling pipes that circulate cool liquid through the concrete. The goal of this method is to lower the maximum temperature reached within the concrete and to increase its cooling period (Gajda and Vangeem, 2002). If used correctly, post cooling can be beneficial in allowing earlier removal of formwork and reducing the amount of time needed for cooling. (Bobko et al., 2013)

Figure 2.3 Embedded Cooling Pipes (http://www.newwrighthouse.blogspot.com)

2.2.3.4 Adopting Insulation

Insulation or insulated formwork is often used to warm the concrete surface and reduce the temperature gradient, which in turn minimizes the potential for thermal cracking. Once the temperature difference of the internal and external surface of the concrete is not exceeded 20^0, thermal cracks will be insignificant (ACI 207, 1995). For most mass pours, surface insulation does not appreciably increase the maximum concrete temperature, but

it can significantly decrease the rate of cooling. Insulation often has to remain in place for several weeks or longer. Removing it too soon can cause the surface to cool quickly so that crack appears. (Bobko et al., 2013)

2.3 BAGASSE ASH AND PERVIOUS STUDY

2.3.1 Bagasse Ash

Sugarcane is an important food crop for tropics and subtropics. It is the major raw material used for sugar production. After crushing of sugarcane in sugar mills and extraction of juice from prepared cane by milling, the discarded fibrous residual matter of cane is called bagasse. Bagasse is very commonly used as fuel in boilers in the sugar mills for cogeneration process. After burning in the cogeneration boiler, bagasse ash is collected in a baghouse filter and is disposed locally, which causes severe environmental problems. (Raja, 2014; De Belie et al, 2018).

For every ten tons of sugarcane crushed, a sugar factory produces nearly three tons wet bagasse ash. The combustion yields ashes containing high amounts of unburned matter like silica and alumina oxides. Studies recommend that sugarcane bagasse ash could be used as cement replacement material to improve quality and reduce the cost of concrete. (Srivastava et al., 2015; Mahmud et al., 2018)

Figure 2.4 Sugarcane, Sugarcane Bagasse, and Bagasse Ash Respectively

2.3.2 Abundance of Bagasse Ash in Ethiopia

In recent years, the government of Ethiopia (GOE) has made considerable investments for boosting the country's capacity to produce sugar. With these investments, the GOE envisions the country becoming one of the world's ten largest sugar producers by 2023 (USDA Foreign Agricultural Service, 2015). Collaborating existing industries with the

future ones, the total bagasse ash to be disposed is estimated to be 1.9 million tons per year. (Geremew, 2017)

Figure 2.5 Bagasse Deposit at Metehara Sugar Factory

2.3.3 Previous Works on Bagasse Ash Concrete

Geremew (2017) studied the appliance of bagasse ash in rigid pavements. In addition to the mechanical properties testing, the heat evolution of a concrete specimens containing SCBA was measured. As it is shown in study, bagasse ash attenuates the total heat of hydration and enhanced the mechanical properties of concrete specimens. Srivastava et al. (2015) carried out experimental studies with different cement to bagasse replacement ratios for examining the mechanical properties of concrete. Low weight concrete with good mechanical properties can be assured with 10% replacement level. Furthermore, tolerating slight reduction in strength of concrete, bagasse can replace the cement up to 20%.

Reddy et al. (2013) utilizes bagasse ash for enhancing the chloride and corrosion resistance of concrete. Cement has been replaced by equivalent weight of bagasse ash. Meanwhile, gypsum was used to ensure workability of a mortal. Fifteen percent of replacement level is found to be the optimum. Reddy et al. (2013) had also studied the heat liberation of mixture contain bagasse ash and found that, hydration heat of concrete specimens was reduced.

According to Suliman et al., (2011), bagasse acts as a class F fly ash. The chemical composition result shows that silica-di-oxide content varies from 56.7-58.02%. On the

other hand, bagasse is a nonvolatile, incombustible, and thermally altered mineral. Sathiya et al. (2010) had also examined that, three-oxide component (SiO_2, Al_2O_3, Fe_2O_3) found in bagasse ash were account more than 75% of the total mineral content. Moreover, the loss of ignition was within the limit as it is prescribed in the ASTM C 618-00 manual.

Hailu (2012) used Wonji sugar cane factory bagasse ash for inspecting the development mechanical property of concrete containing SCBA. Volume-based replacement method was used in order to ensure the workability of the mortal and create a fixed paste volume for all replacement ratio.

2.3.4 Chemical Composition of Bagasse Ash

Taking in to account chemical composition (Percentage of oxides), alkaline and loss of ignition (LOI), bagasse has been classified in either class C or F fly ash (Belie et al., 2018). One of the major factor for utilization of bagasse is the amount LOI; the non-mineral material should have not exceeded the limit proposed by standards. The unburned carbon particles in SCBA are usually the largest contributor to the loss of ignition. (Abdulkadir et al., 2014)

CHAPTER 3 MATERIAL AND METHODS

3.1 MATERIAL

Physical and chemical characterization of construction materials conducted according to ACI and ASTM standards at AAiT material laboratory. The particular details are presented on the following sections.

3.1.1 Aggregate

Aggregate is a comprehensive term, which includes fine and coarse aggregate. At least three-quarter of concrete is occupied by aggregate; it is not surprising that its quality is of considerable importance. (Neville, 2011)

3.1.1.1 Fine Aggregate

Fine aggregate generally consists of natural sand or crushed stone with most particle smaller than 5mm (0.2in). The fine aggregate was collected from Legehar commercial construction material site. The sand was properly washed and packed in plastic bag for controlling its moisture content. The physical property of sand is summarized in Table 3.1& 3.2.

Table 3.1 Summary Physical Property of Fine Aggregate

No.	Property	Standard	Value
1	Silt Content	Dinku. A	3.4%
2	Fineness Modules	ASTM C 136-84	2.61
3	Moisture Content	ASTM C 566- 84	1.62%
4	Dry Rodded Unit Weight	ASTM C 29 – 97	1524.39kg/m3
5	Bulk Specific Gravity	ASTM C 127 – 88	2.41
6	Absorption Capacity	ASTM C 127 – 88	2.74

Table 3.2 Gradation of Fine Aggregate

Sieve Size	Weight Retained (g.)	Percent Retained (%)	Cumulative Retained (%)	Cumulative Passing (%)
4.75mm	0	0	0	100
2.36mm	30	6	6	94
1.18mm	75	15	21	79
0.6mm	130	26	47	63
0.3mm	210	42	89	11
0.15mm	45	9	98	2
Pan	10	2	100	0

According to ASTM C-33-01, the upper and lower bound of percentage cumulative passing for fine aggregate in each sieve size is specified. The local fine aggregate satisfies ASTM C-33-01 requirement. `

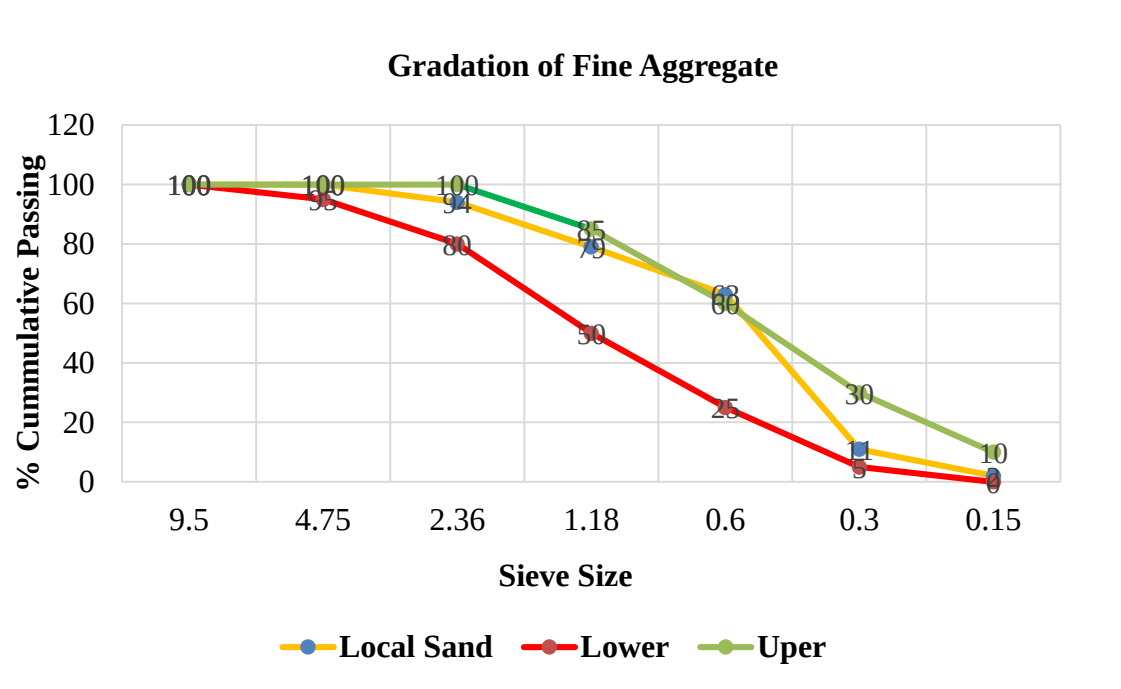

Figure 3.1 Gradation of Local Fine Aggregate and ASTM C-33-01 Requirement

3.1.1.2 Coarse Aggregate

Crushed rock was used as a coarse aggregate for this study. Table 3.3 & 3.4 show the physical properties of coarse aggregate.

Table 3.3 Summary Physical Property of the Coarse Aggregate

No.	Test Description		Standard	Value
1	Nominal Aggregate Size		ASTM D 448 – 98	25mm
2	Moisture Content		ASTM C-566- 84	0.81%
3	Bulk Unit. Wt.		C 29/C 29M – 97	1641.79kg/m^3
4	Dry Rodded unit wt.		C 29/C 29M – 97	1598.65kg/m^3
5	Absorption Capacity		ASTM C 127 – 88	1.52%
6	Specific Gravity	Bulk	ASTM C 127 – 88	2.75
		Bulk(SSD)		2.80%
		Apparent		2.88

Table 3.4 Gradation of the Coarse Aggregate

Sieve Size(mm)	Weight Retained (kg)	Percent Retained (%)	Cumulative Retained (%)	Cumulative Passing (%)
37.5	0	0	0	100
25	5.01	34.26	34.26	65.74
19	3.66	24.4	58.66	41.34
12.5	3.51	23.4	82.06	17.94
9	1.315	8.76	90.82	9.18
4.75	1.285	8.56	99.38	0.62
Pan	0.09	0.62	100	0

Figure 3.2 shows the local coarse aggregate gradation in adjacent the upper and lower boundaries according to ASTM-33-01.

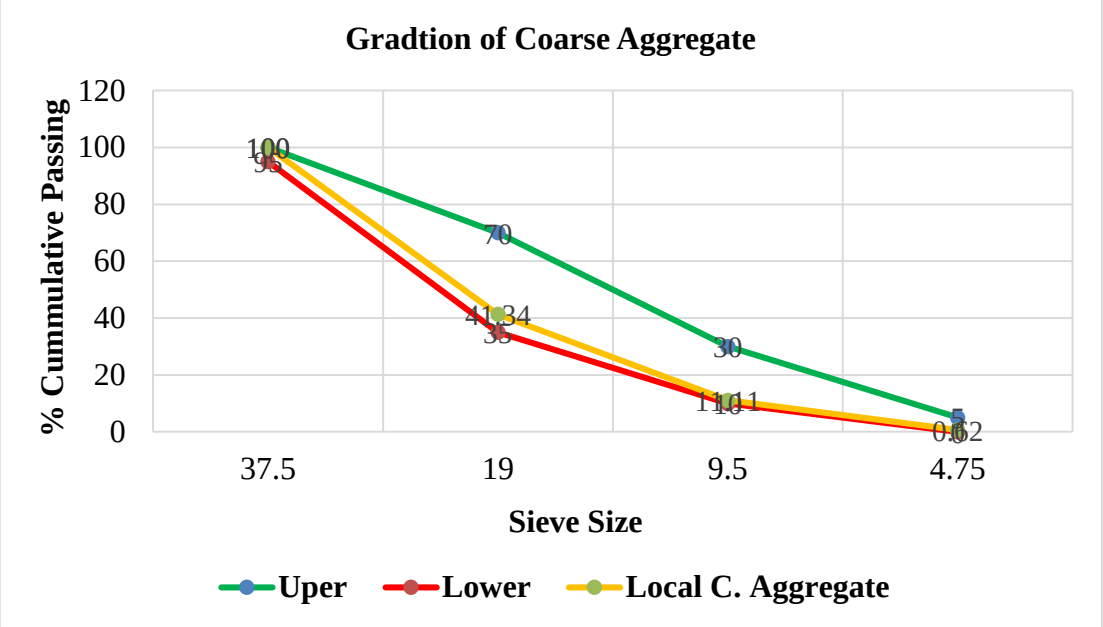

Figure 3.2 The Gradation of Local Coarse Aggregate and ASTM C-33-01 Requirement

3.1.2 Cement

The cement material used was Type-1 Portland cement (42.5-N) from Dangote cement factory. The chemical and physical properties of the cement were examined and reported simultaneously with bagasse ash data.

3.1.3 Bagasse Ash

3.1.3.1 Physical Properties

The bagasse ash was collected from Wonji sugar factory byproduct dumping area. After bagasse ash was left to dry for certain amount of time, it was filtered using a 300-µm sieve for removing the unburned carbon particles.

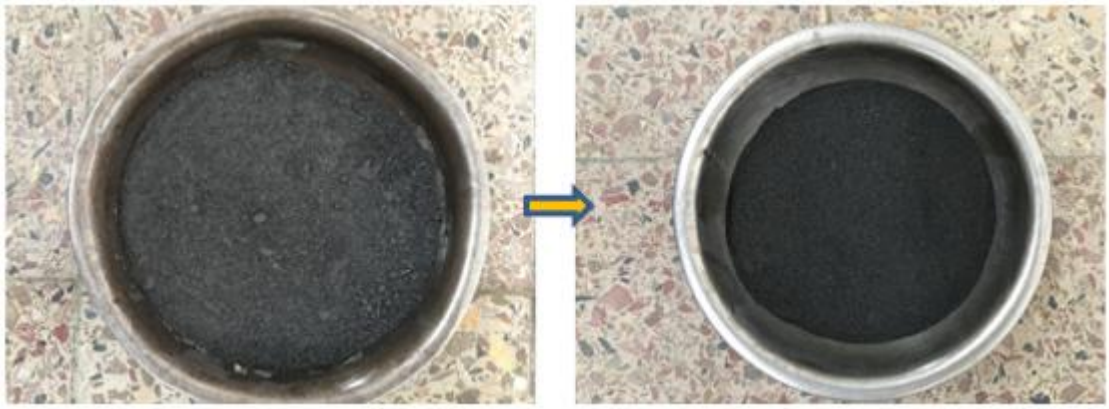

Figure 3.3 Bagasse Ash before and after Sieving

Gradation: pozzolana assets might be dependent on the fineness of bagasse ash. As long as the bagasse ash composition is fine and free from unburned carbon particles, it could ensure the early age mechanical properties of the concrete.

Table 3.5 Gradation of Bagasse Ash and Cement

Sieve Size	Wt. of B.A Retained (g.)	Percent Retained (%)	Cumulative Retained (%)	Cumulative Passing (%)	Cumulative Passing of Cement (%)
150 µm	45	9.09	9.09	92.91	100
125 µm	50	10.11	19.2	80.8	97.9
75 µm	180	36.36	55.96	44.44	95.5
63 µm	65	13.13	68.69	31.31	85.8
32 µm	145	29.29	97.98	2.02	4.7
Pan	10	2.02	100	0	0

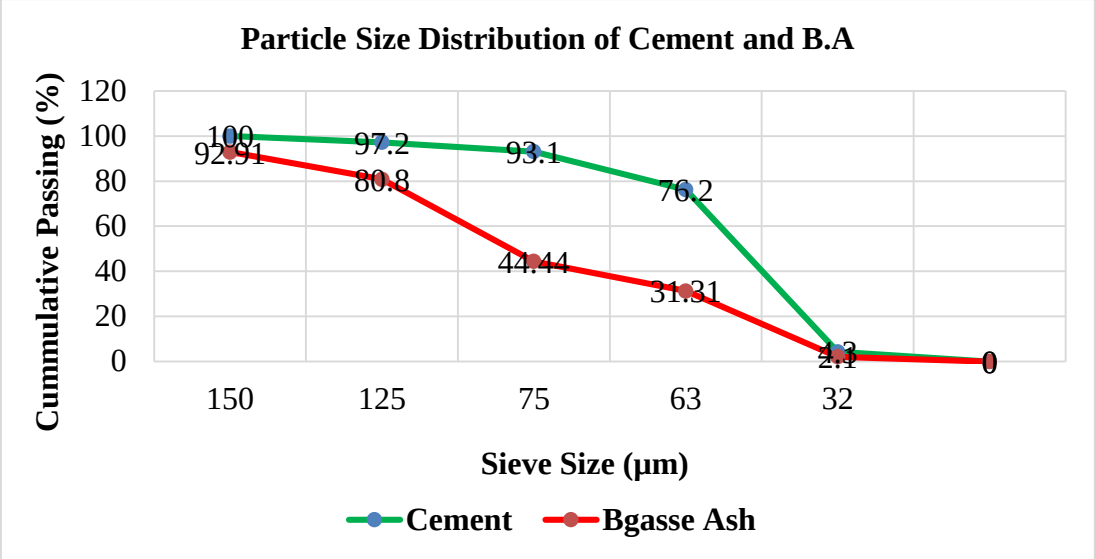

Figure 3.4 Particle Size Distribution of Cement and Bagasse Ash

Specific Gravity: The specific gravity of cement and bagasse ash was examined according to ASTM C188–17 standard procedures were found to be 3.15 and 2.14 respectively. The weight of bagasse ash used for volume-based replacement relays on its specific gravity.

Specific Surface Area (**Blaine Air-Permeability Test):** The specific area of the bagasse ash is determined according to ASTM 2 204-00 using Blaine air permeability apparatus. The specific area of bagasse ash is found to be 3177.3 cm^2/g.

3.1.3.2 Chemical Properties

X-Ray Diffraction: XRD is a technique used to determine the mineral properties of a crystalline solid. When a solid is exposed to X-Rays of a particular wavelength, layers of atoms diffract and produce a pattern of peaks, which characterize the minerals present in the material (Cullity, 1977).

Silica is the major mineral in pozzolana materials. The silica in amorphous phase is known to be more reactive than in crystalline form (Siddique Rafat and Khan Mohammed Iqbal. 2011). Quartz, Cristobalite, and Glass are all different phases of Silica. Amorphous materials like glass, do not produce sharp diffraction peaks (Cullity, 1977). As shown in the Figure 3.6, the X-Ray is scattered in many directions leading a large bump distributed in a wide range (02 Theta) instead of high intensity narrower peaks.

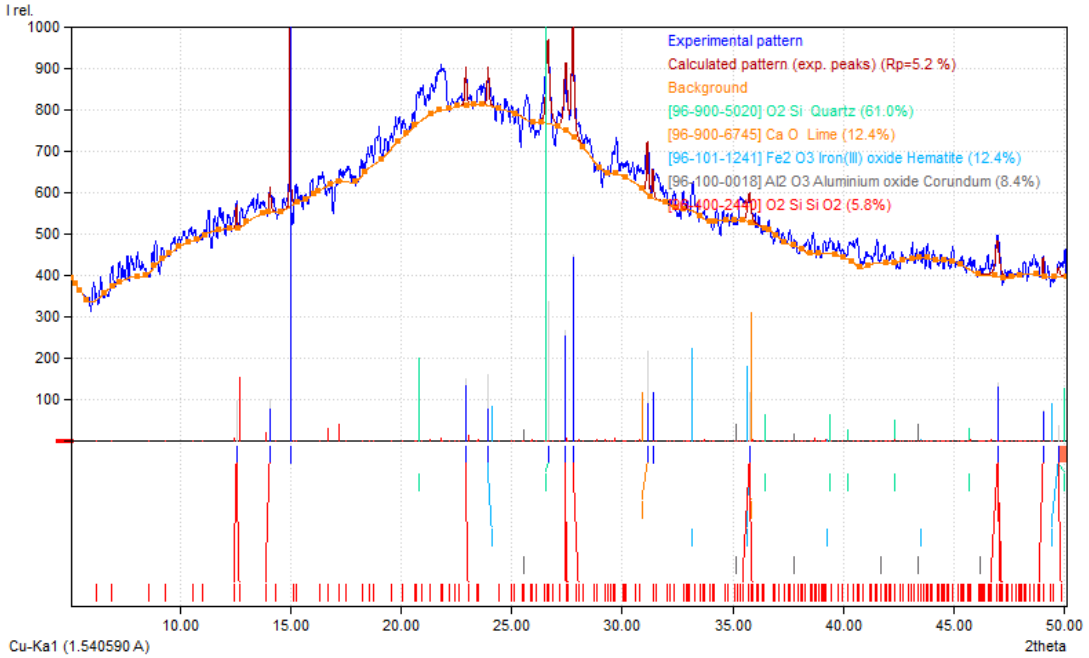

Figure 3.5 X-Ray Diffraction Result of Local Bagasse Ash

The percentage of compounds are quantified using match software (See figure 3.5). However, the results are not necessarily compatible with complete silica analysis and requires XRD professionals for a more accurate analysis.

Complete Silica Analysis: The chemical property of bagasse ash and cement had been examined at Ethiopian Geological and Survey. The experiment result is reported in Table 3.6.

Table 3.6 Chemical Property of Cement and Bagasse Ash

Compounds	Bagasse Ash (%)	Cement (%)
SiO_2	68.6	26.62
Al_2O_3	9.04	6.08
Fe_2O_3	5.24	4.82
CaO	1.52	55.30
MgO	1.36	1.1
Na_2O	1.84	0.2
K_2O	2.44	0.16
MnO	0.12	0.01
P_2O_5	0.51	0.08
TiO_2	0.13	0.24
H_2O	1.8	0.51
LOI	7.91 < 10	3.43
SiO_2+ Al_2O_3+Fe_2O_3	83.18 > 75	-

The local bagasse ash satisfies the criteria specified in ASTM-C 618-00 (standard specification for coal fly ash and raw or calcined natural pozzolana for use as a mineral admixture in concrete). This local pozzolana possesses higher silica content and it can be characterized under Class-F pozzolana materials: indeed, it would insure secondary hydration activity.

3.1.4 Water

Mixing water must not contain substances that cause degradation in quality like strength development, loss of workability, or steel corrosion in harmful quantities. The water used is from AAiT water supply pipe. Odor, Color, unusual tests were checked.

3.2 METHODS

The methods applied in order to achieve the objectives are elaborated in this section. It includes mixture design, test setups for both mechanical property and thermal experimental programs.

3.2.1 Mixture Design

The mixture design is accomplished using ACI 211.1-91 standard procedure. Specified compressive strength of 25 MPa. (Required average compressive strength, 33 MPa.) was pre-assigned for the control group. The quantity of each ingredient for the control group is summarized in Table 3.7.

Table 3.7 Quantity of Material Required Per Metric Cube of Concrete

No.	Material	Weight of material (kg/m3)
1	Water	190
2	Cement	334.51
3	Coarse aggregate	1046.52
`4	Fine aggregate	763.03

Using the above mixture proportion, a trial strength check had been carried out and confirmed the prescribed strength. In case of partial replacement of cement using bagasse ash, volume-based replacement method was adopted. Volume based replacement is

preferred in order to produce equal paste volume, that ensures justified comparison within all mixes. According to ACI 211.1-91 while using pozzolana material, Equation 3.1 can be used for determining the weight of pozzolana material as a function of the volume of replacement.

$$F_w = \frac{1}{1+\left(3.15/G_p\right)\left(\frac{1}{F_v}-1\right)} \quad \text{.....[Eq 3.1]}$$

Where: F_w = Weight of pozzolana

G_p = Specific gravity of pozzolana

F_v = Percentage volume replacement level

Table 3.8 Quantity of Bagasse Ash for Each Replacement Level

Mixture Id.	Replacement Level (%)	Weight of Bagasse ash (kg/m^3)	Weight of Cement (kg/m^3)	Water/Binder (Adjusted) By Weight	Water/Binder (Adjusted) By Volume
BA-0	0	0	334.5	0.568	0.559
BA-6.5	6.5	15.08	312.76	0.579	0.560
BA-13	13	30.82	291.02	0.591	0.562
BA-20	20	48.36	267.6	0.601	0.566

Where: - BA-0 = Control group with 100% OPC

BA-6.5 = Mixture with 6.5 % of bagasse ash and 93.5% OPC

BA-13 = Mixture with 13 % of bagasse ash and 87% OPC

BA- 20 = Mixture with 20 % of bagasse ash and 80% OPC

Since the weight of total binder decrease as an increase in bagasse ash replacement level, the water to binder ratio (in weight basis) will increase in some extent as shown in Table 3.8.

3.2.2 Mixing, Vibrating, and Curing Condition

Pemat mixer has been used for mixing as specified in ASTM C-192. After all ingredients were mixed for 3 min; it was left to rest for 3 min followed by 2 min final mixing. Mixing

machine was lubricated with water in order to prevent it from absorbing mixing water. The slump of each freshly mixed concrete is measured according to ASTM C-143.

Figure 3.6 Measuring Slump of Fresh Concrete

Placing of concrete into the mold is done according to ASTM C-192 specification using scoop, and shovel. The molds were half filled, vibrated, and then filled to top level before they vibrated again. In order to ensure a proper consolidation external vibrator is used. After the molds were fully filled, it has been kept in a rigid surface that is free from any vibration and disturbance. The specimens were removed from the mold at a time of 24 ± 8 hours, and has been kept in water container for providing a consistent curing condition. The specimens were removed from the water tank and placed at room temperature prior to testing.

(a) (b)

Figure 3.7 (a) Mixing Machine (b) Curing Condition

3.2.3 Test Setup and Procedure

3.2.3.1 Mechanical properties

Advanced testing methods combined with accurate analysis techniques is required for solid understanding of material property of young concrete. ASTM manual is adopted for clarifying the test setups and procedures.

Compressive Strength: Provides a general indication of concrete quality. Compressive strength was determined using 15*15*15cm^3 cubical concrete cores at the laboratory. This test method consists of applying a compressive axial load at loading rate from 0.15-0.3Mpa/sec to specimen until failure occurs (ASTM C-39). The compressive strength of the specimen can be calculated by dividing the load attained during the test by the cross-sectional area of the specimen. The universal compression testing machine used in this study is capable of determining both the failure load and stress.

Figure 3.8 Compressive Strength Test Setup

Tensile Strength: Tensile strength of concrete can be conducted using direct uniaxial and indirect methods such as flexural and splitting strength experiments. The direct tensile strength test is a good approach for determining concrete uniaxial tensile capacity. The drawback of this method is that, precise test set up is needed in order to avoid uncertainties.

Splitting tensile strength test was used for this research. This method consists of applying a diametric compressive force along the length of a cylindrical concrete specimen at a rate of 689 to 1380 KPa/min until failure occurs (ASTM C-496-71). The state of stress in the plane of loading is uniform tension perpendicular to this plane (Timoshenko & Goodier 1970). The tensile stress is written in Equation 3.1 (ASTM C-496-71).

$$\sigma = \frac{2*P}{\pi DL} \quad \text{.....(3.1)}$$

Where : P = Applied load at failure

D= Diameter of cylinder

L= Length of cylinder

Flexural Strength: A third-point load experiment has been adopted for determining the flexural capacity as specified in ASTM C 78–00.

Figure 3.9 Flexural Strength Test Setup

The flexural strength of concrete using third-point load test can be calculated using Equation 3.2 (ASTM C 78–00).

$$\sigma = \frac{FL}{WD^2} \quad \text{.....(3.2)}$$

Where: F= Failure load

L= Length of specimen

W= Width of specimen

D= Avarage depth of specimen

3.2.3.2 Thermal Property

The heat of hydration has been determined by a semi-adiabatic temperature rise experiment. The semi adiabatic temperature rise experiment is carried out because it had a similar property with adiabatic temperature rise owing small loss of heat with time. Therefore, the heat compensation method for estimating the adiabatic temperature rise using semi adiabatic tests is required. The heat compensation method can be implemented by considering flat curve at the point where temperature rise is maximum.

Molds made from plywood with a dimension of 30cm width, 30cm length and 40cm height are used for pouring the concrete in. The plywood is insulated using 10cm thickness Styrofoam to prevent the heat from escaping.

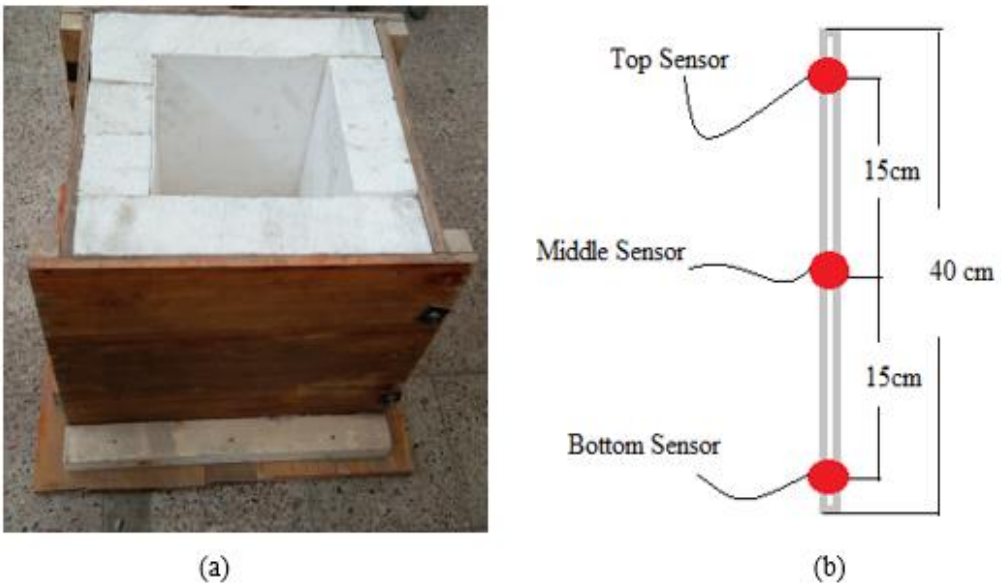

Figure 3.10 (a) Insulated Plywood Mold (b) Location of Sensors Throughout Depth

The upper part of the concrete mold is left open to simulate effect of ambient temperature. The temperature sensor has been embedded in the concrete at three places, top, center and bottom part as shown in Figure 3.11. Temperature is measured for each 30-minutes interval using thermocouples until the maximum heat is perceived. The temperature reading took six days, including night sessions. For three different ambient temperatures and four different replacement ratios, twelve specimens were cast.

Figure 3.11 Demolding and Demolishing Concrete Samples for Reusing Thermocouples

3.2.3.3 Temperature Chamber

In order to simulate the effect of ambient temperature on the heat evolution of the concrete specimens which contain different dosages of bagasse ash, temperature chamber is constructed in the AAiT material laboratory. It was capable of simulating 25^0, 35^0, 45^0 C ambient temperatures.

Layout: The chamber has an internal dimension of 1.2m width, 3m length and 1.28m height. As shown in Figure 3.12, the Chamber was constructed from bricks. The door which serve as an entrance for the specimens is made-up of plywood and insulated by Styrofoam. The chamber is capable of accommodating three concrete samples at a time.

Figure 3.12 Chamber on Progress of Construction

Controlling System: In order to control the room temperature (chamber temperature), computer algorism is developed with the help of Arduino software. LM-35 temperature sensor is used to read the chamber's temperature; so that it will feed continues data to the monitoring device. After the Arduino received the data sent from the temperature sensor, it will translate information and command the relay attached at heaters. The heaters increase and decrease (on and off) the temperature, to produce constant internal ambient temperature.

Figure 3.13 Final Setup of Temperature Chamber with its Full Controlling System

CHAPTER 4 RESULT AND DISCUSSION

This chapter discusses the result obtained as outlined in chapter three. The outcomes gained from the experimental program presented into two major parts: The first section addresses the mechanical strength development of concrete followed by the thermal investigations.

4.1 FRESH CONCRETE PROPERTIES

Optimization of pozzolana in concrete mixture might affect the fresh property of concrete. The average slump value for each replacement level is reported in Table 4.1.

Table 4.1 Average Slump Value for Each Mixture

Mixture Id.	Replacement Level (%)	Water/Binder	Average Slump Value (mm)
BA-0	0	0.567	52
BA-6.5	6.5	0.579	38
BA-13	13	0.591	29
BA-20	20	0.601	17

As indicated in Table 4.1, loss of workability was detected with an increment in level of replacement. The physical and chemical features of bagasse ash could be the cause for this situation. Furthermore, the bagasse ash used in this study have 7.89% of loss of ignition that should be taken in to account for the phenomena.

4.2 HARDENED CONCRETE PROPERTIES

4.2.1 Compressive Strength

To study the early age compressive strength development of concrete, experiments have been carried out at one, two, three, seven and twenty-eight days for 0%, 6.5%, 13% and 20% cement-bagasse ash replacement levels. For each mixture, three specimens were tested and the average results are reported in Table 4.2.

Table 4.2 Average Compressive Strength

Mixture Id.	Average Compressive Strength (Mpa.)				
	Day-1	Day-2	Day-3	Day-7	Day-28
BA-0	8.49	11.9	16.14	23.92	29.19
BA-6.5	8.35	11.26	16.06	23.77	30.20
BA-13	7.7	10.54	15.13	23.38	31.13
BA-20	10.01	11.69	14.39	20.34	28.49

- ***Remark:*** *an additional paste volume has been introduced on mixture "BA-20" for insuring workability so that it is voided from the comparison between mixtures.*

Although reduction in early age compressive strength development was observed, the cement-bagasse ash blends of 6.5 % and 13% replacement level satisfied the strength requirement at late age of testing (See Table 4.2). Higher strength was obtained on concrete specimens containing bagasse ash compared to pure cement concrete (control group).

The pozzolana reaction depends on hydration of cement particles. Bagasse ash is an inert material until it gets base solution from hydration of cement. Therefore, the reason for a drop in compressive strength at early age is that, enough calcium hydroxide (base solution) could not be available for the nonce. As the cement hydration continues, concentration of calcium hydroxide will be critical; Consequently, pozzolanic reaction initiates. Thus, it would not be surprising that pozzolana reaction magnifies at latter ages.

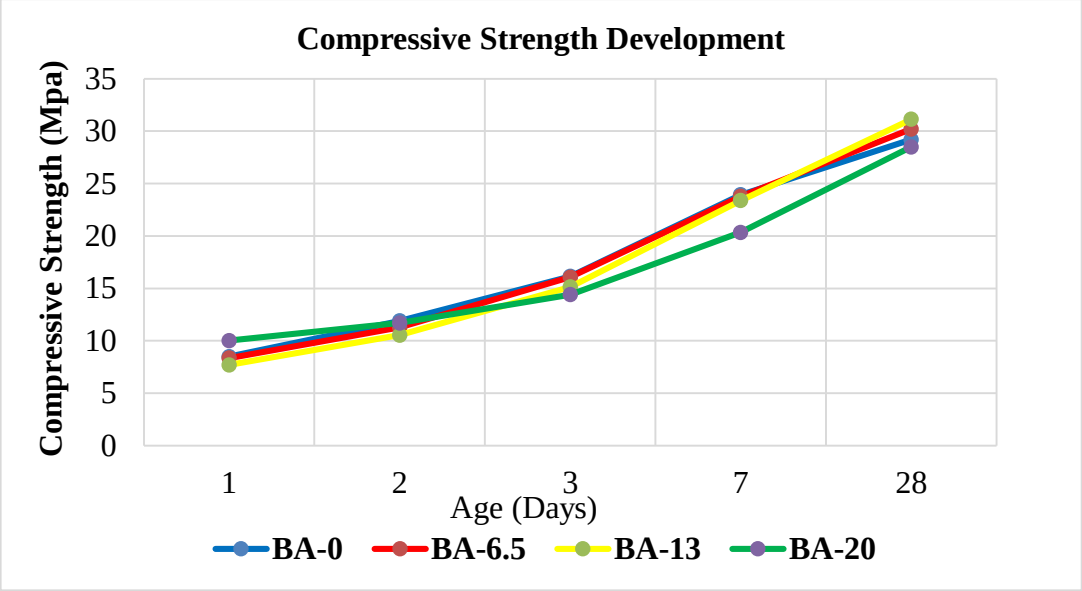

Figure 4.1 Average Compressive Strength Development

The strength gains over time not only resulted due to reaction between pozzolana material and calcium hydroxide but also from the contribution of bagasse ash in facilitating the ordinary hydration process. Neville A.M (2011) states, after cement complexes (E.g. C_3S) reacts with water, calcium hydroxide (byproduct of hydration) will act as a thin film around the remaining cement compounds like C_2S; meanwhile, it will alter left over chemical reactions. The introduced bagasse ash absorbs calcium hydroxide solution from hydration products; Therefore, it will facilitate the ordinary hydration process and ensures ultimate strength development.

As shown in Figure 4.1, early age strength development of concrete containing 20% of sugarcane bagasse ash exceeds other mixtures. Since the first mix was harsh for cast, an additional paste volume was introduced in the concrete mix for ensuring workability. The cement paste added by controlling the water to binder ratio disrupted the early age mechanical property of concrete contains 20% bagasse ash. Full compressive strength result is documented in Appendix A, Table A.1.

4.2.2 Splitting Tensile Strength

The tensile strength is the key property of concrete directly interrelated with early age cracking. Although premature failure considered as drawback of splitting tensile experiment, it has not been noticed throughout this study.

Figure 4.2 (a) Test Set up of Splitting Tensile Strength Test (b) Test Specimen after Failure

The splitting strength testes have been conducted at one, two, three, seven and twenty-eight days. The average splitting tensile strength results are shown in Table 4.3.

Table 4.3 Average Splitting Tensile Strength of Concrete

Mixture Id.	Average Splitting Tensile Strength (Mpa)				
	Day-1	Day-2	Day-3	Day-7	Day-28
BA-0	0.76	1.55	1.86	2.14	2.69
BA-6.5	0.69	1.17	1.73	2.03	2.87
BA-13	0.57	0.88	1.44	1.97	2.92
BA-20	0.41	0.8	1.31	1.55	2.38

Figure 4.3 shows that, the tensile strength also enhances with time. Looking at late age strength development, pozzolanic reactivity induced by replacing cement using 6.5% and 13% of bagasse ash has ensured the desired strength (Control group).

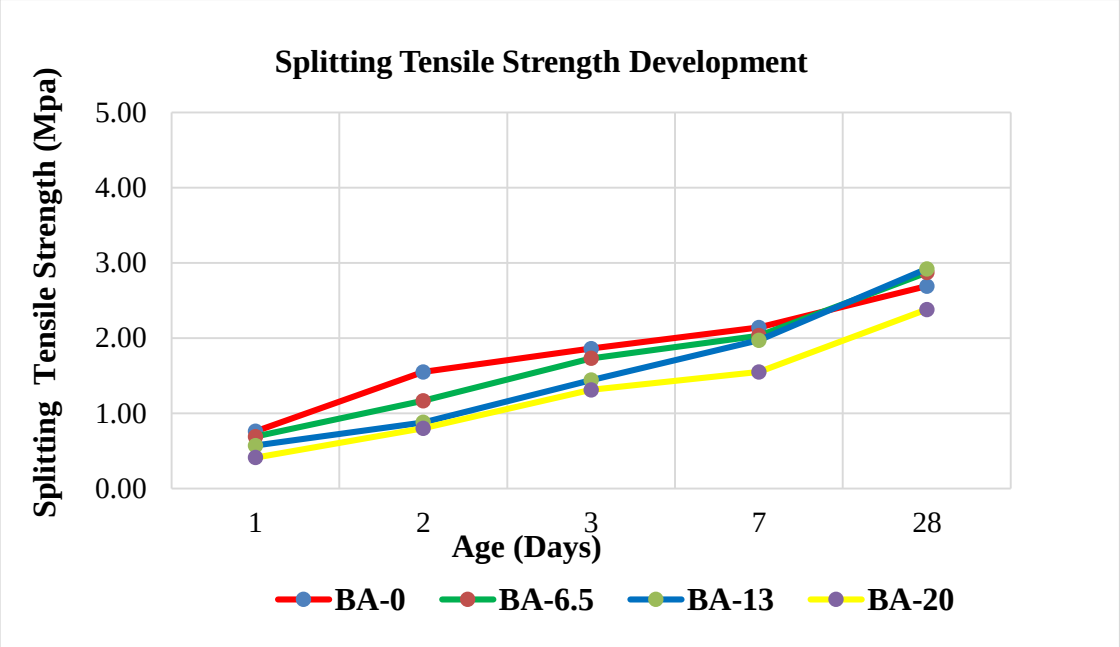

Figure 4.3 Splitting Tensile Strength Development

According to Mehta and Monterio (2006), micro cracking originates in the interfacial transition zone (ITZ) and cracking develops as load is applied. Empty voids could be formed in ITZ while water escapes from large aggregate surface in a form of bleeding. The progress of hydration (C-S-H formation) will eventually fill those empty voids and densify the ITZ. Optimizing bagasse ash in concrete mixture up to 13% replacement level further enhances tensile strength in a way, an additional C-S-H and ettringite will be induced from pozzolanic reaction. Substitution of weak calcium hydroxide layer found in ITZ by a more densified ettringite indeed increases the tensile capacity.

Remarkable early age tensile strength drop is observed on concrete samples containing bagasse ash (See Figure 4.3). According to chemical characterization, the local bagasse ash takes Class-F fly ash property. This pozzolana depends on hydration of cement and do not possesses self-hardening behavior; therefore, it could be major reason for reduction in early age splitting strength.

4.2.3 Flexural Strength

As shown in Table 4.4, flexural strength of concrete contains 6.5% and 13% bagasse ash shows relatively higher value than the control group in late age of testing. On the other

hand, replacing of cement by bagasse ash up to 20% reduces both the early and late age flexural strength development of concrete.

Table 4.4 Average Flexural Strength

Mixture Id.	Average Flexural Strength (Mpa)				
	1 Day	2 Days	3 Days	7 Days	28 Days
BA-0	0.6	1.45	1.68	2.78	4.7
BA-6.5	0.65	1.33	1.58	2.9	5.0
BA-13	0.45	1.25	1.46	2.9	5.55
BA-20	0.38	1	1.35	2.3	3.95

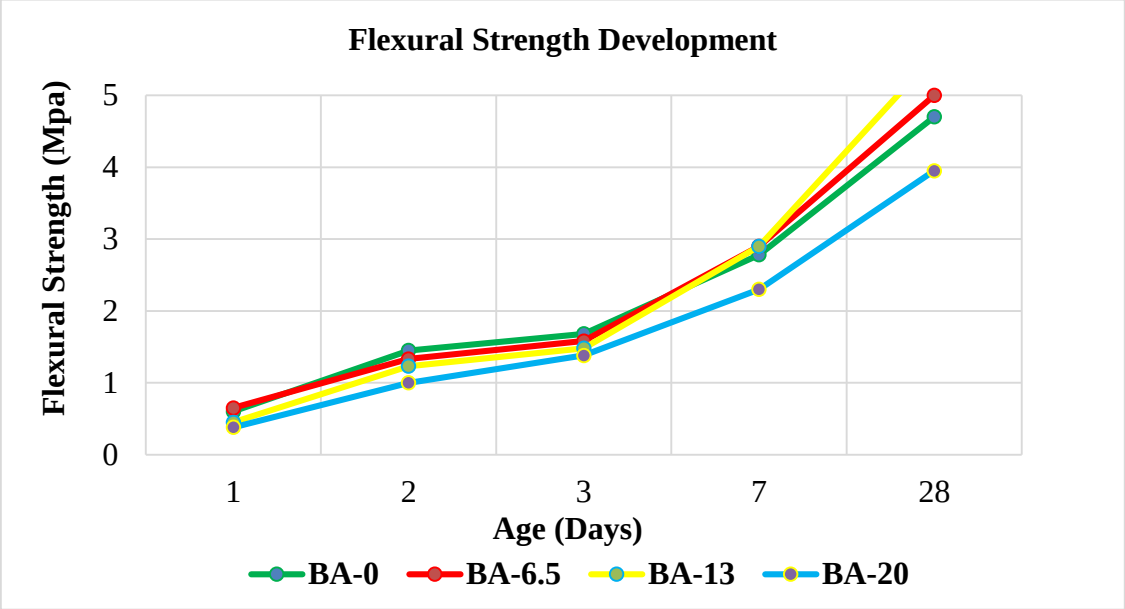

Figure 4.4 Flexural Strength Development

Portlandite (Calcium hydroxide) constitute 20 to 25 percent of the volume of solids in the hydrated paste. The strength-contributing potential of Portlandite is limited as a result of considerably lower surface area (Mehta and Monterio, 2006). The bagasse ash present in the hydrated paste undergoes a chemical reaction with Portlandite to create additional C-S-H and needle-shaped prismatic crystals (ettringite). Both as inert filler and pozzolanic reactivity, bagasse ash in concrete enhanced the quality of cement paste and the micro structure of the transition zone between the binder matrix and the aggregate. (See Table 4.4).

4.3 EARLY AGE THERMAL PROPERTIES

The effect of ambient temperature on hydration heat of concrete containing bagasse ash is studied using temperature chamber. The internal heat evolution of concrete specimens was examined under 25.15º, 35.54º and 43.77º C average ambient temperatures. The ambient temperatures history is shown from Figure 4.5-4.7.

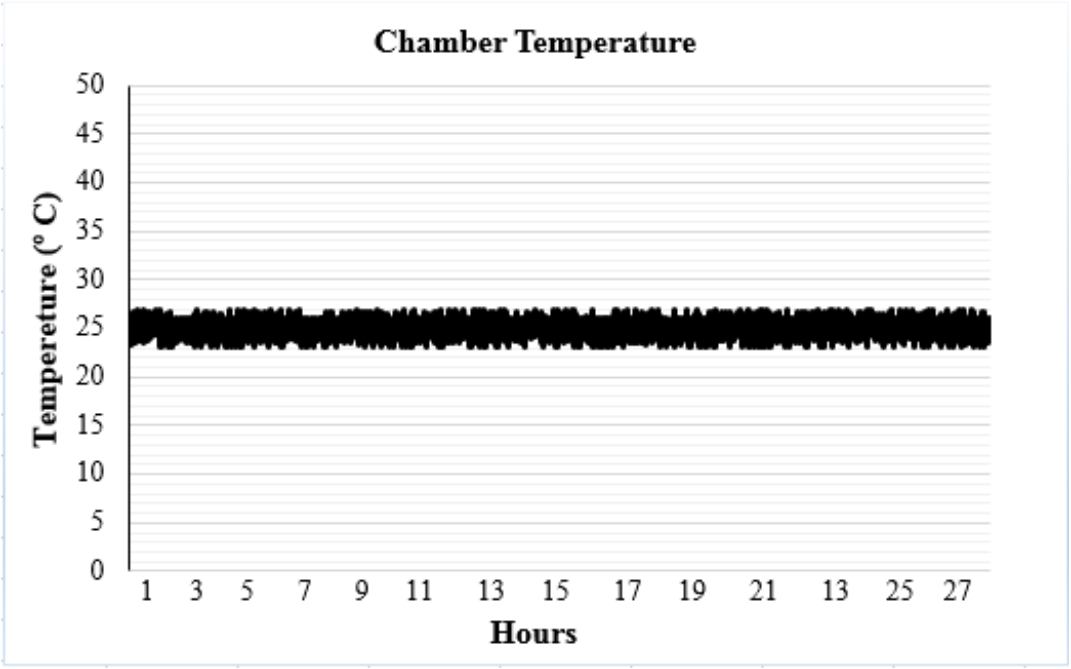

Figure 4.5 25.15º C Average Ambient Temperature History

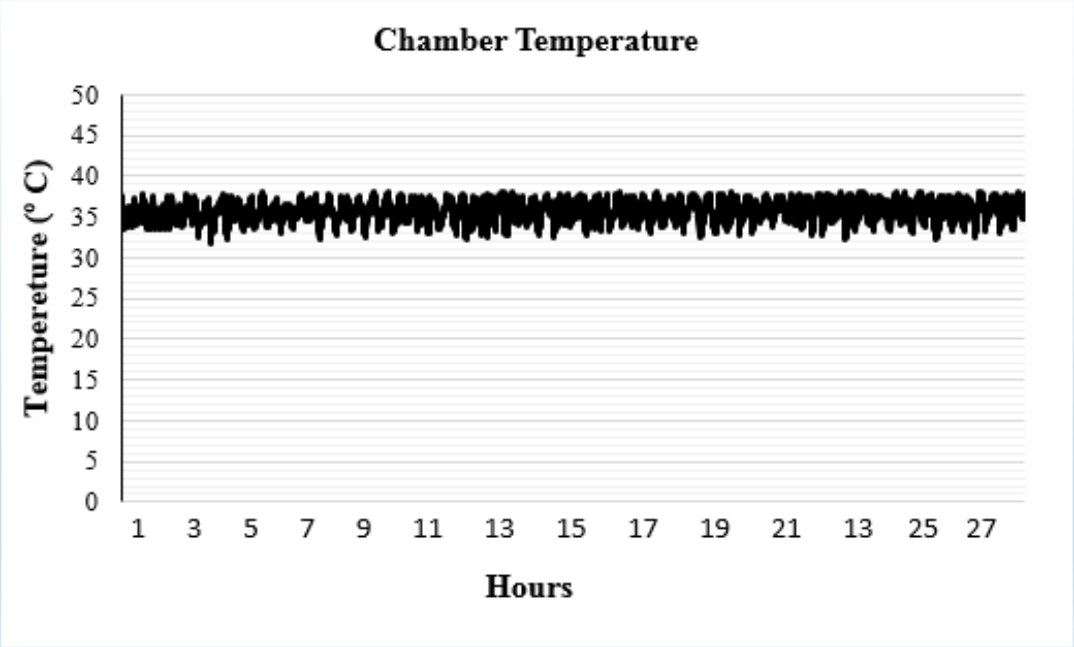

Figure 4.6 35.54º C Average Ambient Temperature History

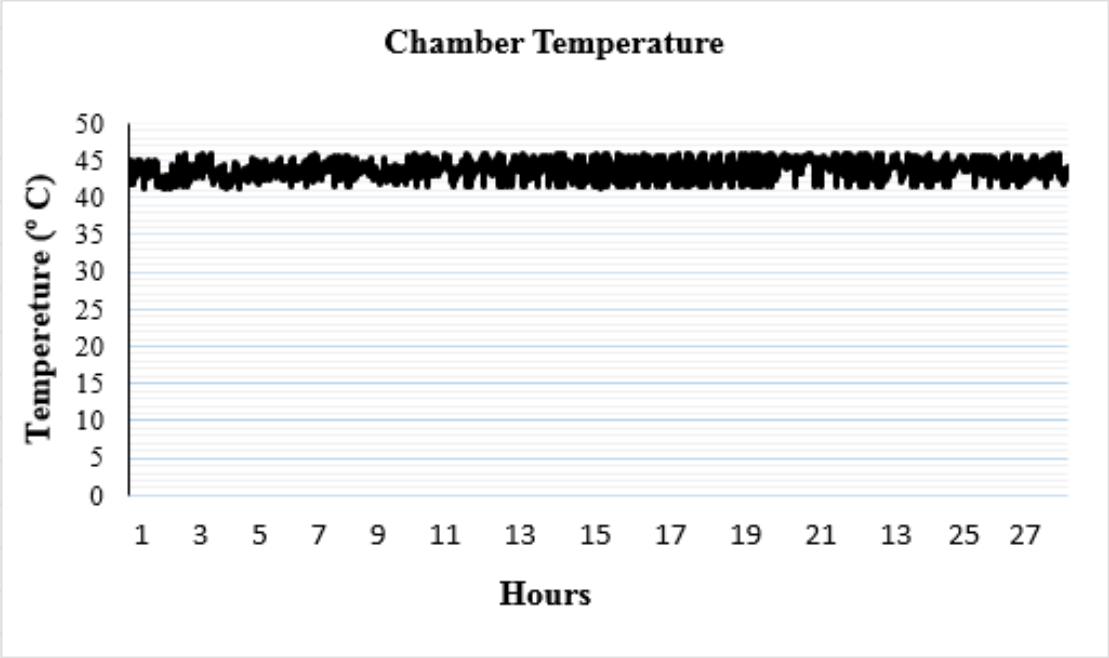

Figure 4.7 43.77º C Average Ambient Temperature History

4.3.1 Effect of Ambient Temperature on Heat Evolution

The peak temperature gauges, for each replacement level under different ambient conditions and corresponding time of measurements are summarized in Table 4.5.

Table 4.5 Peak Temperature in Concrete Specimens

Mixture Code	Position	Ambient Temperature					
		25.15^0C		35.64^0C		43.77^0C	
		Hour	Temp. (^{0}C)	Hour	Temp. (^{0}C)	Hour	Temp. (^{0}C)
BA-0	Top	17	36.9	14.5	38.2	17.5	47.5
	Middle	16.5	41.2	15.5	43.7	18.5	48.9
	Bottom	16.5	43.9	16.5	47	19	51.4
BA-6.5	Top	17.5	35.5	15.5	37.3	19	45.5
	Middle	16.5	38.5	17	42.2	21	46.1
	Bottom	16	41.3	18	45.3	22	48.7
BA-13	Top	18	33.8	16	36.7	20	43.5
	Middle	17.5	36.4	16.5	40.2	21.5	44.8
	Bottom	18	39.3	18.5	42.7	23	46.4
BA-20	Top	20	32.3	17	35.2	16.5	39.9
	Middle	19.5	35	18.5	38.9	18.5	40.8
	Bottom	19	37.3	20	41.4	19	43

As pre stated by ACI 207(1995), the semi adiabatic temperature rise experiments outcome of this study clearly shows that, the hydration heat liberation of concrete specimens escalates as the ambient temperature increase. The temperature rise-time curve, magnitude of maximum temperature gauge, early age reaction rate, thermal gradient, cooling rate of concrete are all under the influence of ambient condition. The temperature profile through different ambient temperatures for each concrete mixture is shown from Figure 4.8-4.19.

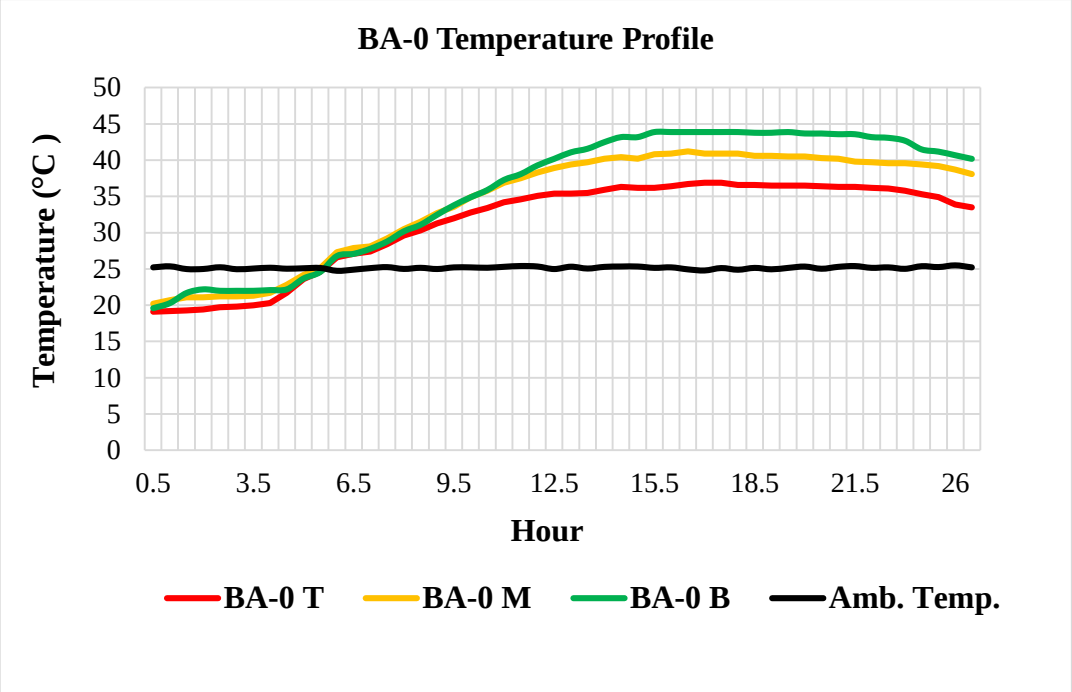

Figure 4.8 Temperature Profile of Control Specimen at 25.15^0 Ambient Temperature

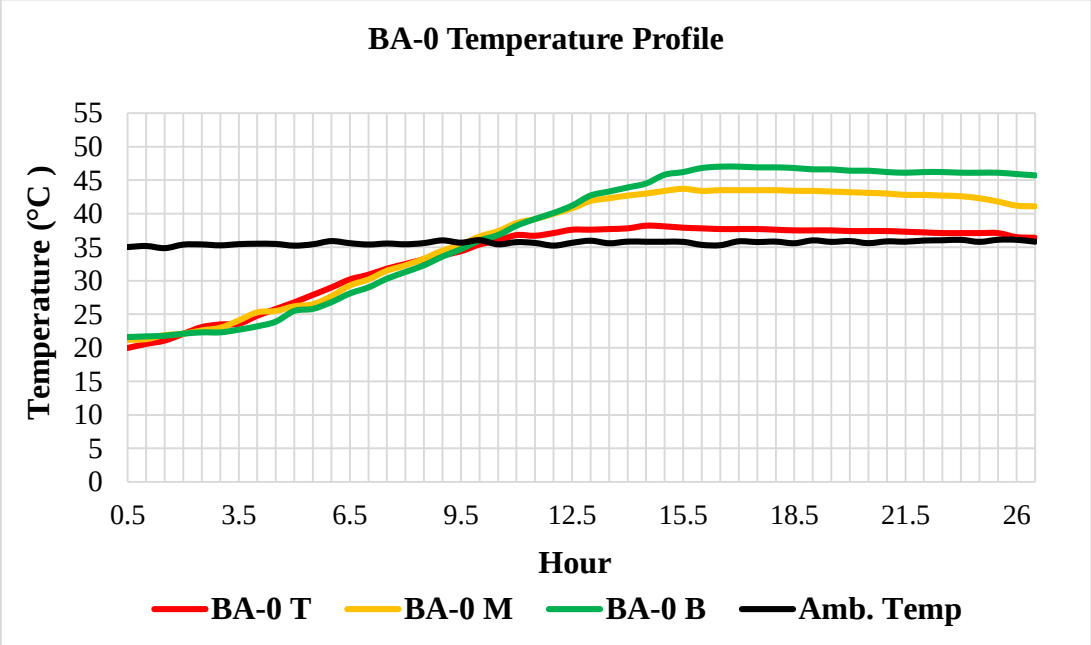

Figure 4.9 Temperature Profile of Control Specimen at 35.54^0 Ambient Temperature

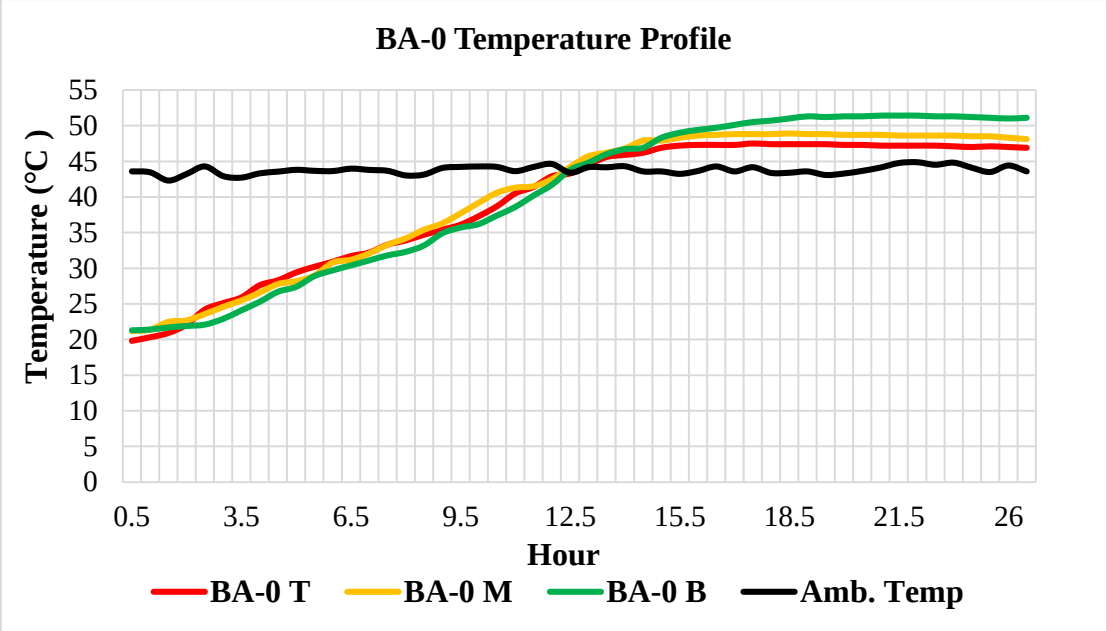

Figure 4.10 Temperature Profile of Control Specimen at 43.77^0 Ambient Temperature

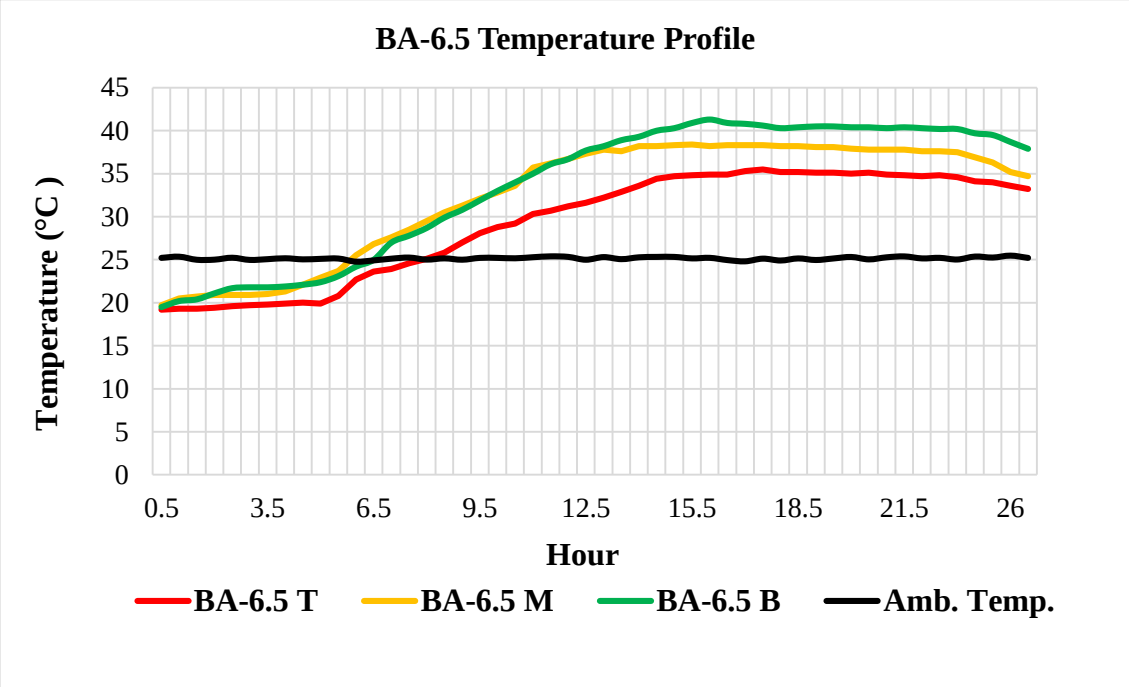

Figure 4.11 Temperature Profile of Concrete Specimen Contain 6.5% BA at 25.15^0 Ambient Temperature

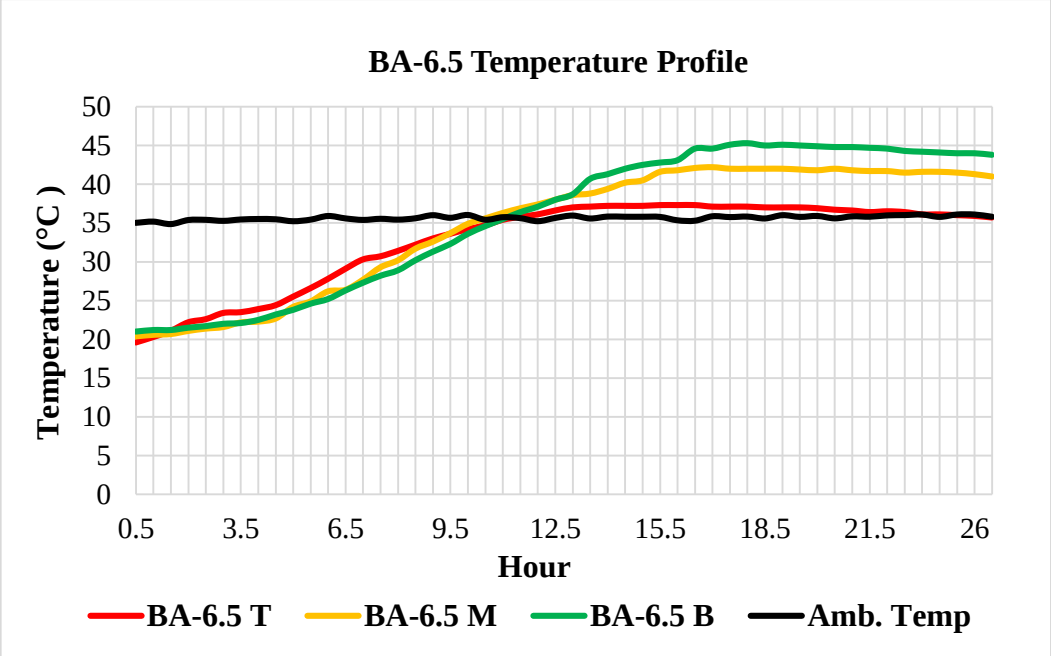

Figure 4.12 Temperature Profile of Concrete Specimen Contain 6.5% BA at 35.54^0 Ambient Temperature

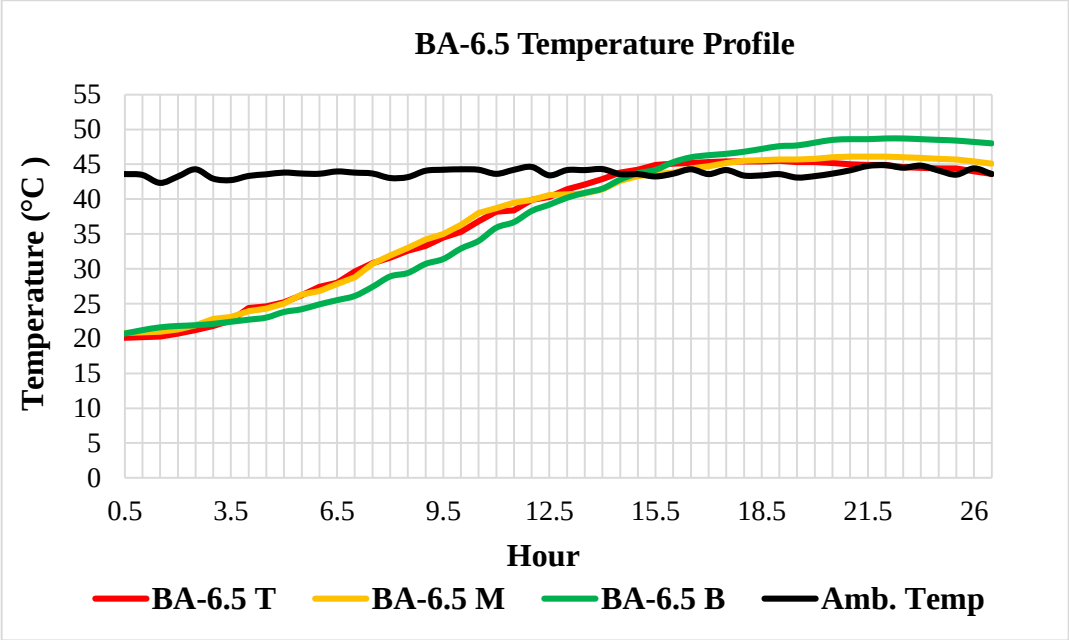

Figure 4.13 Temperature Profile of Concrete Specimen Contain 6.5% BA at 43.77^0 Ambient Temperature

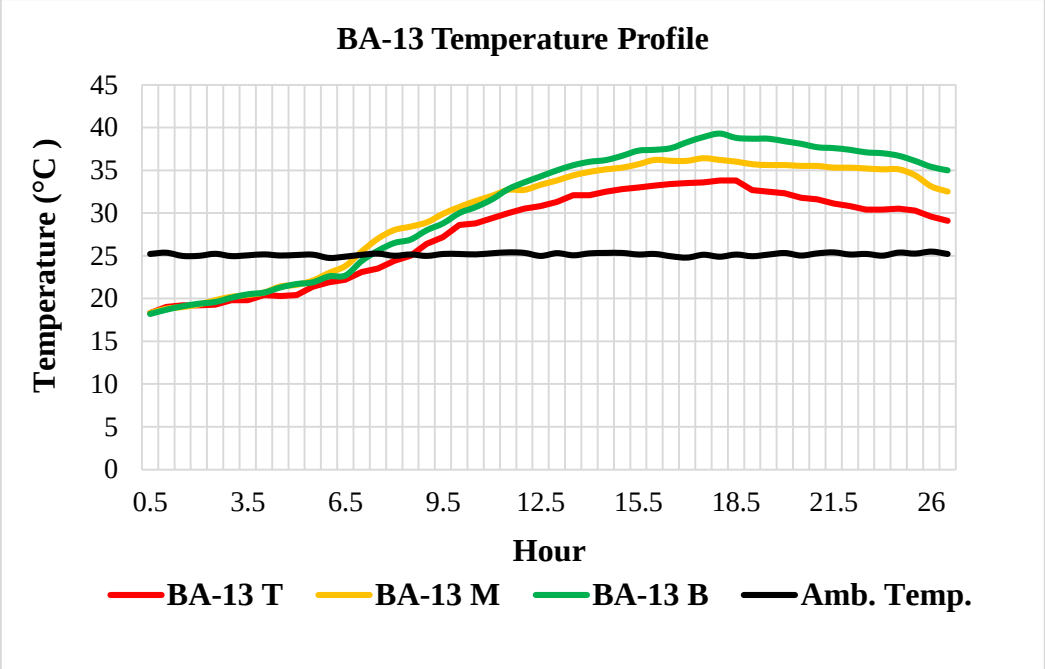

Figure 4.14 Temperature Profile of Concrete Specimen Contain BA 13% BA at 25.15^0 Ambient Temperature

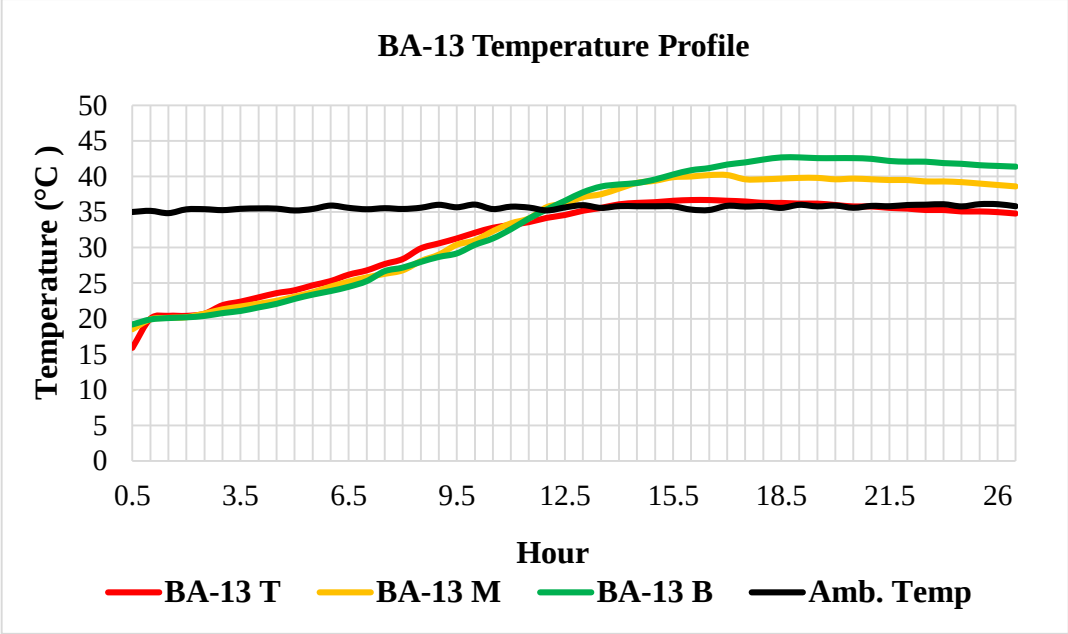

Figure 4.15 Temperature Profile of Concrete Specimen Contain 13% BA at 35.54^0 Ambient Temperature

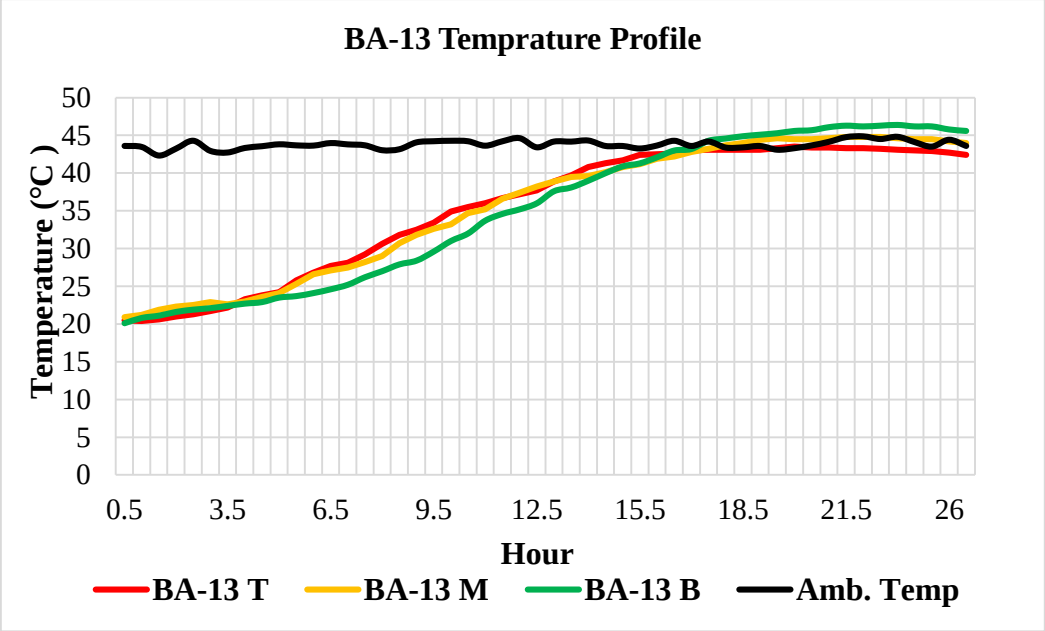

Figure 4.16 Temperature Profile of Concrete Specimen Contain 13% BA at 43.77^0 Ambient Temperature

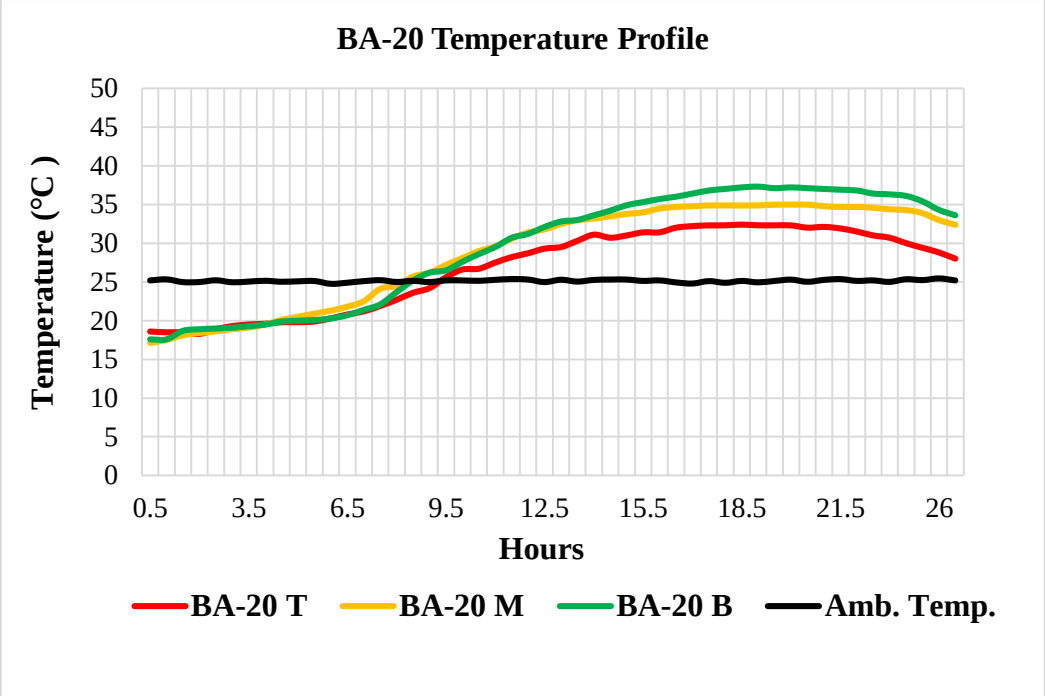

Figure 4.17 Temperature Profile of Concrete Specimen Contain 20% BA at 25.15^0 Ambient Temperature

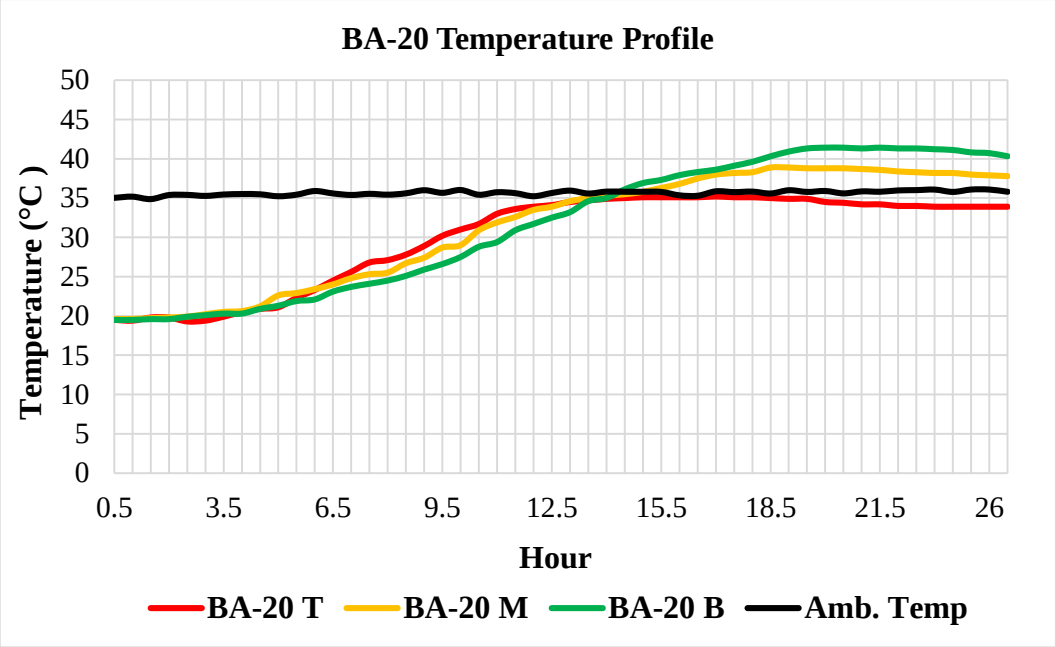

Figure 4.18 Temperature Profile of Concrete Specimen Contain 20% BA at 35.54^0 Ambient Temperature

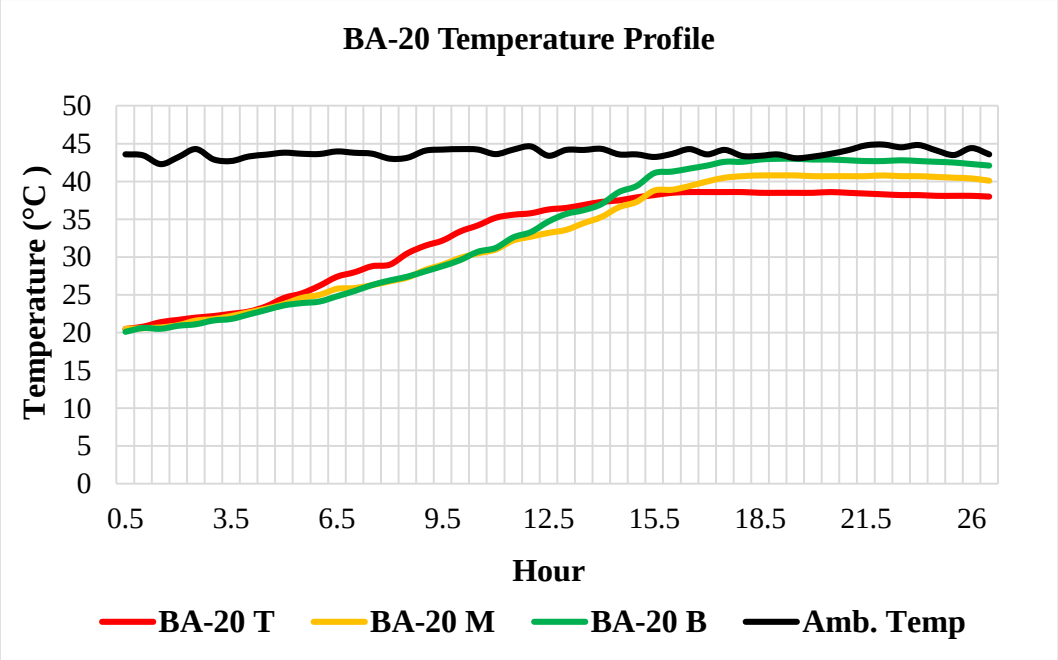

Figure 4.19 Temperature Profile of Concrete Specimen Contain 20% BA at 45.77^0 Ambient Temperature

Figures 4.8-4.10 show the temperature profile of cement concrete at 25.25º, 35.54º and 43.77º C. The peak temperature was gauged at the bottom part of specimen since insulation have been provided at surface of concrete in all direction except the upper part, which was left open intentionally. The insulation (Styrofoam) allows the interior concrete to reach a higher temperature by slowing the diffusion of heat generated from the hydration of cement and chamber temperature radiation. The covering also insulates the concrete surface from the ambient temperature cycles which decreases the temperature drop between the mid-depth and the covered surface.

The peak temperature induced at bottom part of control specimen increased by 17% as the ambient temperature changed from 25.15^0 to 43.77^0 C. In addition, the time required to reach peak temperature of 43.9^0 C was decreased from 16.5 hours to 12.5 hours. In case of concrete containing 6.5%, 13% and 20% dosages of bagasse ash, the ultimate temperature was decreased but the heat evolution corresponding to ambient temperature was significantly influenced.

According to Siddique and Mohammed (2011), pozzolana reaction is slow, releasing heat over a long period of time and not taking place at a very early age of hydration. Similarly, in this study, the effect of bagasse ash on the pattern of hydration heat is pronounced. Temperature profile spectacles, the first 4-6 hour of hydration was slow for all mixes at 25.15^0 C ambient temperature. The control group reaction starts to accelerate even for the first 2-3 hours as the ambient temperature increases. On contrast, mixture contain 13% and 20% of bagasse ash heat liberation rate is relatively slower even in higher ambient temperature (See Figures 4.8 - 4.19).

The maximum temperature differential generally occurred when the maximum internal temperature occurred. The concrete specimens monitored show that, the temperature gradient is trivial over the middle portion of the member and relatively steep towards the surface. Thus it is clear that the temperature drop within a concrete specimen from bottom depth to the exposed surface is not linear, but rather most of the temperature drop occurs near the exposed concrete surface. As a result, current guideline using a linear distribution for estimation of thermal stress developed due to internal heat of hydration comes in to question.

Thermal gradient within section of specimen was decreased by more than 52% for all mixtures after the ambient vary from 25.15^0 to 43.77^0 C. At higher ambient temperature, diffusion of heat from top surface of concrete to the surrounding medium is insignificant. Beside higher ambient transfers heat to the surface of concrete specimen such that, the thermal gradient between top and bottom surface remains low. On the other hand, the thermal gradient increased up to 38% as the ambient changed from 25.15^0 to 35.53^0 C. This phenomenon was surprising but it had a logical background. Relatively intermediate ambient temperature may not have significant effect in heating the top surface of specimen, rather it will facilitate the internal rate of hydration and increase the core temperature concurrently resulting an increment in thermal gradient.

According to ACI 207 (1995), the temperature difference between the ambient temperature and concrete structure should be less than 20^0 C in order to avoid thermal shock. The temperature difference between the cement concrete and ambient (25.15^0) was 18.75^0 C; slightly less than the value specified by ACI 207. Under ambient temperatures of 35.54^0 and 43.77^0 C, the thermal gradients are 11.46^0 and 7.63^0 C respectively; less risky than the former.

Although cold area concreting has favorable effect in mitigating cracking risk (Since the rate of hydration will decrease), it could create potential problems too. In cold ambient temperature, massive concrete structures undergo rapid loss of heat to surrounding medium, which is a reason for thermal gradient and thermal shocks (See Figures 4.8, 4.11, 4.14, 4.17). Thus, emphasis should have to be given for mass concrete placements in cold areas.

4.3.2 The Effect of Bagasse Ash on Early Age Heat Evolution

In previous section, the effect of ambient temperature on rate of reaction and heat liberation of concrete specimens containing pure cement and different dosages of bagasse ash was discussed. This session will particularly discuss the effect of bagasse ash on the heat evolution of concrete mixtures. The Figures 4.20-4.28 show the semi-adiabatic temperature data of different concrete mixtures.

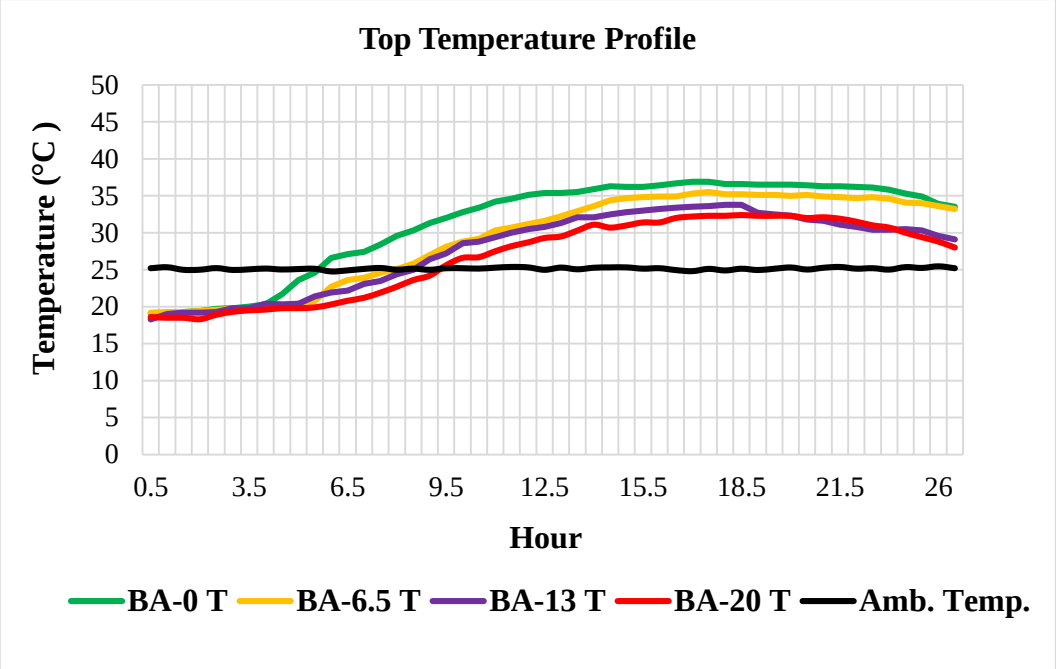

Figure 4.20 Top Temperature Profile of Different Mixture Specimens at 25.15^0 Ambient Temperature

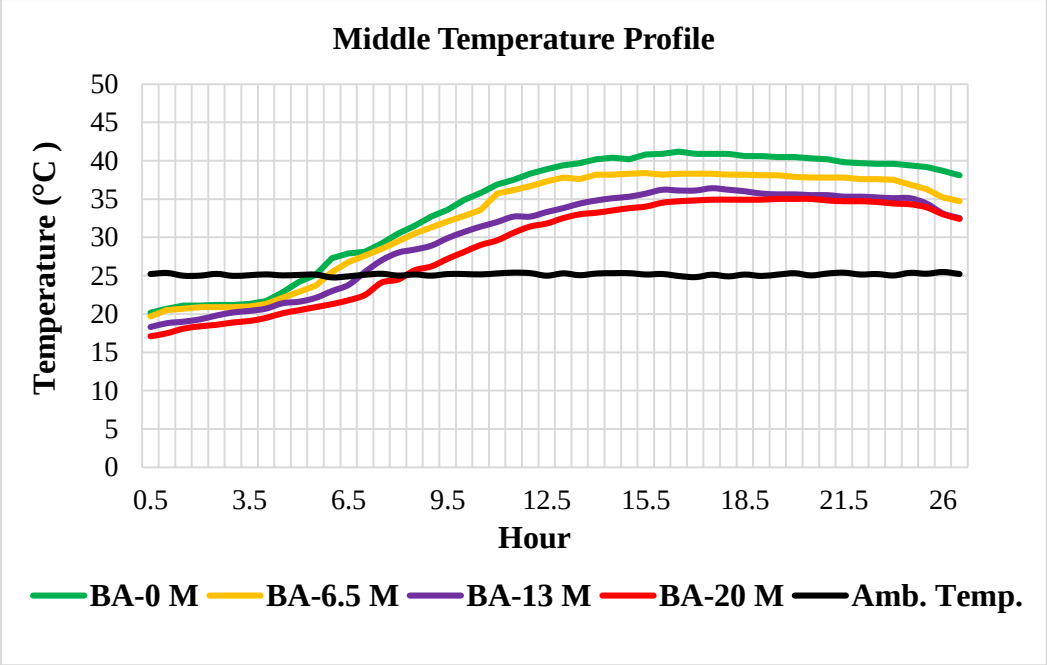

Figure 4.21 Middle Temperature Profile of Different Mixture Specimens at 25.15^0 Ambient Temperature

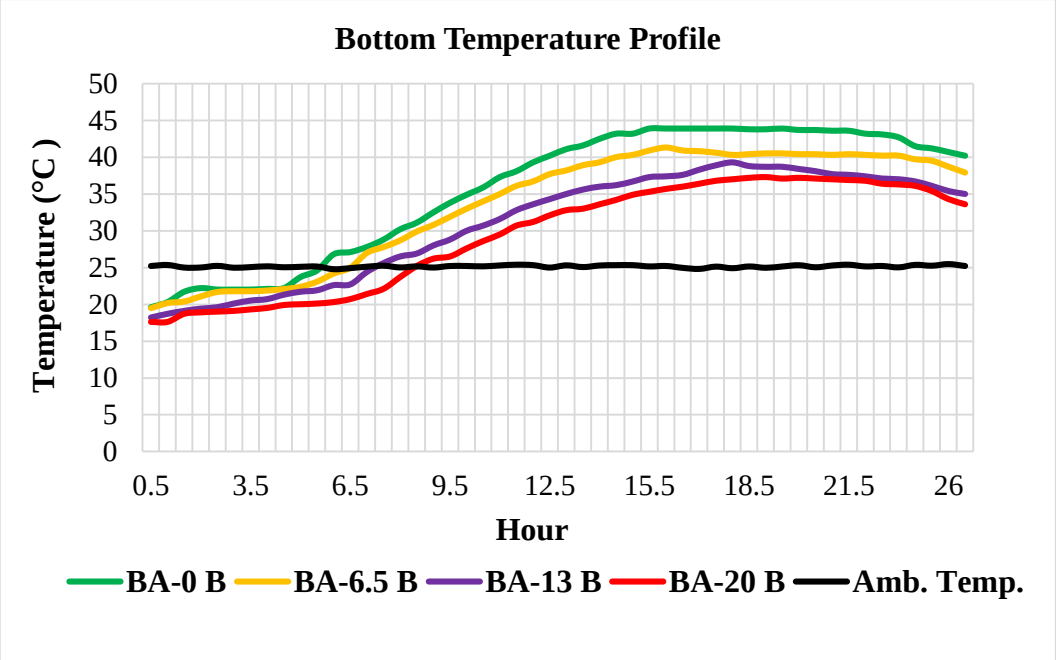

Figure 4.22 Bottom Temperature Profile of Different Mixture Specimens at 25.15^0 Ambient Temperature

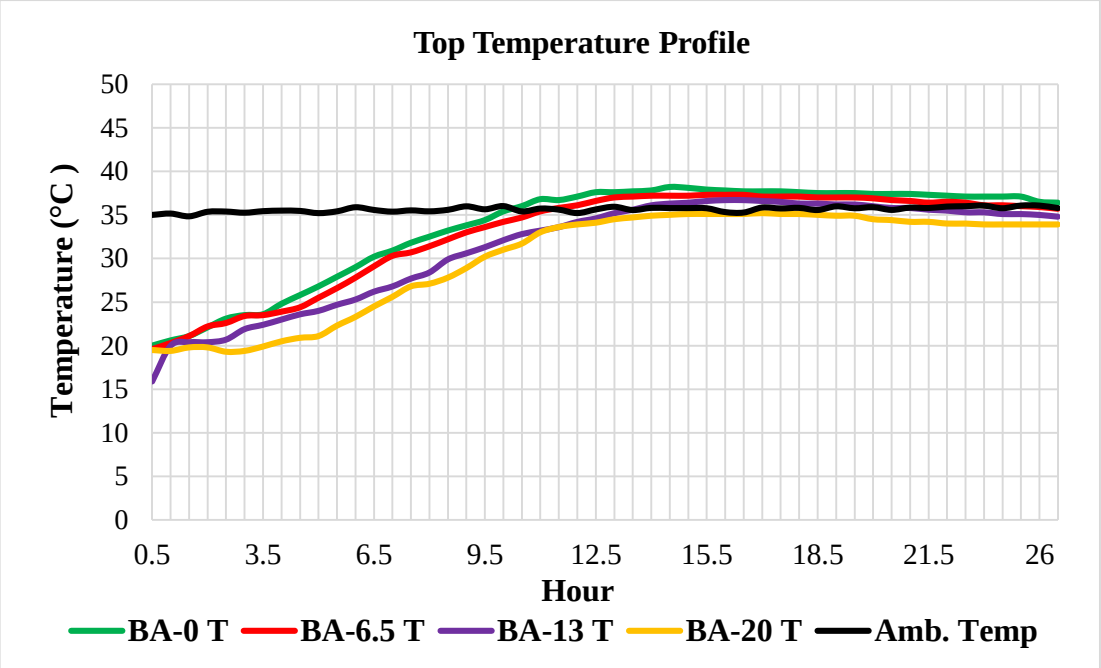

Figure 4.23 Top Temperature Profile of Different Mixture Specimens at 35.54^0 Ambient Temperature

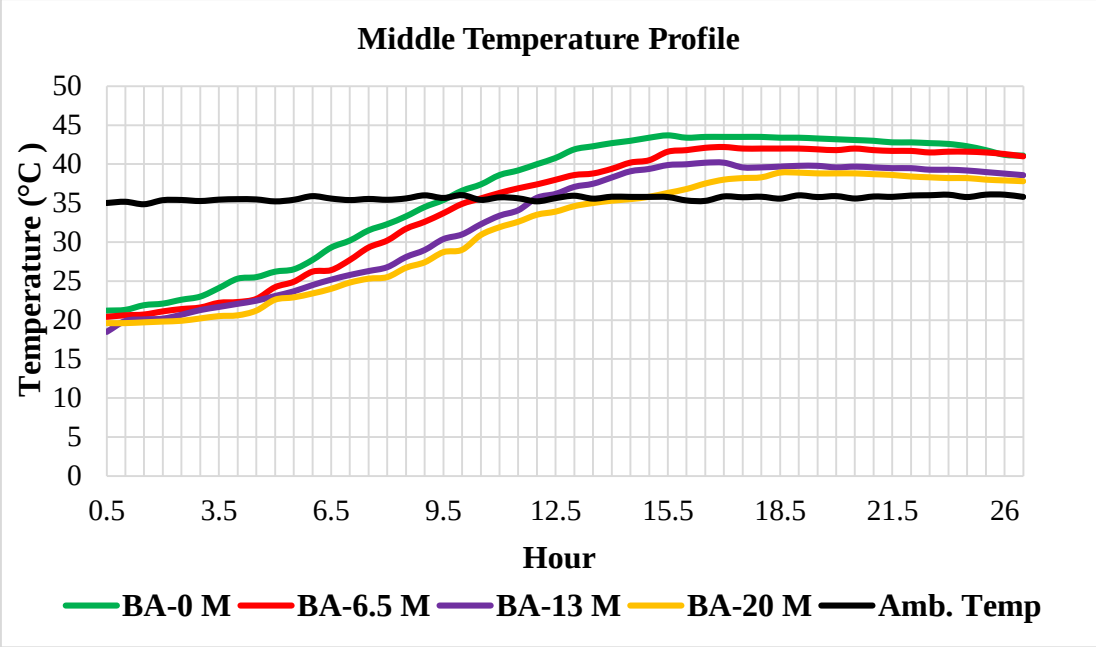

Figure 4.24 Middle Temperature Profile of Different Mixture Specimens at 35.54^0 Ambient Temperature

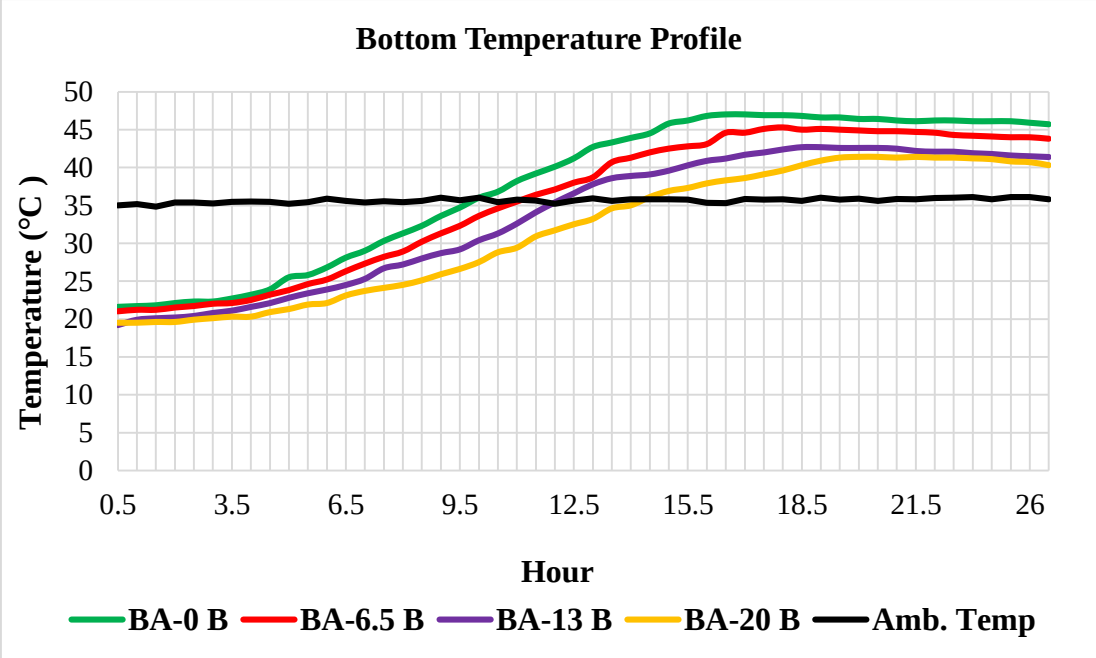

Figure 4.25 Bottom Temperature Profile of Different Mixture Specimens at 35.54^0 Ambient Temperature

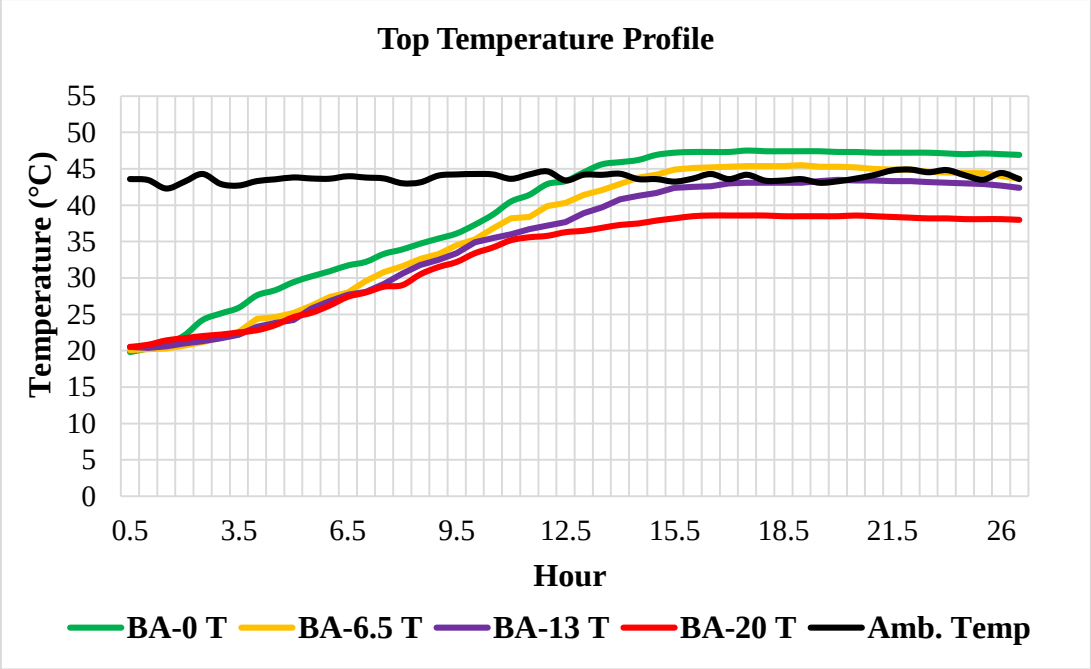

Figure 4.26 Top Temperature Profile of Different Mixture Specimens at 43.77^0 Ambient Temperature

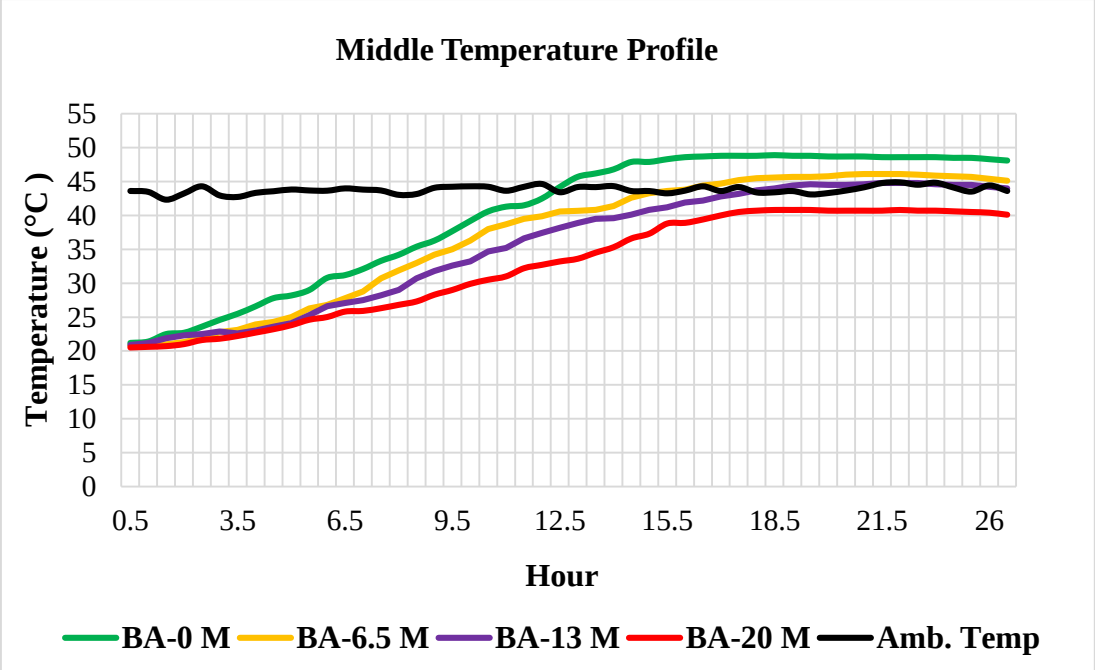

Figure 4.27 Middle Temperature Profile of Different Mixture Specimens at 43.77^0 Ambient Temperature

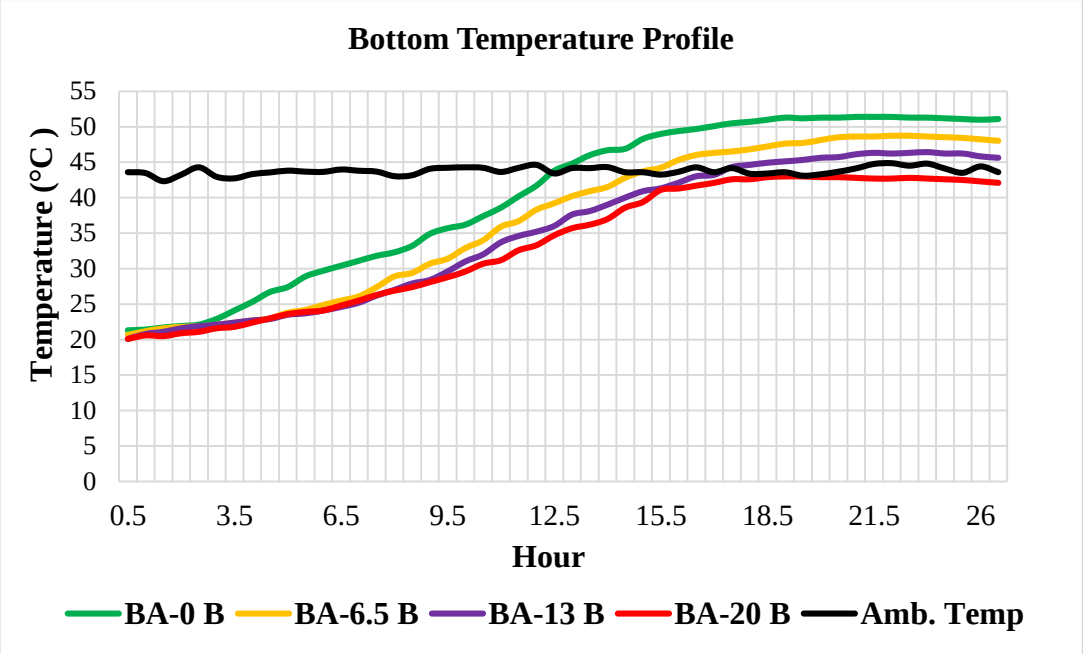

Figure 4.28 Bottom Temperature Profile of Different Mixture Specimens at 43.77^0 Ambient Temperature

The presence of bagasse ash in concrete mixture has dropped the total heat liberated from concrete specimens. The decline in temperature is detected throughout the depth of all concrete specimens containing bagasse ash. Replacing 20% of cement using bagasse ash can drop the peak temperature of cement concrete specimens by 15%, 11.9% and 16.3% for 25.15^0, 35.54^0 and 43.77^0 C ambient condition respectively. This is of immense advantage in massive concrete placement where cooling, following a large temperature rise, can lead to cracking. Likewise, using bagasse ash in 6.5% and 13% replacement level reduce the overall temperature rise of the concrete depending on ambient conditions, however the effect is less due to lower replacement level.

The decrease in temperature appears to be due to the inertness of the bagasse ash at early age. On the other hand, low calcium pozzolana (Local bagasse ash) does not possess self-cementitious property; Therefore, it will not react rapidly with water and release excessive heat just like ordinary Portland cement. Furthermore, bagasse ash bind calcium ions effectively (calcium complexation) without releasing it for desired amount of time, so the hydration is delayed and early age heat evolution is retarded.

Optimization of bagasse ash in concrete shows remarkable shift in temperature rise-time curve. Replacing 13% of cement using bagasse ash elongates the time required to reach 39^0 C internal temperature of specimen by 6, 3.5, and 3 hours under 25.15^0, 35.54^0 and 43.77^0 C ambient temperature respectively. Shifting the temperature rise-time curve by elongating the time required to attain peak magnitude have an optimistic impact in a way, concrete gets additional time for strength development before the thermal load exerted.

Moreover, reduction of thermal gradient is observed as the cement-bagasse replacement level increases. In the case of 13% replacement level, the thermal gradient of cement concrete was decreased by 21.4%, 31.81% and 25.64% for 25.15^0, 35.54^0 and 43.77^0 C ambient temperature respectively.

As shown in the Figures 4.21-4.25, the temperature profile of each concrete mixture do not commence at similar temperature gauge. Since the concrete mixtures were not cast all together, there was a variation of initial temperature until the specimens placed in the chamber. Thus, concrete mixtures casted at lower ambient temperature will eventually show a relatively slow reaction rate compared with the high initial casting temperature. The initial concrete temperature affects the rate of heat liberation which is essential for concrete in a semi-adiabatic environment (moderate mass concrete placements). Pre-cooling of concrete is among the “initial temperature reduction techniques”, which can be used to reduce the internal temperature rise by decreasing the rate of heat generation. The lower rate of heat liberation provides a longer time for heat to dissipate which decreases the potential for thermal cracking due to a thermal gradient within a concrete structure.

CHAPTER 5 FINITE ELEMENT MODELING

In recent years, with advancement in computing technology, significant progress in finite element approach tools have been observed. Finite element analysis based confirmation tools (softwares packages) are helpful in identifying obstacles at early stage of design, reducesing prototyping cost, gaining perceptions on phenomenon which cannot be easily dignified in physical tests, etc. Hacon-3 finite element sofware is used to simulate hardining concrete under different ambient tempretures. The input parameters, modeling issues and finally results are discussed here after.

5.1 MODEL DESCRIPTION

Finite element modeling is used for validating the result obtained from experimental programs. Concrete samples used in experimental programs were modeled with corresponding dimensions, physical properties and different boundary condition including ambient temperature. Moreover, investigation of thermal crack risk, and parametric study was undertaken using this finite element software.

5.2 ABOUT HACON-3 FES

Hacon-3 finite element software was developed for simulation of temperature and stress in hardening concrete structures. The software is open source and can handle a two dimensional and axisymmetric problems. Modeling the stage of construction, introducing ambient temperature, modeling insulation and formworks, creating cement parameters are important features of this software. Additionally, modeling of creep, stress induced thermal strain, autogenous shrinkage and development of crack can be studied using this FES.

5.3 INPUT PARAMETERS

The Input data for numerical study are according to previously done experiments and relevant mathematical formulation/relation proposed in literatures.

5.3.1 Specific Heat Capacity

Specific heat capacity is the amount of heat needed to change the temperature of 1g of material by 1°C (Lawrence, 2016). A typical value of specific heat capacity for concrete ranges from 0.92–1.00 kJ/kg°C according to ACI 207 and 840 to 1170 J/kg°C as per Neville (2011). For this study 840 J/kg°C was adopted.

5.3.2 Thermal Conductivity

Thermal conductivity is a thermo-physical measure of how much heat can be transferred through a material of conductive flow (Neville, 2011). The thermal conductivity of concrete is affected by various parameters including the type of aggregate, moisture content, porosity of the concrete and degree of hydration. According to ACI-207, the thermal conductivity of concrete is in the range of 7.1 to 10.6 kJ/mh°C. In this study thermal conductivity; 8 kJ/mh°C is taken.

5.3.3 Coefficient of Thermal Expansion

Coefficient of thermal expansion describes how the size of an element changes due to a change of temperature. According to Meyers (1951), The linear coefficient of thermal expansion of hydrated cement paste varies between $11 \times l0^{-6}$ and 20×10^{-6}/°C. The coefficient of thermal expansion used in this study is $10*10^{-6}$ per °C.

5.3.4 Thermal Diffusivity

Thermal diffusivity is a measure of easiness or difficulty of concrete undergoing temperature change (ACI 207, 1995). The range of typical values of diffusivity of ordinary concrete is between 0.002 and 0.006m2/h (Neville, 2011). An average value of 0.004 m^2/h is specified for modeling.

5.3.5 Total Heat of Hydration

Degree of hydration of concrete is the foremost important parameter for simulating the early age thermal behavior of a structure (Lawrence, 2009). For common cement types, the hydration is exothermic reaction and up to 500J/g (120 cal/g) energy can be liberated (Neville, 2011). Heat of hydration is not the same for all mixtures. It depends on the chemical compositions of cement, proportion of each compositions and addition of supplementary materials. The hydration heat can be expressed mathematically using Equation 5.1 & 5.2 (Schindler and Folliard, 2005).

$$H_{cem} = 500\rho C_3S + 260\rho C_2S + 866\rho C_3A + 420\rho C_4AF + 624\rho S0_3 + 1186\rho\, freeCao + 850\rho Mgo$$
.....(5.1)

Where:- ρ = is the percentage fraction of the i^{th} compounds in the cement

To account the heat of hydration from supplementary cementitious materials, the equation can be further modified as

$$Hu = \rho_{cement} * H_{cement} + \rho_{flyash} * H_{flyash}$$
.....(5.2)

where: $H_{flyash} = 1800\rho_{cao}\, j/g$ or $209j/g$

ρ = percentage of fly ash

However, heat of hydration for total amount of cement is affected by the chemical compositions interaction. The heat of hydration is given by Equation 5.3 (Neville, 2011).

$136(C_3S) + 62(C_2S) + 200(C_3A) + 30(C_4AF)$ ……...……...(5.3)

The specific heat of hydration for cement with different cement-bagasse ash replacement ratio is computed as per Equation 5.1, 5.2 & 5.3 and summarized in Table 5.1.

Table 5.1 Ultimate Heat of Hydration for Different Mixtures

Mixture Id.	Ultimate heat of hydration(j/g)
BA-0	220.63
BA-6.5	208.04
BA-13	192.29
BA-20	177.44

All the specified input parameters may not represent concrete specimens containing bagasse ash; However, a relatively convenient value is specified for the finite element modeling.

5.4 MODELING

5.4.1 Geometry

The first task in modeling is creating nodes. The nodes are then connected using lines or curve elements. Surface has been created by selecting the desired lines in counter clock wise direction. Hacon-3 provides an option for selecting 3, 5 or 8-noded elements. 8

nodded elements are used for this modeling. Meshing was done by specifying the desired amount of columns and rows in the finite element software.

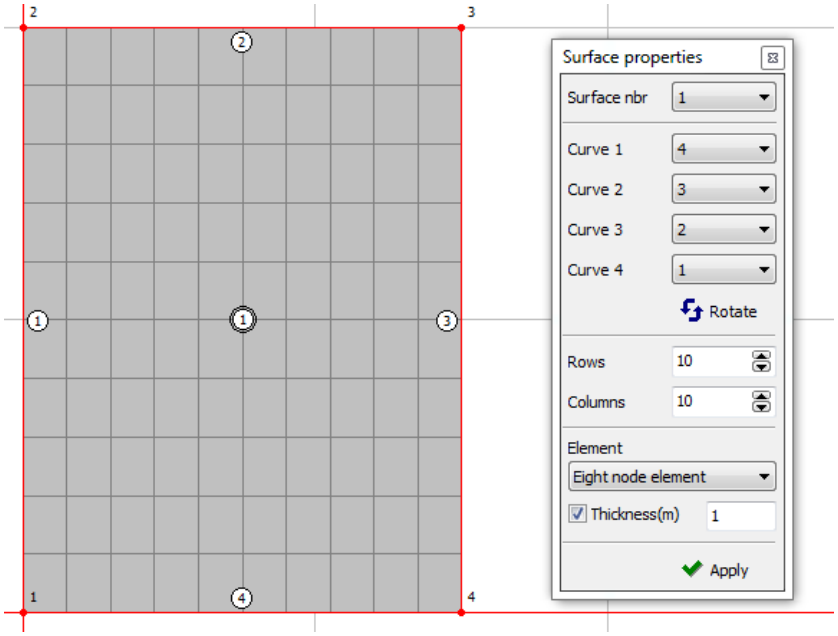

Figure 5.1 Meshing and Element Property

5.4.2 Material

In Hacon-3 there are some predefined materials such as concrete, rock and soil. K-40 concrete material is used, but the default material property was latter modified. In material session; placing temperature, cement content, water/binder, ultimate heat of hydration and time for initiation of maturity are all defined.

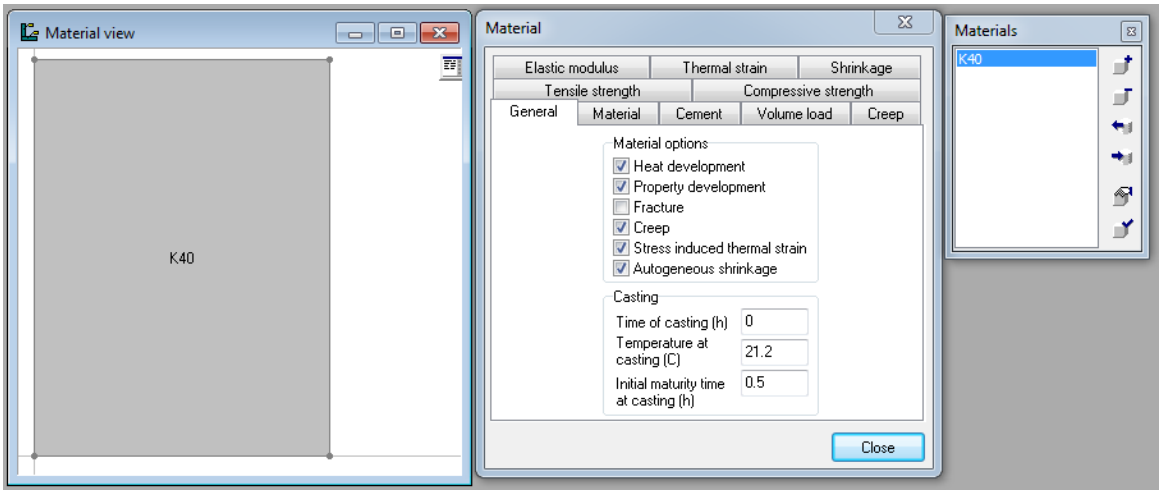

Figure 5.2 Material Modeling Tab in Hacon-3

5.4.3 Boundary Conditions

After all, the boundary conditions are the critical governing factor for simulating the thermal analysis later for staggered structural analysis. The base and sides of the concrete has been fixed in order to get worst case scenario. The concrete specimens were insulated in three directions (the top surface will remain exposed so that the effect of ambient temperature can be simulated). Hacon-3 provides different insulating materials; Moreover, other materials of different physical properties can be introduced. A 10 Cm thickness Styrofoam is modeled with its corresponding insulation property.

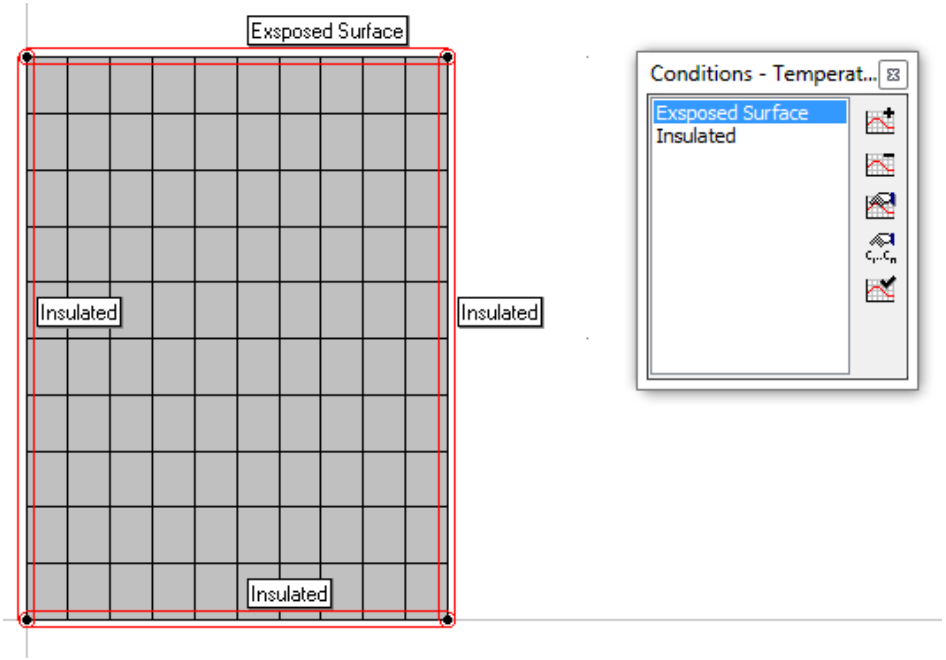

Figure 5.3 Assigned Boundary Conditions on Specimen Surface

5.4.4 Analysis

Before the analysis began, Hacon-3 offers calculation setting in order to choose the desired time step, analysis type and output arrangement. The analysis was carried out for each 30-minutes time step; Therefore, the outcomes will be compatible with experimental program.

5.5 RESULT AND DISCUSSION

5.5.1 Hydration Heat Simulation

Since the specimen was insulated in all directions except the upper part, the peak temperature of all concrete specimens simulated in Hacon-3 was located at the bottom part.

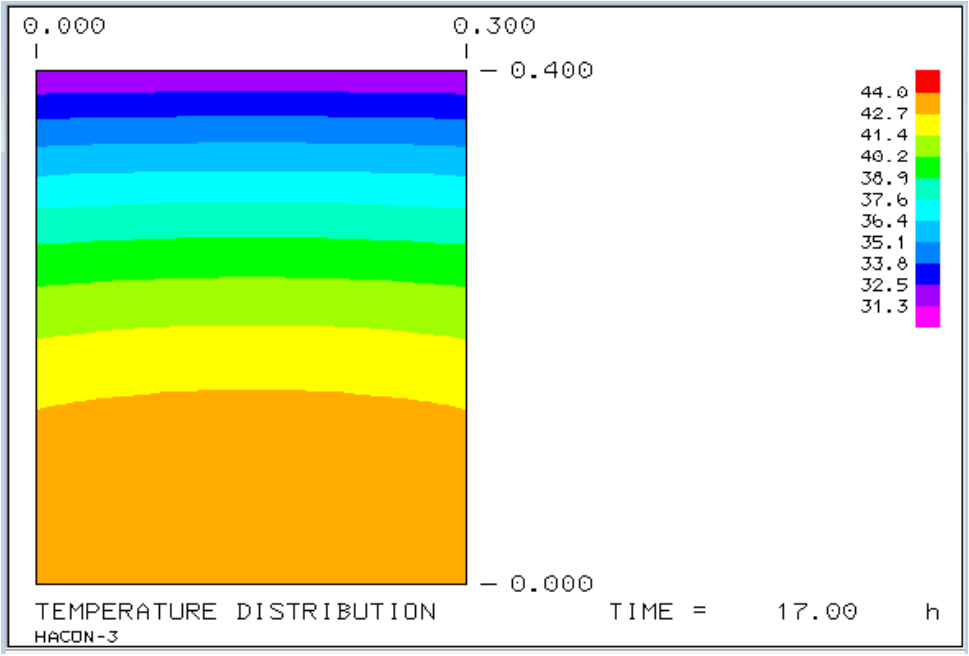

Figure 5.4 Temperature Profile of the Control Group at 25.15^0 Ambient Temperature

Figure 5.4 shows that, peak temperature is 44^0 C and occurred 17 hours later after casting. The results from finite element analysis show a good agreement with the experimental outcomes in terms of predicting locations, magnitude and time delay of peak temperatures.

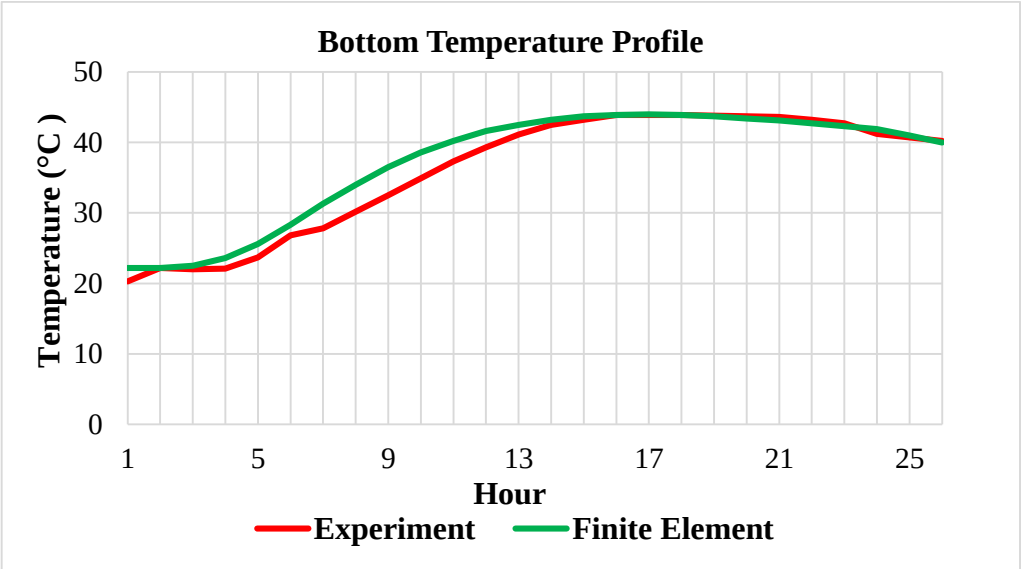

Figure 5.5 Bottom Temperature Profile at Ambient Temperature 25.15^0 C

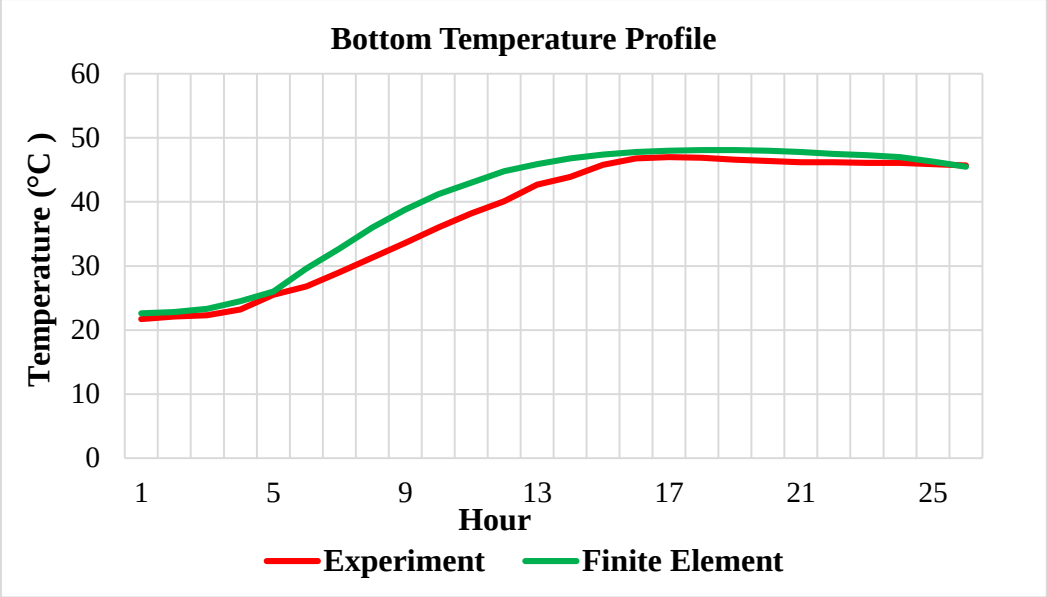

Figure 5.6 Bottom Temperature Profile at Ambient Temperature of 35.54^0 C

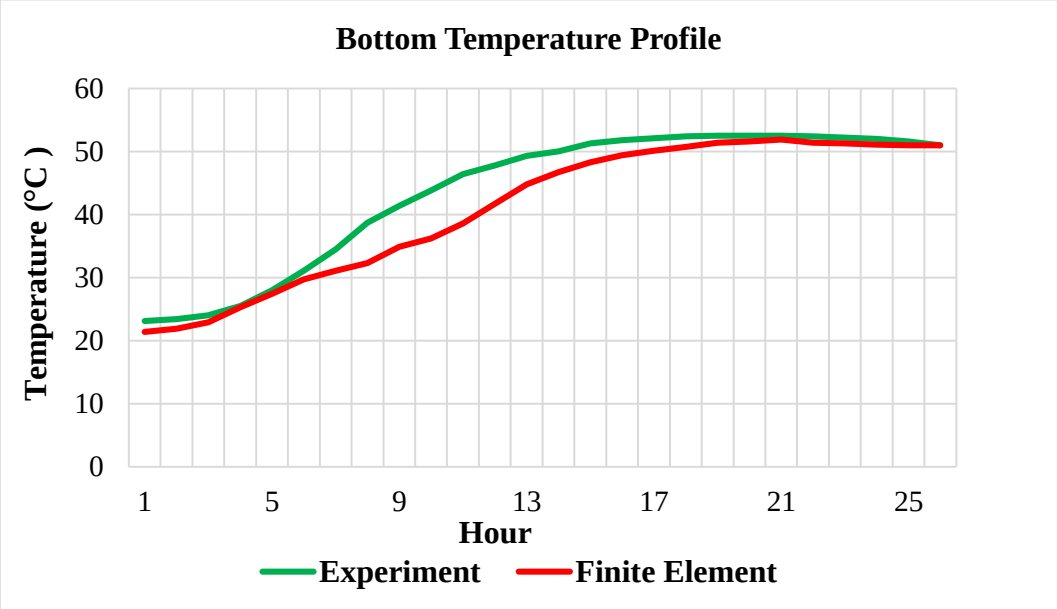

Figure 5.7 Bottom Temperature Profile at Ambient Temperature of 43.77^0 C

It can be observed from Figure 5.5-5.7, thermal responses under different ambient temperature are well predicted using Hacon-3 finite element software.

5.5.2 Cracking Risk Simulation

Cracking start to initiate when the crack index is greater than 100%. Which means the stress induced by combined action of thermal and structural loads exceeds the strength of concrete.

The thermal cracking risk for the first 24 hours is trivial for all scenarios. As temperature increases the concrete attempts to expand, indeed the specimen will be under compression at the time of heat evolution. Usually the compressive strength of concrete is adequate to resist those minor compression forces. Moreover, the cracking risk plot is flatted for certain duration because specimen is under compression and tensile stress are almost zero. (See Figures 5.12-5.14).

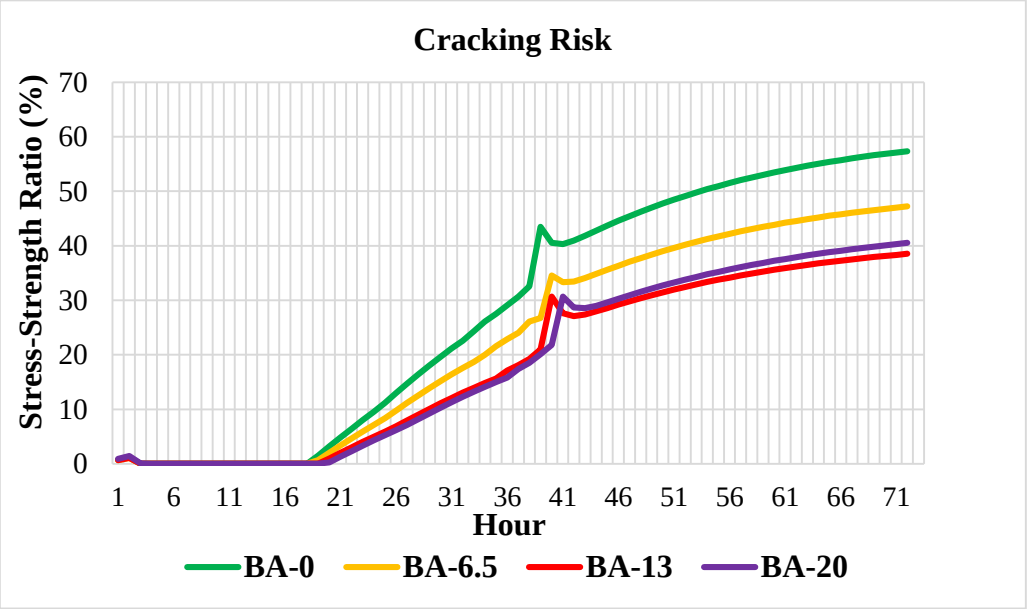

Figure 5.8 Cracking Risk at Ambient Temperature of 25.15^0

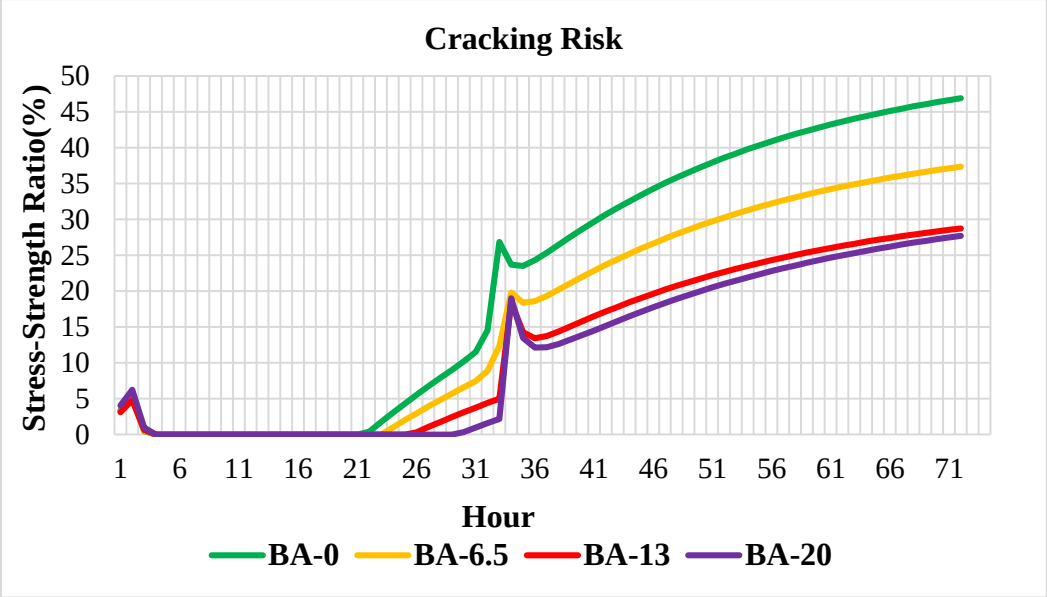

Figure 5.9 Cracking Risk at Ambient Temperature of 35.54^0

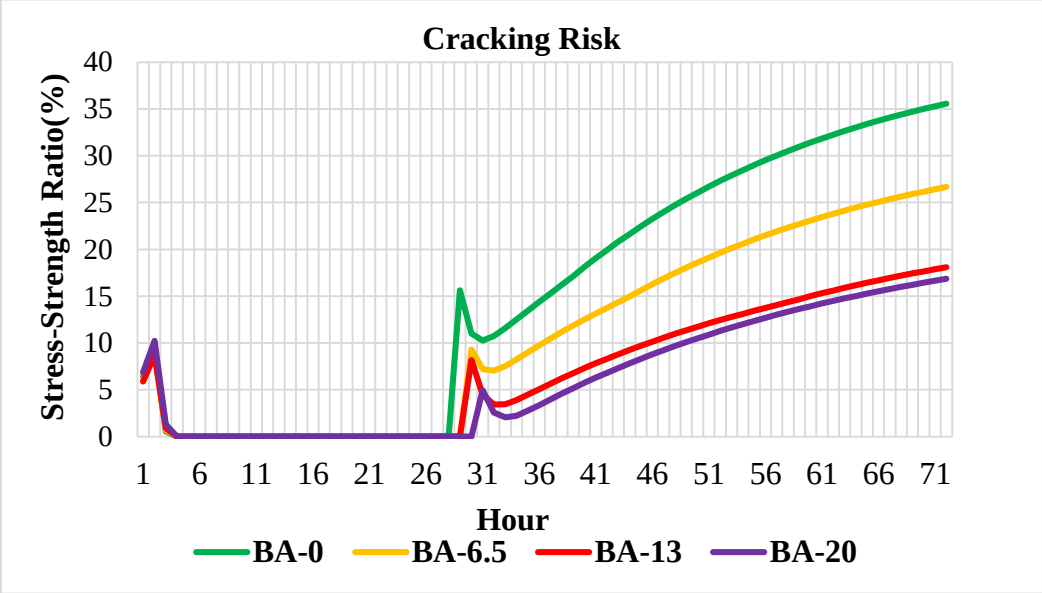

Figure 5.10 Cracking Risk at Ambient Temperature of 43.77^0

The tensile stress being minimal at the time of heat evolution does not mean that, the peak temperature will not influence thermal cracking, rather consequences get manifested on cooling stage of concrete. As it can be seen in the Figure 5.8-5.10, the cracking risk increase on the cooling phase as the tensile stress increases. Ambient temperature affects not only the heat liberation but also the cracking risk. The 72 hours cracking risk decrease up to 18.29%, 37.9% as the ambient varies from 25.15^0 to 35.54^0 and 43.77^0 C respectively.

When the ambient temperature increases, the heat loss from the concrete decrease so that it will elongate the time for concrete contraction. Even though higher ambient temperature lowers the ultimate cracking risk by increasing the maturity of concrete and decreasing the tensile stress, it will increase the cracking risk at the very early age.

Introducing bagasse ash to a concrete mixture played a role in reducing thermal cracking risk. Thermal cracking risk after 72 hours is reduced by 17.68%, 32.83% and 29.34% after 6.5%, 13% and 20% of cement is replaced by bagasse ash respectively. Replacing cement up to 20% using bagasse ash clearly increased thermal risk in the first 16 hours for all ambient temperatures. Decreases in mechanical property of concrete containing 20% of bagasse ash is attributed to the phenomena. Although optimization of supplementary materials such as bagasse ash reduce the heat evolution, compatibility with strength requirement should be checked.

5.5.3 Influence of Insulation on Thermal Gradient

As discussed in literature section, researchers recommend adoption of insulation in mass concrete structure for reducing thermal gradient. Different size concrete specimens were modeled with and without insulation. The outcomes were alarming.

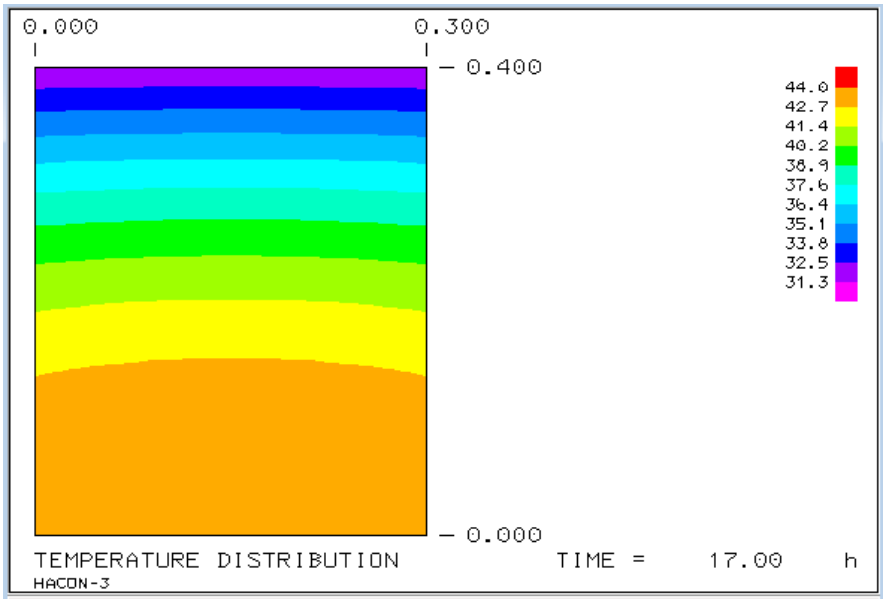

Figure 5.11Temperature Profile of Insulated Concrete at 25.15^0 C Ambient Temperature (Size: 0.3m*0.4m)

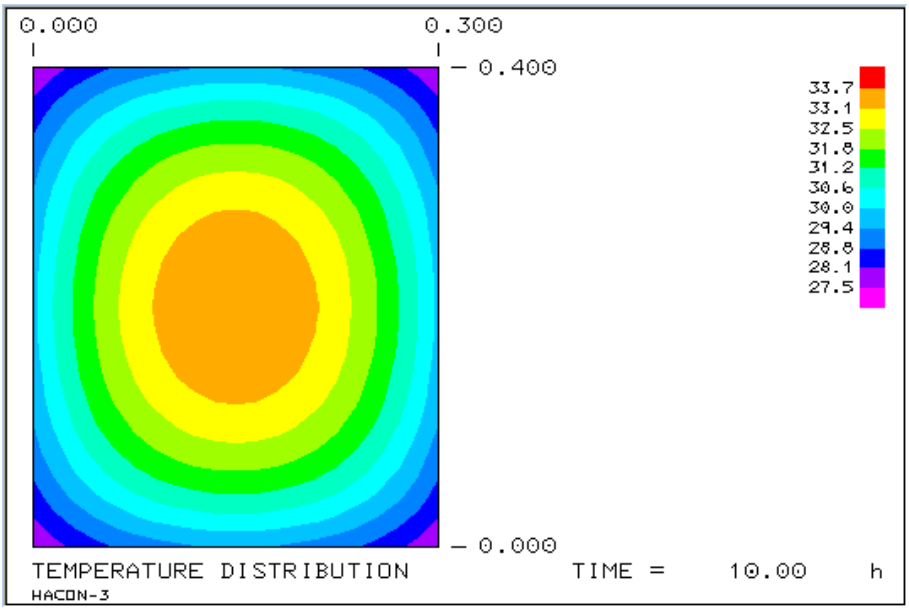

Figure 5.12 Temperature Profile of not Insulated Concrete at 25.15^0 C Ambient Temperature (Size: 0.3m*0.4m)

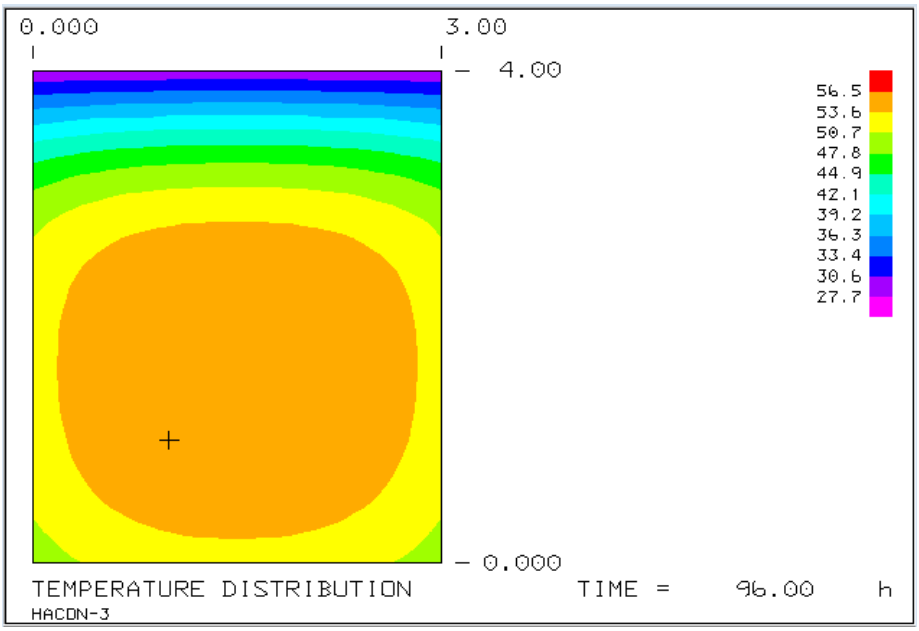

Figure 5.13 Temperature Profile of Insulated Concrete at 25.15^0 C Ambient Temperature (Size: 3m*4 m)

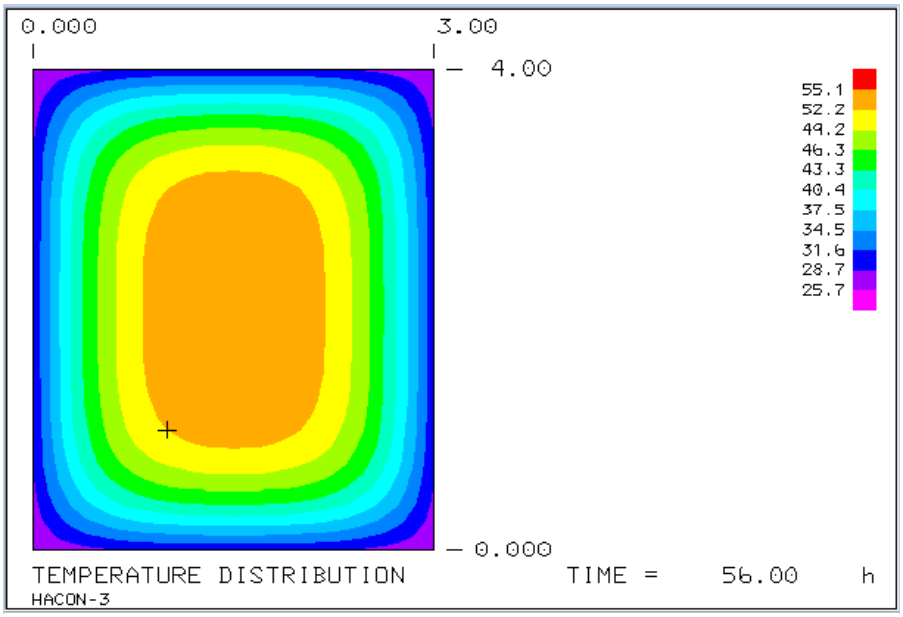

Figure 5.14 Temperature Profile of not Insulated Concrete at 25.15^0 C Ambient Temperature (Size: 3m*4 m)

As shown in Figures 5.11 & 5.12, for Specimen size: 0.3m*0.4m, the thermal gradient of insulated concrete is greater than non-insulated one. On contrast, when the size of specimen increases, providing insulation effectively reduces the thermal gradient as shown in Figures 5.13 & 5.14.

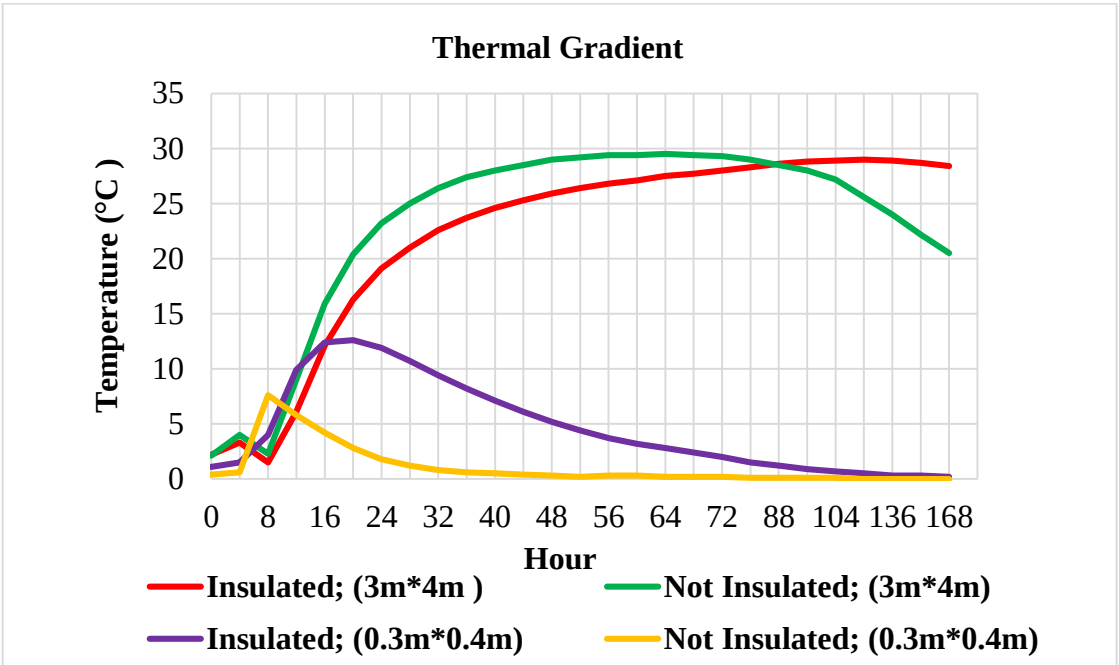

Figure 5.15 Thermal Gradient of Insulated and Concrete without Insulation

It can be seen in Figure 5.15 that; the rate of cooling is significantly decreased due to provision of insulation. Slow rate of cooling has positive impact in lowering thermal risk. Despite the merits, it cannot be thought that provision of insulation will decrease the thermal gradient for all cases. Thermal gradient is affected by so many factors such as; Insulation condition, size of concrete structures, material properties and environmental conditions. Therefore, before proposing insulation for mitigating thermal cracking risk in mass concrete structures, comprehensive analyses should be carried out for each specific projects.

5.5.4 Influence of Specimen Size on Thermal Gradient

Concrete specimens with four different section dimension were modeled in Hacon-3. The thermal gradient-time curve is shown in Figure 5.16.

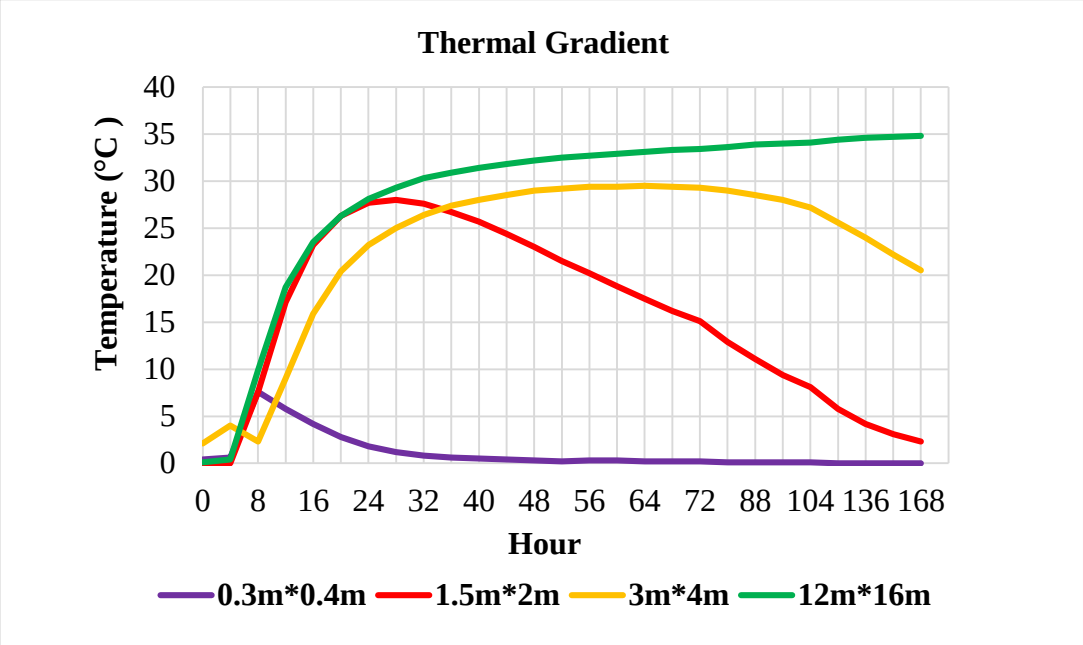

Figure 5.16 Thermal Gradient of Different Size Concrete Specimens

As the size of concrete specimen increases, internal heat will rise, but the outer surface of concrete temperature converges to the ambient temperature. Thus, thermal gradient will increase for an increment in specimen size. The cooling rate and temperature rise are also factors influenced by size of concrete specimen.

CHAPTER 6 CONCLUSION AND RECOMMENDATION

6.1 CONCLUSION

The main objective of this research was to understand early age thermal and mechanical properties of concrete contain bagasse ash under different ambient temperatures. The goal was achieved by undertaking experimental programs on concrete specimens encompassing different cement-bagasse ash proportions. Along the way, many significant conclusions were drawn and are stipulated below.

- Optimization of bagasse ash in concrete should be inclusive of early age strength development. In the present study, the early age strength development of concrete containing bagasse ash was retarded; However, strength enhancement was observed at late age of testing.
- Ambient temperature significantly affects both cement concrete and concrete containing bagasse ash. Although reduction in peak temperature up to 16.3% is observed while replacing cement by bagasse ash, heat liberation of all mixtures increase as the ambient temperature rises.
- Concrete specimens of all mixtures experienced higher thermal gradient at lower ambient temperature; Therefore, cold area concrete placements should get proper attention.
- Incorporating bagasse ash in concrete reduced thermal gradient inside the specimens. Moreover, this pozzolana decreased the total heat of hydration and elongated the time required for the occurrence of peak temperature by retarding early age chemical reactions.
- Thermal cracking risk has been dropped while using bagasse ash as partial cement replacing material. However, using a higher dosage of bagasse ash could retard the strength development and consequently escalates the risk of cracking.
- Adapting insulation at surface of concrete structures is not always a wise choice for minimizing thermal gradients. Since thermal gradient depends on factor such as insulation, size of concrete structures, material properties and environmental conditions, comprehensive studies and design should be carried out for each specific projects.

6.2 RECOMMENDATIONS FOR FUTURE WORK

While maintaining the favorable property in the retarding heat of hydration, other studies should be undertaken for enhancing the early age strength development of concrete containing bagasse ash. In this thesis, semi adiabatic temperature rise experiment was carried out, but this was not precise in predicting concrete temperature. Studies incorporating isothermal calorimetry and adiabatic temperature rise experiments should follow through.

In the present study, cracking risk is simulated using finite element software; However, Tensile Strength Testing Machine (TSTM) and Cracking Frame can be implemented for better investigations.

REFERENCE

Abdulkadir T. S., Oyejobi D. O., Lawal A.A. (2014). Evaluation of sugarcane bagasse ash as a replacement for cement in concrete works. *ACTA TEHNICA CORVINIENSIS – Bulletin of Engineering Tome*, 71-76. ISSN 2067 – 3809

ACI Committee 207. 207.1R-05. (2005). Guide to Mass Concrete. American Concrete Institute, Farmington Hills, Mich.

ACI Committee 207. 207.2R-07. (2007). Report on Thermal and Volume Change Effects on Cracking of Mass Concrete. American Concrete Institute, Farmington Hills, Mich.

ACI Committee 116. 116R-00. (2000). Cement and Concrete Terminology. American Concrete Institute, Farmington Hills, Mich.

ACI 211.1-91. (2002). Standard Practice for Selecting Proportions for Normal, Heavyweight, and Mass Concrete. American Concrete Institute, Farmington Hills, Mich.

ASTM C 150. (2000). Standard Specification for Portland cement. American Society for Testing and Materials. West Conshohocken, PA.

ASTM C 469. (2002). Standard Test Method for Static Modulus of Elasticity and Poisson's Ratio of Concrete in Compression. American Society for Testing and Materials. West Conshohocken, PA.

ASTM C 618-00. Standard Specification for Coal Fly Ash and Raw or Calcined Natural Pozzolana for Use as a Mineral Admixture in Concrete. American Society for Testing and Materials. West Conshohocken, PA.

ASTM C 136-84. (2001). Standard Test Method for Sieve Analysis of Fine and Coarse Aggregates. American Society for Testing and Materials. West Conshohocken, PA.

ASTM C 566-84. (1997). Standard Test Method for Total Evaporable Moisture Content of Aggregate by Drying. American Society for Testing and Materials. West Conshohocken, PA.

ASTM C 29-97. (1997). Standard Test Method for Bulk Density ("Unit Weight") and Voids in Aggregate. American Society for Testing and Materials. West Conshohocken, PA.

ASTM C 127-88. (2001). Standard Test Method for Density, Relative Density (Specific Gravity), and Absorption of Coarse Aggregate. American Society for Testing and Materials. West Conshohocken, PA.

ASTM C-33-01. (2001). Standard Specification for Concrete Aggregates. American Society for Testing and Materials. West Conshohocken, PA.

ASTM D 448-98. (1998). Standard Classification for Sizes of Aggregate for Road and Bridge Construction. American Society for Testing and Materials. West Conshohocken, PA.

ASTM C 204-00. (2000). Standard Test Method for Fineness of Hydraulic Cement by Air-Permeability Apparatus. American Society for Testing and Materials. West Conshohocken, PA.

ASTM C-192. (2002). Standard Practice for Making and Curing Concrete Test Specimens in the Laboratory. American Society for Testing and Materials. West Conshohocken, PA.

ASTM C-143 /C 143M–00. (2000). Standard Test Method for Slump of Hydraulic-Cement Concrete American Society for Testing and Materials. West Conshohocken, PA.

ASTM C-39/C 39M. (2003). Standard Test Method for Compressive Strength of Cylindrical Concrete Specimens. American Society for Testing and Materials. West Conshohocken, PA.

ASTM C-496. (1996). Standard Test Method for Splitting Tensile Strength of Cylindrical Concrete Specimens. American Society for Testing and Materials. West Conshohocken, PA.

ASTM C 78-00. (2001). Standard Test Method for Flexural Strength of Concrete (Using Simple Beam with Third-Point Loading). American Society for Testing and Materials. West Conshohocken, PA.

Awad Yasir, Mohamed Allah, Khalifa Shihab Ali, Hassan Abd Elwahab. (2017). Effects of sugarcane's bagasse ash additive on Portland cement properties. *International Journal of Sustainable Development Research, 3*(6), 85-89. ISSN: 2575-1832.

Ayub Tehmina, Khan Sadaqat Ullah, and Memon Fareed Ahmed. (2014). Mechanical characteristics of hardened concrete with different mineral admixtures: A review. *The Scientific World Journal,*1-15. doi: http://dx.doi.org/10.1155/2014/875082

A. Bahurudeen, A. V. Marckson, Arun Kishore, and M. Santhanam. (2014). Development of sugarcane bagasse ash based Portland pozzolana cement and evaluation of compatibility with superplasticizers. *Construction and Building Materials*, 68, 465 – 475.

Belie Nele De, Soutsos Marios, Gruyaert Elke. (Ed.). (2018). Properties of fresh and hardened concrete containing supplementary cementitious materials. The Ghent University, Belgium: Springer.

B. D. Cullity. (1977). Elements of x-ray diffraction (2nd Ed.). Addison-Wesley Publishing Company Inc. ISBN:0-201-01174-3.

Bobko Christopher (Dr.), Rudolf Seracino(Dr.), Zia Paul (Dr.) and Edwards Andrew. 2013. Crack free mass concrete footings on bridges in coastal environments (4-8). Mann Hall, USA.

CEB-FIP. (1990). Textbook on behavior, design and performance updated knowledge of the CEB/FIP model code. Lausanne, Switzerland. ISSN 1562-3610.

Chini Abdol R. and Parham Arash. (2005). Adiabatic temperature rise of mass concrete in Florida (5-14). Gainesville, USA.

Ethiopian Mapping Authority (EMA). (1988). The national atlas of Ethiopia. EMA, Addis Ababa.

Gajda John and Martha Vangeem. (2002). Controlling temperature in mass concrete. *Concrete International*. 59-61.

Geremew Miheret. (2017). Bagasse ash as a partial substitute of cement on concrete rigid pavement (unpublished master's thesis). Addis Ababa University, Addis Ababa, Ethiopia.

Hailu Biruk. (2011). Application of sugar cane bagasse ash as a partial replacement material (published master's thesis). Addis Ababa University, Addis Ababa, Ethiopia.

Hösthagen Anders. (2017). Thermal crack risk estimation and material properties of young concrete (unpublished academic thesis). Luleå University of Technology. Sweden.

Ji Guomin. (2008). Cracking risk of concrete structures in the hardening phase: Experiments, material modeling and finite element analysis (published doctoral thesis). The Norwegian University of Science and Technology, Trondheim, Norway.

Joshua Opeyemi, Matawal D.S., Akinawumi T.D, Olusola K.O. (2018). Development of fully pozzolanic binders for sustainable construction whole cement replacement in concrete application. *International journal of civil engineering and technology, 9*(2),1-12. ISSN:0976-6316

Kim Soo Geun. (2010). Effect of heat generation from cement hydration on mass concrete placement (unpublished master's thesis). Iowa State University, Iowa.

Klemczak Barbara and Knoppik Agnieszka Wróbel, 2011. Early age Thermal and Shrinkage Cracks in Concrete Structures Influence of Curing Conditions. *Archives of Civil Engineering*, 96-117. doi: 10.2478/ace-2013-0004

Lee M H, Khil B S and Yun H D. (2014). Influence of cement type on heat of hydration and temperature rise of the mass concrete. *Indian Journal of Engineering & Materials Sciences, 21*, 536-542.

Lawrence Adrian M. (2009). A finite element model for the prediction of thermal stresses in mass concrete (published doctoral dissertation). University of Florida, USA.

Lawrence Adrian, Mang Tia, Tu Anh Do, David Verdugo, Sangyoung Han, Mohammed Almarshoud, Brandon Ferrante, Ananya Markandeya. (2016). Maximum heat of mass concrete (17-20). University of Florida. USA.

Lagundžija Sandra and Thiam Marie. (2017). Temperature reduction during concrete hydration in massive structures (unpublished masters project). Stockholm, Sweden.

Mehta, P. K. and P.J.M. Monterio. (2006). Concrete: Microstructure, Properties, and Materials. 3rd Edition. McGraw-Hill, Inc. New York. USA.

Mahmud Safayat, Islam Md. Imamul, Ali Rubieyat Bin, Hasan Md. Mahadi. (2018). Investigation on the workability and compressive strength of concrete by using bagasse ash from sugar mill. *An International Scientific Journal*, (191-201), ISSN: 2392-2192.

Mohamed Saad Morsy and Mohamed Heikal. (2004). effect of curing temperature on the thermal expansion and phase composition of hydrated limestone-slag cement. Building Physics Department, Building Research Center, 48 (3), 110-116.

Meadows Jason Lee. (2007). Early-age cracking of mass-concrete structures (unpublished master's thesis). Auburn University, Auburn, Alabama.

Mikulcic Hrvoj, Vujanovic Milan, Markovska Natasa, Rist V. FILL, Ban Marko, Duci Neven (2013). CO_2 emission reduction in the cement industry. *The Italian Association of Chemical Engineering,35,* 703-708. doi: 10.3303/CET1335117.

Moses Priji. E., Dr. Perumal S.B. (2016). Hydration of cement and its mechanisms. *journal of civil and mechanical,13*(6), 17-31. ISSN: 2320-334X.

National Ready Mixed Concrete Association. (2009). Thermal cracking of concrete. *Technical information.* Silver Spring, USA.

Nehdi Moncef & Soliman Ahmed M. (2011). Early-Age Properties of Concrete: Overview of Fundamental Concepts and State of the Art Research". Engineering Journal.

Neville A.M. (2011). Properties of concrete (5^{th} Ed). Pearson Education Limited, United Kingdom (2018). ISBN: 0273755803.

Portland Cement Association. (1997). Portland cement, concrete, and heat of hydration. *Concrete technology today,18*(2), Skokie, USA.

Quero VGJ, Martinez FML, Garcia PM, Tiburcio CG, Nava JCG. (2013). Influence of sugar-cane bagasse ash and fly ash on the rheological behavior of cement pastes and mortars. *Construction Build Materials*, 40: 691–701.

Radovanvic Sanda. (1998). Thermal and structural finite element analysis of early age mass concrete structures (unpublished master's thesis). University of Manitoba, Winnipeg, Manitoba.

Raja Krovvidi Bangar. (2014). Behavior of sugarcane bagasse ash concrete when exposed to various temperature and cooled at room temperature (unpublished master's thesis). Gitam University, India.

Reddy G. Nithin Kumar, Vardhan G. Harsha, Reddy S. Vijaya Bhaskar. (2013). Partial replacement of cement in concrete with sugarcane bagasse ash and its behavior in aggressive environments. *Civil and mechanical engineering journal*, 29-35. ISSN: 2320–334X.

Siddique Rafat, Khan Mohammed Iqbal. (2011). Supplementary cementing materials. Springer. Heidelberg. ISSN 1612-1317.

S. L. Meyers. (1951). How temperature and moisture changes may affect the durability of concrete. Rock Products, 153–7.

Schindler, A. K., and Folliard, K. J. (2005). Heat of hydration models for cementitious materials. *ACI Materials Journal, 102*(1), 24-33.

Smith Samuel J. (2007). The development of thermal and mechanical property tests for mass concrete (unpublished master's thesis). University of Florida, USA.

Srivastava Er. Shubham and Shukla Er. Puneet Kumar. (2015). Studies on partial replacement of cement by bagasse ash in concrete. *International journal for innovative research in science & technology*, *2*(3), 43-45. ISSN: 2349-6010.

Srinivasan R. and Sathiya K. (2010). Experimental Study on Bagasse Ash in Concrete. *International Journal for Service Learning in Engineering, 5*(2), 60-66. ISSN 1555-9033.

Suliman Mohamed Eljack and Almola Samah M. Fudl. (2011). The use of sugarcane bagasse ash as an alternative local pozzolanic material: study of chemical composition. *A scientific journal of COMSATS, 17*, 65-69.

Tang Kangkang (PhD), Millard Steve (PhD), Beattie Greg (PhD). (2015). Early-age heat development in GGBS concrete structures. *Proceedings of the Institution of Civil Engineers*, *168*(SB8), 551-553. doi: 10.1680/stbu.14.00089.

Townsend, C.L. (1981). Control of cracking in mass-concrete structures. United States Government Printing Office, USA.

USDA Foreign Agricultural Service. (2015). Assessments of commodity and trade issues. Made by USDA staff. Addis Ababa.

Ulm, F.J., Coussy, O., 1998. Couplings in early-age concrete: from material modeling structural design. *International Journal of Solids and Structures, 35*, 31–32, ISSN: 4295–4311.

Wang Kejin, Hu Jiong, Ge Zhi. (2014). The influence of cement fineness and water to cement ratio on mortal early age heat of hydration. *Construction building and material,50,* 657-663.

APPENDIX A

MECHANICAL PROPERTIES DATA

Table A.1 Compressive Strength Experiment Data, 0% and 6.5% Replacement Level

Mixture Code	Test Date	Failure Load (KN)	Stress (Mpa)	Avg. (Mpa)	Mixture Code	Test Date	Failure Load (KN)	Stress (Mpa)	Avg. (Mpa)
BA-0	1	215.7	9.59	8.49	BA-6.5	1	201.4	8.95	8.35
		191.9	8.53				185.5	8.25	
		165.7	7.36				176.3	7.84	
	2	288.2	12.81	11.9		2	240.1	10.67	11.26
		292.6	13.01				252.4	11.22	
		222.3	9.88				267.3	11.88	
	3	399.6	17.76	16.14		3	386.2	17.16	16.06
		310.8	13.81				326.7	14.52	
		378.8	16.84				367.7	16.34	
	7	538.2	23.9	23.92		7	506.5	22.51	23.77
		523.4	23.35				556.6	24.74	
		551.9	24.84				541.9	24.08	
	28	677.2	30.12	29.19		28	654.5	30.12	30.2
		633.4	28.15				692.1	30.76	
		659.5	29.32				669.2	29.74	

Table A.2 Compressive Strength Experiment Data, 13% and 20 % Replacement Level

Mixture Code	Test Date	Failure Load (KN)	Stress (Mpa)	Avg. (Mpa)	Mixture Code	Test Date	Failure Load (KN)	Stress (Mpa)	Avg (Mpa).
BA-13	1	160.4	7.13	7.7	BA-20	1	233.1	10.36	10.01
		202.2	8.13				238.3	10.59	
		176.5	7.84				204.5	9.09	
	2	235.2	10.46	10.54		2	234.5	10.42	11.69
		268.4	10.93				304.7	12.54	
		230.4	10.24				272.9	12.13	
	3	324.2	14.41	15.13		3	326.3	14.5	14.39
		343.5	15.26				310.8	13.81	
		354	15.73				334.6	14.87	
	7	524.9	23.33	23.28		7	424.4	18.86	20.34
		508.8	22.61				456.9	20.31	
		537.9	23.91				491.8	21.86	
	28	663.9	29.51	31.13		28	627.6	27.89	28.49
		719.8	31.99				675.9	30.03	
		717.5	31.89				624.8	27.77	

Table A.3 Flexural Strength Experiment Data, 0% and 6.5% Replacement Level

Mixture Code	Test Date	Failure Load (KN)	Stress (Mpa)	Avg. (Mpa)	Mixture Code	Test Date	Failure Load (KN)	Stress (Mpa)	Avg. (Mpa)
BA-0	1	1.2	0.6	0.6	BA-6.5	1	1.4	0.7	0.7
		1.2	0.6				1.4	0.7	
	2	3.1	1.55	1.45		2	2.8	1.4	1.33
		2.7	1.35				2.5	1.25	
	3	3.3	1.65	1.68		3	3.2	1.6	1.58
		3.4	1.7				3.1	1.55	
	7	6.2	3.1	2.95		7	5.9	2.95	2.9
		5.6	2.8				5.7	2.85	
	28	10.2	5.1	4.7		28	10.2	5.1	5
		8.6	4.3				9.8	4.9	

Table 4.4 Flexural Strength Experimental Data, 13 % and 20 % Replacement Level

Mixtue Code	Test Date	Failure Load (KN)	Stress (Mpa)	Avg. (Mpa)	Mixture Code	Test Date	Failure Load (KN)	Stress (Mpa)	Avg. (Mpa)
BA-13	1	1	0.5	0.45	BA-20	1	0.7	0.35	0.38
		0.8	0.4				0.8	0.4	
	2	2.4	1.2	1.25		2	2	1	1
		2.6	1.3				2	1	
	3	2.8	1.4	1.46		3	2.8	1.4	1.35
		3	1.5				2.6	1.3	
	7	6	3	2.9		7	4.3	2.15	2.3
		5.6	2.8				4.9	2.45	
	28	10.8	5.4	5.55		28	8.3	4.15	3.95
		11.4	5.7				7.5	3.75	

Table A.5 Splitting Tensile Strength Experiment Data, 0% and 6.5% Replacement Level

Mixture Code	Test Date	Failure Load (KN)	Stress (Mpa)	Avg. (Mpa)	Mixture Code	Test Date	Failure Load (KN)	Stress (Mpa)	Avg. (Mpa)
BA-0	1	44.5	0.63	0.76	BA-6.5	1	55.7	0.79	0.69
		62.9	0.89				41.8	0.59	
	2	118	1.67	1.55		2	82.9	1.17	1.17
		100.9	1.43				81.9	1.15	
	3	135.2	1.91	1.86		3	118.2	1.67	1.73
		127.7	1.81				126.4	1.78	
	7	149.1	2.11	2.14		7	148.7	2.10	2.03
		153.7	2.17				138.7	1.96	
	28	194.4	2.47	2.69		28	218.3	2.78	2.87
		227.9	2.90				232.6	2.96	

Table A.6 Splitting Tensile Strength Experimental Data, 13 % and 20 % Replacement Level

Mixture Code	Test Date	Failure Load (KN)	Stress (Mpa)	Avg. (Mpa)	Mixture Code	Test Date	Failure Load (KN)	Stress (Mpa)	Avg. (Mpa)
BA-13	1	38.2	0.49	0.57	BA-20	1	29.8	0.38	0.41
		50.9	0.65				34.2	0.44	
	2	64.5	0.82	0.88		2	56.2	0.72	0.8
		73.7	0.94				69.3	0.88	
	3	107.2	1.36	1.44		3	97.8	1.24	1.31
		119.3	1.52				107.8	1.37	
	7	153.3	1.95	1.97		7	126.9	1.62	1.55
		156.2	1.98				115.5	1.47	
	28	224.4	2.86	2.92		28	185.3	2.35	2.38
		233.6	2.97				189	2.41	

APPENDIX B

SEMI ADIABATIC TEMPERATURE RISE

Table B.1 Semi Adiabatic Temperature Rise Data at Average Ambient Temperature of 25.15^{0}C

Hours	Mixture Code												Amb. Temp.
	BA-0			BA-6.5			BA-13			BA-20			
	T	M	B	T	M	B	T	M	B	T	M	B	
0.5	19.1	20.2	19.6	19.2	19.7	19.5	18.3	18.3	18.2	18.6	17.1	17.6	25.21
1	19.2	20.7	20.3	19.3	20.5	20.2	19	18.8	18.7	18.5	17.5	17.6	25.35
1.5	19.3	21.1	21.7	19.3	20.7	20.4	19.2	19	19.1	18.5	18.1	18.7	24.99
2	19.4	21.1	22.2	19.4	20.9	21.1	19.2	19.3	19.4	18.3	18.4	18.9	25
2.5	19.7	21.2	22	19.6	20.9	21.7	19.3	19.8	19.6	18.9	18.6	19	25.23
3	19.8	21.2	22	19.7	20.9	21.8	19.8	20.2	20.1	19.3	18.9	19.1	24.97
3.5	20	21.3	22	19.8	21	21.8	19.8	20.4	20.5	19.5	19.1	19.3	25.06
4	20.3	21.7	22.1	19.9	21.3	21.9	20.4	20.7	20.7	19.6	19.5	19.5	25.17
4.5	21.7	22.8	22.2	20	22.1	22.1	20.3	21.4	21.3	19.8	20.1	19.9	25.04
5	23.6	24.2	23.7	19.9	22.9	22.4	20.4	21.6	21.7	19.8	20.5	20	25.1
5.5	24.6	25.1	24.6	20.8	23.7	23.1	21.4	22.1	21.9	19.9	20.9	20.1	25.13
6	26.6	27.3	26.8	22.7	25.5	24.2	21.9	23	22.6	20.3	21.3	20.3	24.76
6.5	27.1	27.9	27.1	23.6	26.8	25	22.2	23.8	22.7	20.8	21.8	20.7	24.91
7	27.4	28.1	27.8	23.9	27.6	27	23.1	25.5	24.4	21.2	22.5	21.4	25.12
7.5	28.4	29.2	28.8	24.6	28.5	27.8	23.5	27	25.6	21.9	24.1	22.1	25.25
8	29.6	30.5	30.2	25.1	29.5	28.7	24.4	28	26.5	22.7	24.5	23.7	25.01
8.5	30.3	31.5	31.1	25.8	30.5	29.9	25	28.4	26.9	23.6	25.7	25.2	25.15
9	31.3	32.7	32.5	27	31.3	30.8	26.4	28.9	28	24.2	26.2	26.2	25
9.5	32	33.6	33.8	28.1	32.1	31.9	27.2	29.9	28.8	25.6	27.2	26.5	25.21
10	32.8	34.9	34.9	28.8	32.8	33	28.6	30.7	30	26.6	28.1	27.6	25.21
10.5	33.4	35.8	35.9	29.2	33.6	34	28.8	31.4	30.7	26.7	29	28.6	25.16
11	34.2	36.9	37.3	30.3	35.7	35	29.4	32	31.6	27.5	29.6	29.5	25.29
11.5	34.6	37.5	38.1	30.7	36.2	36.1	30	32.7	32.8	28.2	30.6	30.7	25.39
12	35.1	38.3	39.3	31.2	36.7	36.7	30.5	32.7	33.6	28.7	31.4	31.2	25.33
12.5	35.4	38.9	40.2	31.6	37.3	37.7	30.8	33.3	34.3	29.3	31.8	32.1	24.99
13	35.4	39.4	41.1	32.2	37.8	38.2	31.3	33.8	35	29.5	32.5	32.8	25.3
13.5	35.5	39.7	41.6	32.9	37.6	38.9	32.1	34.4	35.6	30.3	33	33	25.06
14	35.9	40.2	42.5	33.6	38.2	39.3	32.1	34.8	36	31.1	33.2	33.6	25.28
14.5	36.3	40.4	43.2	34.4	38.2	40	32.5	35.1	36.2	30.7	33.5	34.2	25.33
15	36.2	40.2	43.2	34.7	38.3	40.3	32.8	35.3	36.7	31	33.8	34.9	25.33
15.5	36.2	40.8	43.9	34.8	38.4	40.9	33	35.7	37.3	31.4	34	35.3	25.15
16	36.4	40.9	43.9	34.9	38.2	41.3	33.2	36.2	37.4	31.4	34.5	35.7	25.22
16.5	36.7	41.2	43.9	34.9	38.3	40.9	33.4	36.1	37.6	32	34.7	36	24.95
17	36.9	40.9	43.9	35.3	38.3	40.8	33.5	36.1	38.3	32.2	34.8	36.4	24.8

17.5	36.9	40.9	43.9	35.5	38.3	40.6	33.6	36.4	38.9	32.3	34.9	36.8	25.12
18	36.6	40.9	43.9	35.2	38.2	40.3	33.8	36.2	39.3	32.3	34.9	37	24.9
18.5	36.6	40.6	43.8	35.2	38.2	40.4	33.8	36	38.8	32.4	34.9	37.2	25.15
19	36.5	40.6	43.8	35.1	38.1	40.5	32.7	35.7	38.7	32.3	34.9	37.3	24.96
19.5	36.5	40.5	43.9	35.1	38.1	40.5	32.5	35.6	38.7	32.3	35	37.1	25.14
20	36.5	40.5	43.7	35	37.9	40.4	32.3	35.6	38.4	32.3	35	37.2	25.32
20.5	36.4	40.3	43.7	35.1	37.8	40.4	31.8	35.5	38.1	32	35	37.1	25.03
21	36.3	40.2	43.6	34.9	37.8	40.3	31.6	35.5	37.7	32.1	34.8	37	25.28
21.5	36.3	39.8	43.6	34.8	37.8	40.4	31.1	35.3	37.6	31.9	34.7	36.9	25.39
22	36.2	39.7	43.2	34.7	37.6	40.3	30.8	35.3	37.4	31.5	34.7	36.8	25.15
22.5	36.1	39.6	43.1	34.8	37.6	40.2	30.4	35.2	37.1	31	34.6	36.4	25.21
23	35.8	39.6	42.7	34.6	37.5	40.2	30.4	35.1	37	30.7	34.4	36.3	25.02
23.5	35.3	39.4	41.5	34.1	36.9	39.7	30.5	35.1	36.7	30	34.3	36.1	25.37
24	34.9	39.2	41.2	34	36.3	39.5	30.3	34.4	36.1	29.4	33.9	35.4	25.25
26	33.9	38.7	40.7	33.6	35.2	38.7	29.6	33.1	35.4	28.8	33	34.3	25.48
28	33.5	38.1	40.2	33.2	34.7	37.9	29.1	32.5	35	28	32.4	33.6	25.21

Table B.2 Semi Adiabatic Temperature Rise Data at Average Ambient Temperature of 35.64 ^{0}C

Hour	Mixture Code												Amb. Temp
	BA-0			BA-6.5			BA-13			BA-20			
	T	M	B	T	M	B	T	M	B	T	M	B	
0.5	20	21.2	21.6	19.6	20.4	21	15.9	18.5	19.2	19.5	19.6	19.5	35.01
1	20.6	21.3	21.7	20.3	20.6	21.2	20	19.9	19.9	19.4	19.6	19.5	35.17
1.5	21.1	21.9	21.8	21.1	20.7	21.2	20.4	20.1	20.1	19.8	19.7	19.6	34.85
2	22.1	22.1	22.1	22.2	21.1	21.5	20.4	20.2	20.2	19.8	19.8	19.6	35.38
2.5	23.1	22.6	22.3	22.6	21.4	21.7	20.7	20.7	20.4	19.3	19.9	19.9	35.40
3	23.5	23	22.3	23.4	21.6	22	21.9	21.3	20.8	19.4	20.2	20.1	35.27
3.5	23.6	24.1	22.7	23.5	22.2	22.1	22.4	21.7	21.1	19.9	20.5	20.3	35.45
4	24.8	25.3	23.2	23.9	22.3	22.5	23	22.1	21.6	20.5	20.6	20.3	35.51
4.5	25.8	25.5	23.9	24.4	22.7	23.2	23.6	22.5	22.1	20.9	21.2	20.9	35.47
5	26.8	26.2	25.5	25.5	24.2	23.8	24	23.1	22.8	21.1	22.6	21.3	35.22
5.5	27.9	26.5	25.8	26.6	24.9	24.6	24.7	23.7	23.4	22.3	22.9	21.9	35.43
6	29	27.7	26.8	27.8	26.2	25.2	25.3	24.5	23.9	23.3	23.4	22.1	35.90
6.5	30.2	29.3	28.1	29.1	26.4	26.3	26.2	25.2	24.5	24.5	24	23.1	35.59
7	30.9	30.2	29	30.3	27.7	27.3	26.8	25.8	25.3	25.6	24.8	23.7	35.39
7.5	31.8	31.5	30.3	30.7	29.3	28.2	27.7	26.3	26.7	26.8	25.3	24.1	35.54
8	32.5	32.3	31.3	31.4	30.2	28.9	28.4	26.8	27.2	27.1	25.5	24.5	35.43
8.5	33.2	33.3	32.3	32.2	31.7	30.2	29.9	28.1	28	27.8	26.7	25.1	35.60
9	33.8	34.5	33.6	33	32.6	31.3	30.6	29	28.7	28.9	27.4	25.9	36.00
9.5	34.4	35.4	34.7	33.6	33.7	32.3	31.3	30.4	29.2	30.2	28.7	26.6	35.66

10	35.4	36.6	36	34.2	34.9	33.6	32.1	31	30.4	31	29	27.5	36.03
10.5	36	37.4	36.8	34.7	35.6	34.6	32.8	32.3	31.3	31.7	30.9	28.8	35.42
11	36.8	38.6	38.2	35.4	36.3	35.5	33.2	33.4	32.6	33	31.9	29.4	35.75
11.5	36.7	39.2	39.2	35.8	36.9	36.4	33.6	34.1	34.1	33.6	32.6	30.9	35.62
12	37.1	40	40.1	36.1	37.4	37.1	34.2	35.7	35.4	33.9	33.5	31.7	35.23
12.5	37.6	40.8	41.2	36.6	38	38	34.6	36.2	36.6	34.1	33.9	32.5	35.65
13	37.6	41.9	42.7	37	38.6	38.7	35.2	37.1	37.8	34.5	34.6	33.2	35.95
13.5	37.7	42.3	43.3	37.1	38.8	40.7	35.6	37.5	38.6	34.7	35	34.6	35.58
14	37.8	42.7	43.9	37.2	39.4	41.3	36.1	38.3	38.9	34.9	35.3	35	35.83
14.5	38.2	43	44.5	37.2	40.2	42	36.3	39.1	39.1	35	35.5	36.1	35.80
15	38.1	43.4	45.8	37.2	40.5	42.5	36.4	39.4	39.6	35.1	35.8	36.9	35.80
15.5	37.9	43.7	46.2	37.3	41.6	42.8	36.6	39.9	40.3	35.1	36.3	37.3	35.78
16	37.8	43.4	46.8	37.3	41.8	43.1	36.7	40	40.9	35.1	36.8	37.9	35.34
16.5	37.7	43.5	47	37.3	42.1	44.6	36.7	40.2	41.2	35.1	37.5	38.3	35.29
17	37.7	43.5	47	37.1	42.2	44.6	36.6	40.2	41.7	35.2	38	38.6	35.87
17.5	37.7	43.5	46.9	37.1	42	45.1	36.5	39.6	42	35.1	38.2	39.1	35.76
18	37.6	43.5	46.9	37.1	42	45.3	36.3	39.6	42.4	35.1	38.3	39.6	35.82
18.5	37.5	43.4	46.8	37	42	45	36.3	39.7	42.7	35	38.9	40.3	35.58
19	37.5	43.4	46.6	37	42	45.1	36.2	39.8	42.7	34.9	38.9	40.9	36.00
19.5	37.5	43.3	46.6	37	41.9	45	36.2	39.8	42.6	34.9	38.8	41.3	35.78
20	37.4	43.2	46.4	36.9	41.8	44.9	36	39.6	42.6	34.5	38.8	41.4	35.90
20.5	37.4	43.1	46.4	36.7	42	44.8	35.8	39.7	42.6	34.4	38.8	41.4	35.59
21	37.4	43	46.2	36.6	41.8	44.8	35.8	39.6	42.5	34.2	38.7	41.3	35.86
21.5	37.3	42.8	46.1	36.4	41.7	44.7	35.6	39.5	42.2	34.2	38.6	41.4	35.81
22	37.2	42.8	46.2	36.5	41.7	44.6	35.5	39.5	42.1	34	38.4	41.3	35.98
22.5	37.1	42.7	46.2	36.4	41.5	44.3	35.3	39.3	42.1	34	38.3	41.3	36.02
23	37.1	42.6	46.1	36.1	41.6	44.2	35.3	39.3	41.9	33.9	38.2	41.2	36.09
23.5	37.1	42.3	46.1	36.1	41.6	44.1	35.1	39.2	41.8	33.9	38.2	41.1	35.79
24	37.1	41.8	46.1	36	41.5	44	35.1	39	41.6	33.9	38	40.8	36.09
26	36.5	41.2	45.9	35.9	41.3	44	35	38.8	41.5	33.9	37.9	40.7	36.09
28	36.4	41.1	45.7	35.7	41	43.8	34.8	38.6	41.4	33.9	37.8	40.3	35.80

Table B.3 Semi Adiabatic Temperature Rise Data at Average Ambient Temperature of 43.77^0 C

Hour	Mixture Code												Amb. Temp
	BA-0			BA-6.5			BA-13			BA-20			
	T	M	B	T	M	B	T	M	B	T	M	B	
0.5	19.8	21.2	21.3	20.1	20.8	20.7	20.5	20.9	20.1	20.5	20.5	20.1	43.59
1	20.3	21.4	21.4	20.2	20.9	21.2	20.4	21.2	20.8	20.8	20.6	20.6	43.46
1.5	20.9	22.5	21.7	20.3	21	21.6	20.6	21.9	21.1	21.4	20.7	20.5	42.30
2	22.1	22.7	21.9	20.7	21.3	21.8	21	22.3	21.6	21.7	21	20.9	43.23
2.5	24.2	23.6	22.1	21.2	21.9	21.9	21.3	22.5	21.9	22	21.6	21.1	44.28
3	25.1	24.6	22.9	21.8	22.8	22.1	21.7	22.9	22.1	22.2	21.8	21.6	42.93
3.5	25.9	25.5	24.1	22.6	23.1	22.4	22.2	22.6	22.4	22.5	22.2	21.8	42.71
4	27.6	26.6	25.3	24.4	23.9	22.7	23.3	23	22.7	22.8	22.7	22.4	43.32
4.5	28.3	27.8	26.7	24.6	24.3	23	23.8	23.6	22.9	23.5	23.2	23	43.55
5	29.4	28.2	27.4	25.2	25	23.8	24.2	24.1	23.5	24.6	23.8	23.6	43.81
5.5	30.2	29	28.9	26.2	26.3	24.2	25.8	25.3	23.7	25.2	24.6	23.9	43.67
6	30.9	30.8	29.7	27.4	26.8	24.9	26.8	26.6	24.1	26.2	25	24.1	43.63
6.5	31.7	31.2	30.4	28	27.8	25.5	27.7	27.1	24.6	27.4	25.8	24.8	43.97
7	32.2	32.1	31.1	29.6	28.8	26.1	28.1	27.5	25.2	28	25.9	25.5	43.80
7.5	33.3	33.3	31.8	30.8	30.7	27.4	29.2	28.2	26.2	28.8	26.3	26.3	43.67
8	33.9	34.2	32.3	31.6	31.9	28.9	30.6	29	27	30.3	26.8	26.9	43.02
8.5	34.7	35.4	33.2	32.6	33	29.4	31.8	30.7	27.9	31.8	27.3	27.4	43.15
9	35.4	36.3	34.9	33.3	34.2	30.7	32.5	31.8	28.4	32.8	28.3	28.1	44.07
9.5	36.1	37.7	35.7	34.5	35	31.4	33.4	32.6	29.6	33.5	29	28.8	44.22
10	37.3	39.2	36.2	35.3	36.3	32.9	34.9	33.2	31	34.7	29.9	29.6	44.28
10.5	38.7	40.6	37.4	36.8	38	34	35.5	34.7	32	35.5	30.5	30.7	44.22
11	40.5	41.3	38.6	38.2	38.7	35.9	36	35.2	33.7	36.5	31	31.2	43.62
11.5	41.4	41.5	40.2	38.4	39.5	36.7	36.7	36.6	34.6	36.9	32.2	32.6	44.21
12	42.9	42.5	41.7	39.9	39.9	38.3	37.2	37.4	35.2	37.1	32.7	33.3	44.63
12.5	43.3	44.2	43.8	40.3	40.6	39.2	37.7	38.2	36	37.6	33.2	34.7	43.41
13	44.5	45.7	44.8	41.4	40.7	40.2	38.9	38.9	37.6	37.8	33.6	35.7	44.17
13.5	45.6	46.2	46	42.1	40.8	40.9	39.7	39.5	38.1	38.2	34.5	36.2	44.17
14	45.9	46.8	46.7	42.9	41.4	41.5	40.8	39.6	39	38.6	35.3	37	44.31
14.5	46.2	47.9	46.9	43.8	42.6	42.8	41.3	40.1	40	38.8	36.6	38.6	43.58
15	46.9	47.9	48.3	44.2	43.3	43.7	41.7	40.8	40.9	39.2	37.3	39.4	43.58
15.5	47.2	48.3	49	44.9	43.6	44.2	42.4	41.2	41.3	39.5	38.8	41.1	43.25
16	47.3	48.6	49.4	45.1	43.8	45.3	42.5	41.9	42.1	39.8	38.9	41.3	43.65
16.5	47.3	48.7	49.7	45.2	44.4	46	42.6	42.2	43	39.9	39.4	41.7	44.28
17	47.3	48.8	50.1	45.3	44.7	46.3	43	42.8	43.2	39.9	40	42.1	43.58
17.5	47.5	48.8	50.5	45.4	45.2	46.5	43.1	43.2	44.3	39.9	40.5	42.6	44.17
18	47.4	48.8	50.7	45.4	45.5	46.8	43.1	43.7	44.6	39.9	40.7	42.6	43.38
18.5	47.4	48.9	51	45.4	45.6	47.2	43.1	44	44.9	39.8	40.8	42.9	43.40

19	47.4	48.8	51.3	45.5	45.7	47.6	43.1	44.4	45.1	39.8	40.8	43	43.58
19.5	47.4	48.8	51.2	45.3	45.7	47.7	43.3	44.6	45.3	39.8	40.8	43	43.08
20	47.3	48.7	51.3	45.3	45.8	48.1	43.5	44.5	45.6	39.8	40.7	42.9	43.29
20.5	47.3	48.7	51.3	45.2	46	48.5	43.4	44.5	45.7	39.9	40.7	42.9	43.66
21	47.2	48.7	51.4	45	46.1	48.6	43.4	44.6	46.1	39.8	40.7	42.8	44.14
21.5	47.2	48.6	51.4	44.9	46.1	48.6	43.3	44.8	46.3	39.7	40.7	42.7	44.76
22	47.2	48.6	51.4	44.9	46.1	48.7	43.3	44.8	46.2	39.6	40.8	42.7	44.88
22.5	47.2	48.6	51.3	44.6	46	48.7	43.2	44.8	46.3	39.5	40.7	42.8	44.52
23	47.1	48.6	51.3	44.5	45.9	48.6	43.1	44.6	46.4	39.5	40.7	42.7	44.81
23.5	47	48.5	51.2	44.4	45.8	48.5	43	44.5	46.2	39.4	40.6	42.6	44.10
24	47.1	48.5	51.1	44.4	45.7	48.4	42.9	44.5	46.2	39.4	40.5	42.5	43.50
26	47	48.3	51	44	45.4	48.2	42.7	44.2	45.8	39.4	40.4	42.3	44.41
28	46.9	48.1	51	43.6	45.1	48	42.4	44	45.6	39.3	40.1	42.1	43.59

APPENDIX C

CHEMICAL PROPERTY OF BAGASSE ASH AND CEMENET

	GEOLOGICAL SURVEY OF ETHIOPIA	Doc.Number: GLD/F5.10.2	Version No: 1
	GEOCHEMICAL LABORATORY DIRECTORATE		Page 1 of 1
Document Title:	Complete Silicate Analysis Report	Effective date:	May, 2017

Issue Date: -03/04/2019

Customer Name:- Amanuel Bersisa Gudisa

Request No:- GLD/TR/151/19

Report No:- GLD/TR/152/19

Sample type:- Ash

Sample Preparation: - 200 Mesh

Date Submitted: - 11/03/2019

Number of Sample:- One (1)

Analytical Result: In percent (%) Element to be determined Major Oxides & Minor Oxides

Analytical Method: $LiBO_2$ FUSION, HF attack, GRAVIMETERIC, COLORIMETRIC and AAS

Collector's code	SiO_2	Al_2O_3	Fe_2O_3	CaO	MgO	Na_2O	K_2O	MnO	P_2O_5	TiO_2	H_2O	LOI
ABG-01	68.60	9.04	5.24	1.52	1.36	1.84	2.44	0.12	0.51	0.13	1.80	7.91

Note: - This result represent only for the sample submitted to the laboratory.

Analysts	Checked By	Approved By	Quality Control
Yirgalem Abriham Tihitna Beletkachew Tizita Zemene Yohanis Getachew Elsa Fisseha Bethelhem Tefera	Dessie Abebe	Gosa Haile	Negash Worku

Table C.1 Chemical Property of Bagasse Ash

	GEOLOGICAL SURVEY OF ETHIOPIA	Doc.Number: GLD/F5.10.2	Version No: 1
	GEOCHEMICAL LABORATORY DIRECTORATE		Page 1 of 1
Document Title:	Complete Silicate Analysis Report	Effective date:	May, 2017

Issue Date: - 23/04/2019

Customer Name:- Kalayu Kifle Aron Birhanu & Amanuel

Request No: GLD/TR/204/19

Report No: GLD/TR/200/19

Sample type: - Powder

Sample Preparation: - 200 Mesh

Date Submitted: - 29/01/2019

Number of Sample: One (1)

Analytical Result: In percent (%) Element to be determined Major Oxides & Minor Oxides

Analytical Method: $LiBO_2$ FUSION, HF attack, GRAVIMETERIC, COLORIMETRIC and AAS

Collector's code	SiO_2	Al_2O_3	Fe_2O_3	CaO	MgO	Na_2O	K_2O	MnO	P_2O_5	TiO_2	H_2O	LOI
cement-1	26.62	6.08	4.82	55.30	1.10	0.20	0.16	<0.01	0.08	0.24	0.51	3.43

Note: - This result represent only for the sample submitted to the laboratory.

Analysts	Checked By	Approved By	Quality Control
Tihitna Beletkachew Yohannes Getachew Tizita Zemene Yergalem Abraham Bethlehem Tefera	Dessie Abebe	Gosa Haile	Negash Worku

Table C.2 Chemical Property of Cement